HIGH RESOLUTION ISOTOPE STRATIGRAPHY OF THE LOWER DEVONIAN

by

Davin Ala

A thesis submitted to the School of Graduate Studies and Research

in partial fulfullment of the requirements

for the degree of M.Sc. in Earth Sciences

OTTAWA-CARLETON GEOSCIENCE CENTRE

AND

UNIVERISTY OF OTTAWA

OTTAWA, CANADA

ISBN 0-612-19924-X

Canada

UNIVERSITÉ D'OTTAWA
UNIVERSITY OF OTTAWA

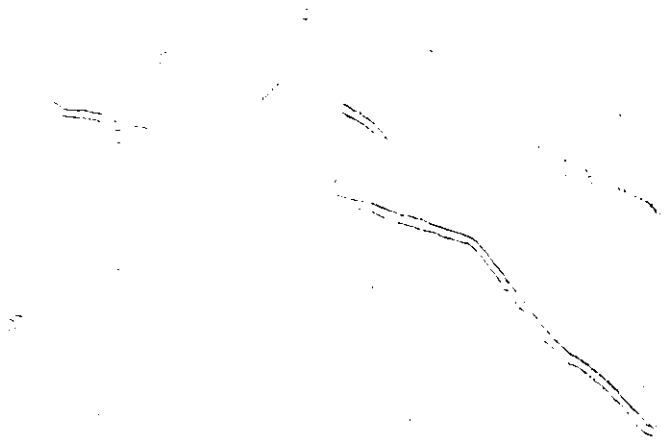

ABSTRACT

A new data set of 53 $^{87}Sr/^{86}Sr$ ratios for the Lower Devonian has been collected from well preserved, and stratigraphically well constrained, brachiopod shells from the Leon region in Spain, western Urals in Russia, Podolia in Ukraine and New York State in the United States. Multiple criteria, including trace element and stable isotope (C, O) analysis, scanning electron microscopy, cathodoluminescence and optical light microscopy, were used to determine the state of preservation of the samples.

One hundred and ten samples were analysed for $\delta^{13}C$, with the results ranging from -1.49 to 5.5 ‰ (VPDB). The carbon isotope trend through the Lower Devonian is characterized by a flat slope within ± 1.5 ‰ of the mean value. One hundred and ten samples were analysed for $\delta^{18}O$, with results that ranged from -8.74 to -1.89 ‰ (VPDB). The oxygen isotope trend through the Lower Devonian is flat, except for the New York State samples which fall ~ 2 ‰ lighter, probably because of the ambient temperature of the coeval sea water.

For $^{87}Sr/^{86}Sr$, the new data set is continuous and consistent for all study areas and shows a decrease from 0.70882 to 0.70782 from the Pridoli to the Emsian/Eifelian boundary. The Lower Devonian trend also fits well with the previously published Middle Devonian data. In detail, a relatively stable $^{87}Sr/^{86}Sr$ ratio for the Lochkovian is followed by a rapid decrease through the Pragian, and by a period of short term small oscillations (2×10^{-4}) in the Emsian and the Eifelian. The observed decline in ^{87}Sr throughout the Lower Devonian may suggest that

the fraction of strontium derived from seawater/mantle interactions is on the increase through the Lower Devonian in relation to strontium derived from sialic sources such as weathering of the continents. Paleogeographic and biogeographic data for this time period suggest that the relative sea level in the Lower Devonian was rising, possibly due to increased spreading rates at MOR's, in accord with the observed strontium isotope trend. In terms of stratigraphic resolution, the slope of the $^{87}Sr/^{86}Sr$ curve for the Lochkovian is too flat to be of utility for correlation purposes. In contrast, the steep slope observed in the Pragian and steep short term fluctuations found in the Emsian may provide stratigraphic resolution on the order of 1-2 Ma.

RÉSUMÉ

De nouvelles données comptant 53 rapports $^{87}Sr/^{86}Sr$ provenant du Dévonien inférieur fut établie à partir de coquilles de brachiopodes bien préservées et stratigraphiquement bien délimitées, recueillies en Espagne, Russie (Urals occidentaux), Ukraine (Podolie) et dans l'état de New York, aux États-Unis. Divers critères, tels les éléments traces et isotopes stable (C,O), microscopes à balayage électronique, à cathodoluminescence et optique, ont servi à déterminer l'état de préservation des échantillars.

Cent dix spécimens furent analysés pour le carbone-13, ayant des valeurs de $\delta^{13}C$ variant entre -1.49 et 5.5 ‰ (VPDB). La tendance isotopique du carbone au cours du Dévonien inférieur se caractérise par une peut douce a ± 1.5 ‰ de la valeur moyenne. Cent dix échantillers furent analysés pour l'oxygène-18, ayant des valeurs s'étalant entre -8.84 et -1.89 ‰ (VPDB). La tendance isotopique pour l'oxygène pendant le Dévonien inférieur est plate, à l'exception des échantillers provenant de l'état de New York, lesquels sont environ 2 ‰ plus légers, probablement dû à la température ambiante de l'eau marine.

En ce qui a trait au rapport $^{87}Sr/^{86}Sr$, la banque de données présentée ici est continue et comparable entre tous les sites étudiés, et présente un déclin de 0.70882 à 0.70782, depuis la limite entre le Pridoli et l'Emsien/Eifelien. Cette tendance du Dévonien inférieur concorde également avec les résultats publiés précédement sur le Dévonien moyeu. De façon plus spécifique, le rapport $^{87}Sr/^{86}Sr$ relativement stable pour le Lochkovien est suive d'un déclin

rapide durant le Pragien, et par un période de faibles oscillations de courte durée (2×10^{-4}) pendant l'Emsien et l'Eifelien. Cette diminution en ^{87}Sr durant le Dévonien inférieur pourrait suggérer un changement d'une source de strontium 'siliclique' à une autre plus influencée par les interactions entre l'océan et le manteau terrestre. Des données paléogéographiques et biogéographiques pour cette période suggèrent une hausse du niveau océanique moyen, possiblement causée par la vitesse grandissante de l'ouverture des continents le lang des dorales mid-océaniques, en accord avec la tendance observée dans les isotopes du strontium. En termes de résolution stratigraphique, la pente du graphique $^{87}Sr/^{86}Sr$ pour le Lochkovien est trop faible pour être utile pour des fins de corrélation. Par contre, la peut abrupte observée pendant le Pragien, et les variations prononcées et à court terme de l'Emsien pourrait fournir une résolution stratigraphique de l'ordre de 1-2 Ma.

ACKNOWLEDGEMENTS

I would like to acknowledge the help and support of my advisor, Prof. Jan Veizer. Dieter Buhl of the Ruhr University in Germany provided the strontium isotope data, John Loop the chemical analysis, Natalie Morisset and Gilles St. Jean gave their patience and help while I learned to use the mass spectrometer and the extraction line, George Mrazek provided polished thin sections for cathodoluminescence, and Lewis Ling from Carleton University assisted with the SEM analysis. I would also like to thank Hélène De Gouffe and Sylvie Downing for all their help.

During my field season, many people assisted and guided me throughout many adventures. In Spain, Prof. Jernando Garcia-Alcalde and Prof. Isabella Mendez-Bedia led me in the field; in the Ukraine, Dr. Gritsenko and Dr. Konstantinenko guided me and a colleague down the Dniester river; in Russia, many people helped me during my two week stay, including Dr. Mizens, Dr. Ivanoff and Dr. Bikbaer who were the leaders of the expedition. Along the way Elena, Luba, Maria and Vera made the trip memorable. Thanks to all.

Finally, I would like to thank my cell mates (Karem Azmy, Johannes Barth, Ajaz Karim and Kevin Telmer) in room 208 who were always there with advice and a smile when I needed it most.

TABLE OF CONTENTS

LIST OF FIGURES

Page

Page

Page

Page

LIST OF TABLES

LIST OF PLATES

1. INTRODUCTION

The Phanerozoic Era was a time of dynamic changes, both in terms of biologic activity and solid Earth evolution. Throughout this interval, strontium, carbon and oxygen isotopic systems of the Earth hydrosphere were also evolving, often reflecting regional environmental changes or in some cases global trends.

Stable isotopes have only recently come into their own as both a stratigraphic tool and as a possible mean of determining the environmental parameters of past oceans. High resolution stratigraphy has recently been proposed as a means of achieving stratigraphic resolution of the same caliber as biostratigraphy, magnetostratigraphy and lithostratigraphy, with strontium isotopes having the highest potential. Carbon and oxygen isotopes, on the other hand, are more suited for paleoenvironmental studies. Nevertheless, the debate is still active and will probably be so for many years to come.

1.1. History

The use of strontium isotopes as stratigraphic tool began with Wickman (1948) who proposed that the $^{87}Sr/^{86}Sr$ ratio of ocean water should vary linearly with time and by measuring the $^{87}Sr/^{86}Sr$ ratio of marine sediments, it should be possible to determine their age. Over the succeeding decades, our knowledge has increased to a point where it is now known that the $^{87}Sr/^{86}Sr$ ratio is not a linear function of time, but exhibits large fluctuations (Peterman et al.,

1970; Veizer and Compston, 1974). This stage has culminated in the classic paper of Burke et al. (1982) that outlined in detail the $^{87}Sr/^{86}Sr$ ratio for the entire Phanerozoic. Subsequent development has focused on improvement of the resolution of the curve and on filling the gaps in the data set. Improved instrumentation, increased collaboration and a greatly increased data set has made this possible. The improved resolution of the curve is due to numerous factors, including improved sample selection criteria, increased instrumental sensitivity and standardization of data. The end result is that the strontium isotope reference curve is approaching the stage when it can compete with other stratigraphic tools.

The secular trend observed in carbon isotopes from marine sediments is not a hot topic in isotope stratigraphy. It is generally agreed that $\delta^{13}C$ in carbonates vary with time (Compston, 1960; Kroopnick et al., 1977 and Veizer et al., 1980). What is in contention, is the effect of biogenetic fractionation. If "vital effect" exists, how great is its effect on the chemistry of the precipitate? (Lowenstam, 1961; Adlis et al., 1988; McConnaughey, 1989; Carpenter and Lohmann, 1995).

Controversy still exists as to the causes of secular $\delta^{18}O$ trend in marine sediments. This trend can be explained by: 1) diagenetic reequilibrium (Degens and Epstein, 1962; Killingley, 1983), 2) warmer Palaeozoic oceans (Knauth and Epstein 1976; Karhu and Epstein 1986), 3) secular variations in the oxygen isotopic composition of sea water with time (Popp et al., 1986; Veizer et al., 1986; Veizer, 1992; Wadleigh and Veizer, 1992); and 4) formation of a globally stratified ocean (Railsback, 1990). For more detail, the reader is referred to Chapter 8.

1.2. Previous Work

To date, very little has been published concerning the isotopic composition of Lower Devonian carbonate samples. The existing data (Veizer et al., 1986; Burke et al., 1982; Brand, 1989a; Gao, 1992 and Lavoie, 1993) is sporadic, containing a half dozen points for strontium, carbon and oxygen isotopes. Depending on the publication, the sampled material was either the secondary layer of the shells of brachiopods (Veizer et al., 1986; Brand, 1989; Lavoie, 1993) or micrite (Gao, 1992). The Paleozoic data set of Burke et al. (1982) is based predominantly on limestone matrix, but includes also carbonate macrofossils, conodonts, dolostones and evaporites.

For strontium isotopes, the published data based on fossils and micrites shows a fairly linear trend with all points lying on or just above the Burke et al. (1982) curve. The data show a decrease from 0.7086 at the Pridoli/Lochkovian boundary to 0.7078 at the Emsian/Eifelian boundary. The existing data for carbon isotopes suggest an overall ^{13}C depletion throughout the Lower Devonian, from as high as 1.8‰ within the Lochkovian to approximately 0.2‰ in the Late Emsian. The oxygen isotope band is approximately 1.5‰ wide and ranges from about -2.5‰ for the early Lochkovian to -5.2‰ during the late Emsian.

1.3. Principal Objectives

This study aims at filling the gaps in the strontium, carbon and oxygen isotope reference

curves for Lower Devonian sea water. The principal goal of this study was to develop a high resolution strontium isotopic curve based on the best preserved shell material, in this case brachiopods collected in 4 regions scattered throughout the globe. The portion of the curve is to be integrated into a master reference curve for the Phanerozoic, currently under construction by researchers in Europe and North America. The results, integrated with the previously published data, may help understand the chemical dynamics of the coeval ocean.

Development of carbon and oxygen isotope curves for the Lower Devonian was a secondary goal, including the possible impact this may have on the issue of the primary versus secondary nature of the observed ^{18}O depletion in Paleozoic (bio)chemical sediment, if compared to their younger counterparts.

2. LOCATION AND GEOLOGY OF THE STUDY AREAS

A total of 177 samples were collected from four regions, New York State of the United States and three areas in Europe (Podolia, Ukraine; Western Urals, Russia; and Cantabrian Mountains, Spain) (figures 2-1, 2-2). The sampled strata cover a time period of 23.8 Ma, from the Pridoli (Silurian) across the Lower Devonian (Lochkovian, Pragian and Emsian) to the Lower/Middle Devonian contact. Correlations between study areas was achieved using standard global conodont biozones (Harland et al., 1990).

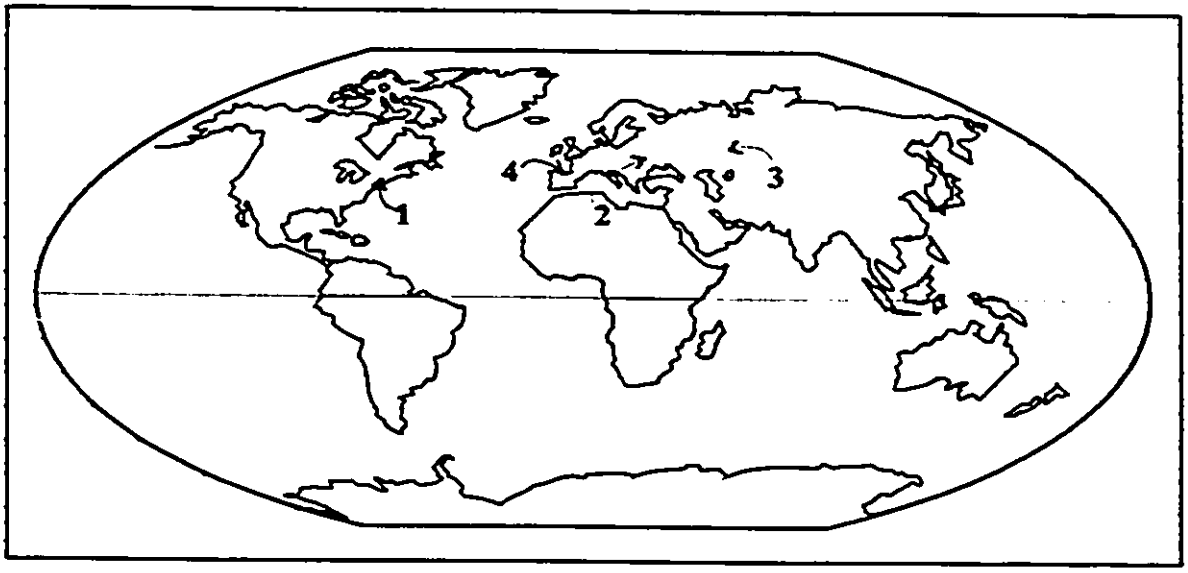

Figure 2-1. World map showing field areas. 1 New York State, 2 Podolia in the Ukraine, 3 Ural Mountains in Russia and 4) northern Spain.

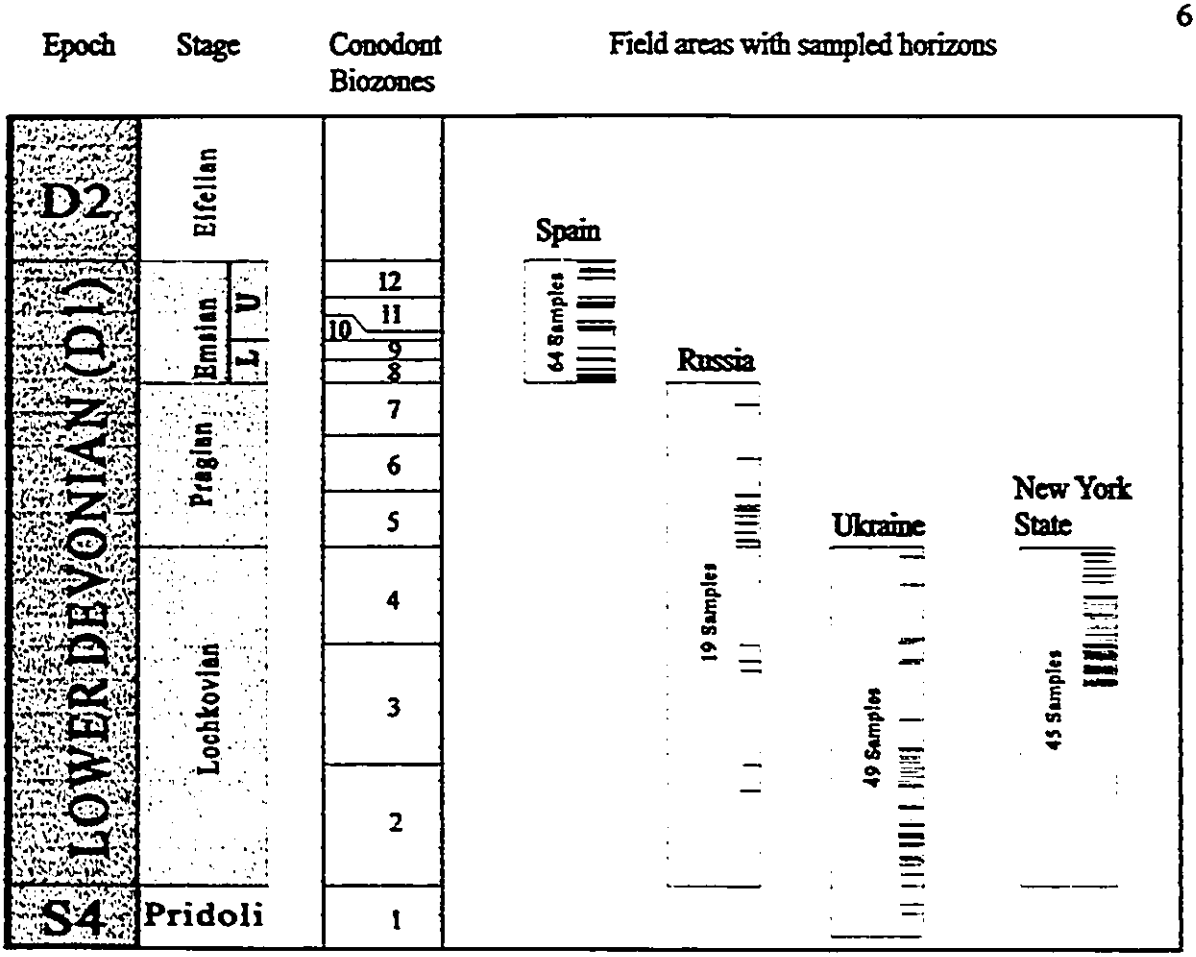

Figure 2-2. Simplified composite brachiopod sample distribution for the studied areas and 177 samples. Conodont biozones numbered 1-12: 1 *Ozarkodina r. eosteinhoznensis*, 2 *Icrinodus w. woschmidti*, 3 *Icriodus w. postwoschmidti*, 4 *Ancyrodelloides Ic. pesavis*, 5 *Eognathus sulcatus*, 6 *Sp. kindlera* 7 *sp. pirinea*, 8 *Polygnathus dehiscens*, 9 *sp. gronbergi*, 10 *sp. laticosti*, 11*?Polygnathus serotinus*, 12 *Polygnathus costatus patulus*. Conodont biozones from Harland et al. (1990) and Carls (1988).

2.1. Podolia, western Ukraine (Lochkovian)

The Lochkovian, and most of the Pridoli ,the latest Silurian, were sampled during the June 19-25, 1994 period. Forty-nine samples were collected (46 from the Lochkovian and three from the Pridoli) along the middle Dniester River in western Ukraine (figure 2-3). The region

can be reached by train, car, or bus from Kiev. Outcrops are located along both banks of the river and its tributaries and are best accessed by boat because of a poor road infrastructure with few river crossings and riverside roads.

For this study, a train was taken from the Ukrainian capital of Kiev 500 km west to the town of Chernivtsi in the foothills of the Carpathian Mountains. From there, a local bus was taken to the village of Zaleshchiki on the north bank of the Dniester River. Once at the river, two inflatable dinghies were utilized to sample 15 outcrops. Field work ended at the town of Kamenets Podol'sk, where a train was caught back to Kiev.

2.1.1. Geology

The Dniester basin of western Ukraine is ideal for this kind of study because of its easy access, well-preserved fossils and simple geology, with little or no folding thus establishing easy bed to bed correlation (Zaika-Novatsky, 1983). The beds strike approximately north-south with an average dip of 2-5° W. This, in addition to the abundance of outcrops and well-preserved brachiopods along both banks of the river, insures a good stratigraphic resolution. The sampled area can be subdivided into four formations: the Skala, Borszczow, Czortkow and Ivane. The Skala Formation is of Pridolian age while the remaining three are of Lochkovian age. The Skala Formation consists of dolomite, marls and dolostone. Limestone beds are present only in localized horizons. In contrast, the Lochkovian formations are composed mostly of interbedded limestone and shale, with minor calcareous clays and argillite in localized

horizons (figure 2-4).

The Raskov Formation of the Pridolian Skala Group was also sampled at three outcrops. Typically these beds consist of interbedded calcareous shales and limestones, often dolomitized. As a result, fossil preservation is generally poor and not reliable enough for use in this study. Only three samples were collected from this formation. One geographically widespread horizon within the Skala Formation consists of a thin bed of bentonite clay. Fossil groups found in this formation include brachiopods, tabulates, conodonts, gastropods and bivalves.

The fossil content of the Lochkovian formations decreases from the Borszczow to the Ivane Formation. The Borszczow Formation can be subdivided into three members: the Tajna, Mitkov and Bogdanov. The fossil assemblage within this formation is diverse with abundant well-preserved fossils. Brachiopod diversity decreases, from coquina in some beds of the Tajna Member to rare shells with some rare beds with abundant shells in the Bogdanov Member. Brachiopod orders include particularly Spiriferida, Strophomenida, and Rhynchonellida, but Orthida, Terabratulida and Lingulida are also present. Other fossil groups include nautiloids, ostracods, bivalves and trilobites.

The Czortkow Formation contains uncommon calcareous beds with abundant fossils that are separated by shales, the latter mostly barren. Fossil groups include nautiloids, ostracods and bivalves. Brachiopods, while present, are generally small although a few larger specimens were found, albeit not in situ.

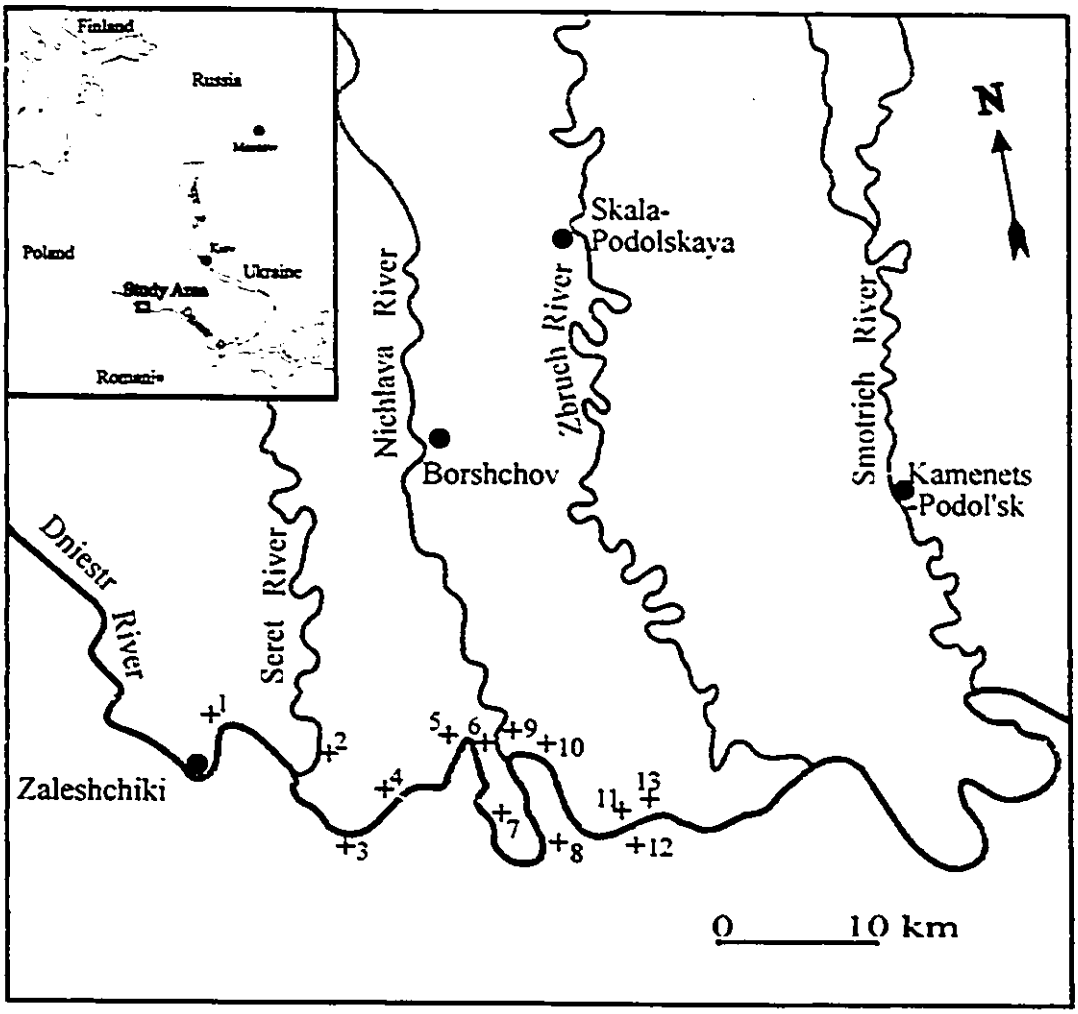

Figure 2-3. Location map for Lochkovian outcrops in Podolia, western Ukraine.

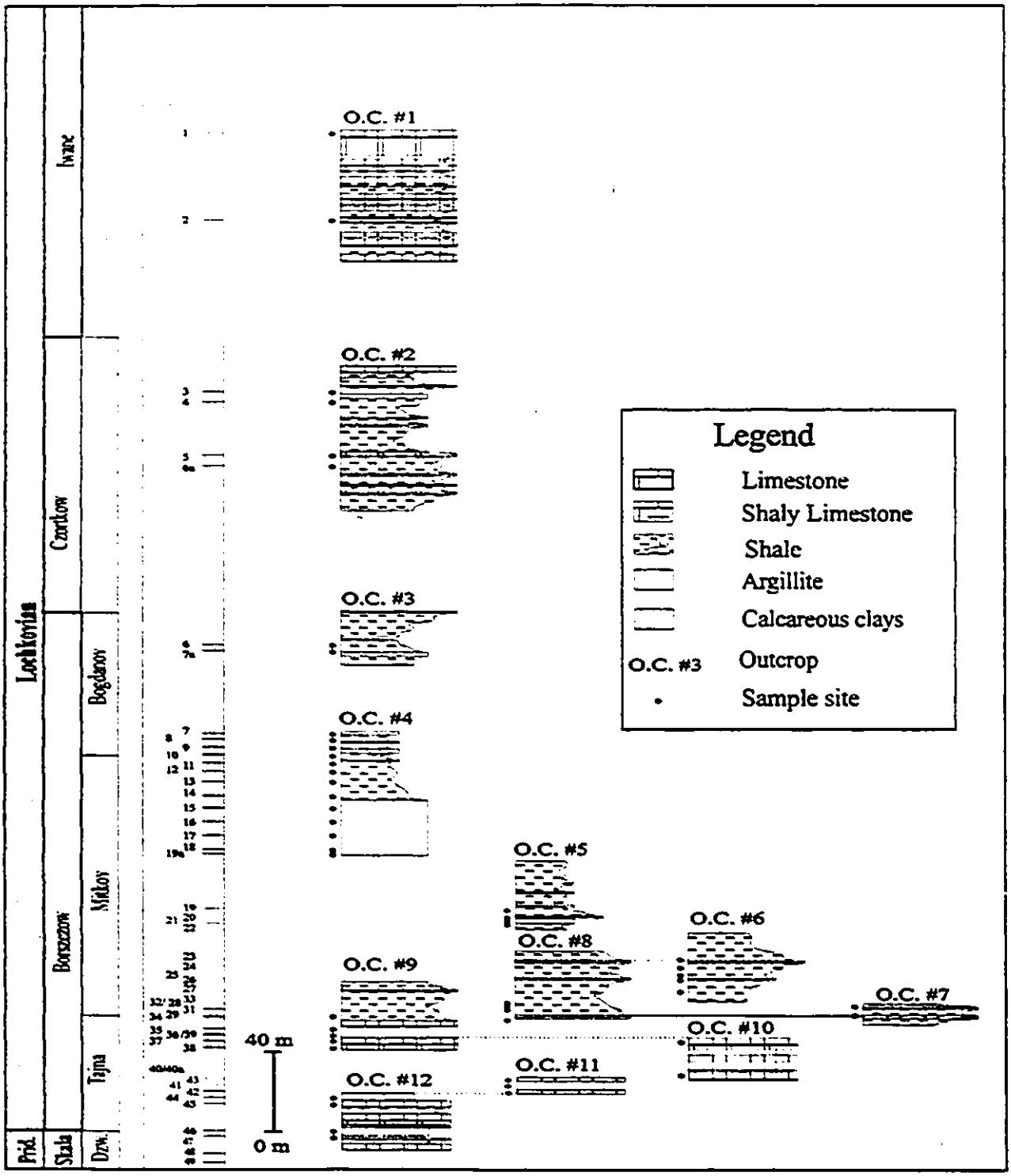

Figure 2-4. Composite stratigraphic log for the Lochkovian of Podolia. Stratigraphy by Nikiforova (1968).

The Ivane Formation has less shale and fewer fossils than the Czortkow Formation. The fossil assemblage is also similar, but trilobite and primitive fish fragments can also be found.

2.2. New York State (Lochkovian)

In the New York State, 45 samples of Lochkovian age were collected from a road cut located within the Coxsackie quadrangle, south of the city of Albany, April 23-24, 1994. The road cut is just past the underpass that runs perpendicular to interstate 81 (I-81) and is located 0.8 km east of Broncks Lake and approximately 10 km NNW of the town of Catskill (figure 2-5).

2.2.1. Geology

The road cut, striking east-west and consisting of limestone with minor shale and chert, is considered one of the best Helderbergian exposures known (Rickard, 1962). It is approximately 100 metres long on the north side of the road and incorporates five formations (Coeyman, Kalkberg, New Scotland, Becraft and Alsen). Samples were only collected from the New Scotland, Becraft and Alsen Formations (figure 2-6). The road cut shows moderate folding with the strikes ranging from 15 ° at the western end to 20 ° at the eastern end of the exposure. Dips increase eastward from 24 °W to a maximum dip of 49 °W.

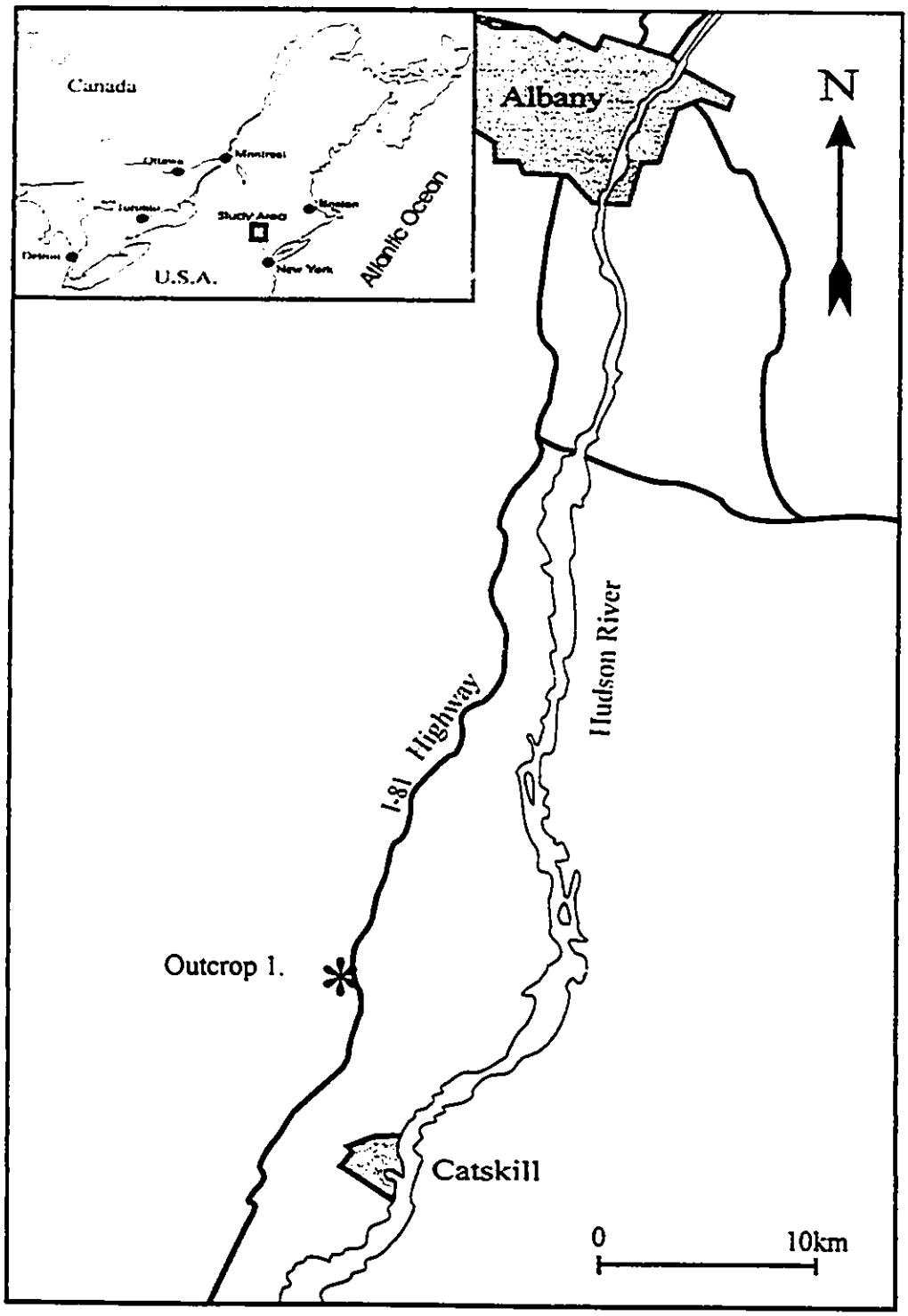

Figure 2-5. Sample locality for the Lochkovian of the New York State.

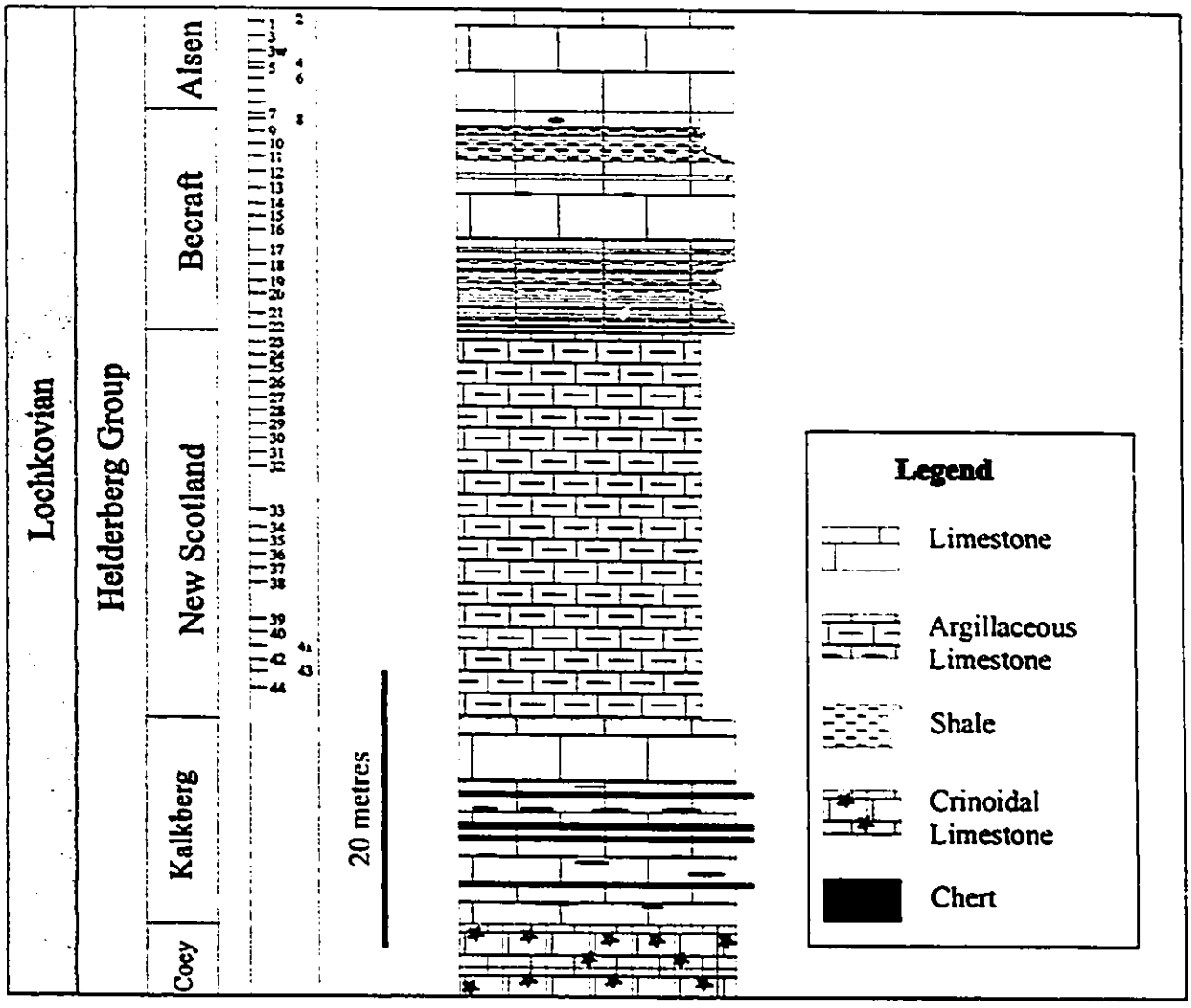

Figure 2-6. Stratigraphic section for the Lochkovian of the New York Helderburg Group. Stratigraphy by Rickard (1962).

Coeymans and Kalkberg Formations

The Coeymans and Kalkberg Formations were not sampled for this study and are included just for completeness. Only the Ravena Member of the Coeymans Formation is present at the Broncks Lake road cut. It forms medium grained massive grey limestone. Brachiopods are rare. The Kalkberg is composed of mostly medium grained limestone with medium to massive bedding. Minor chert exposed as thin beds and nodules up to 10 cm long can be found throughout this formation. Fossil content varies from abundant in the bottom 7 metres to rare in the upper part of the formation.

At Broncks Lake, the Coeymans Formation is 5.15 metres thick and the Kalkberg Formation is 10.30 metres thick. The Kalkberg formation is exposed for approximately 3 metres at the easternmost end of the road cut while the remaining 7.3 metres of the Kalkberg and all of the Coeymans Formation is located along I-81, just north of the underpass.

New Scotland Formation

The New Scotland Formation is composed of argillaceous fine to medium grained limestone with a characteristic shaly weathering profile. The thickness of the formation is 27.88 metres and this represents the thickest New Scotland exposure in the Helderbergian Group.

The New Scotland Formation has few fossils with some beds completely devoid of any

specimens. Generally, the fossils consist of brachiopods, gastropods and crinoids with rare trilobite fragments. The brachiopods are usually small and occur mostly in the same beds.

Becraft Formation

The lower contact of the Becraft Formation with the New Scotland Formation is gradual, with the argillaceous fine to medium grained limestone of the New Scotland Formation gradually changing into inter-layered green shale and limestone. The massive, weathering resistant nature of the upper Becraft produces a characteristic extruding block which overlies the lower Becraft and New Scotland Formations. The lower half of the Becraft formation is composed of thin green shale layers that become less numerous towards the top. The highly resistant cap is composed of massive coarse grained pink crinoidal limestone. At Broncks Lake, the thickness of the Becraft Formation is 16.06 metres.

In the shaly lower half of the Becraft Formation, fossils are common and tend to be dispersed on limestone bedding surfaces, with brachiopods the dominant group. The upper Becraft Formation is a coquina, composed almost exclusively of crinoidal segments and brachiopods. The brachiopods occur mostly as well preserved separated Spiriferida and Strophomenida valves. Some shells have been recrystallized, form coarse grained sparry calcite moulds and partly infilled vugs. Gastropods are a minor component of the coquina.

Rickard (1981) believes that the Becraft Formation represents a shallow high energy sub-

tidal environment. While this may be true for the upper portion of the formation, the lower half with its high shale content was more likely deposited in a quieter shallow water environment.

Alsen Formation

The contact of the Becraft Formation with the overlying Alsen Formation is abrupt, from the pinkish coarse grained massive crinoidal limestone of the Becraft Formation to a blueish grey medium to coarse grained layered limestone. The thickness of the Alsen Formation at Broncks Lake is 7.27 metres. Minor black chert is also present as thin beds and nodules. The weathering surface is generally yellowish brown with some beds having localized rust stains possibly due to assessory iron minerals. It should be noted nevertheless that no pyrite was observed either in the field or in thin sections. The limestone beds range in thickness from 1-20 cm, with the thicker beds predominant.

Fossils in the Alsen Formation include abundant brachiopods that occur as separated valves, crinoid stem segments, gastropods, and digitate bryozoans. The brachiopods, most important to this study, were mostly from the Spiriferida and Strophomenida families. No coupled valves were observed and this, together with lithology, suggests a moderately shallow sub-tidal environment, possibly at or near the wave-base (Rickard, 1981).

2.3. Western Ural Mountains, Russia (Pragian)

The western Urals were sampled for brachiopods over a four day period, July 6-10, 1994. Nineteen samples were collected from three outcrops covering the Lochkovian, Emsian and particularly the Pragian. Three other outcrops were visited, but sampling was not done due to the poor quality of the samples and/or stratigraphic resolution problems and correlation ambiguities. The best access is from Yekaterinburg, an industrial city located on the eastern flank of the central Ural mountains, approximately three flight hours east of Moscow. From Yekaterinburg, the outcrops (figure 2-7) were reached using local roads and tracks in a large military all terrain truck and an inflatable boat (for location #4).

2.3.1.Geology

The sampled field area is located along the western slopes of the Ural mountains within the 2000 km long Uralian fold belt. This belt was formed mostly during the Late Paleozoic Variscan orogeny. It can be divided into a series of longitudinal structural zones known as megazones. The studied area is located within the West Uralian Megazone (Kirel Ivanoff, unpublished) and is composed of thick Middle to Late Paleozoic shallow water sediments. These include reefal and layered limestones as well as some detrital quartz units.

Outcrop #1 (figure 2-8) is located on the Ufa river near the village of Tabulska, approximately two hours or 50 km west of Yekaterinburg. The outcrop is a sporadic series of

exposures overlooking the right bank of the river for a few hundred metres and can only be reached by a four-wheel drive vehicle or by a long hike through the taiga and wetlands. It is composed of massive reefal and layered grey limestone with rare thin shaly units. Near the base of the outcrop, is a unit with massive allochthonous blocks of reefal limestone embedded in thinly layered limestone. While brachiopods were present in these blocks, they were not sampled because they could not be accurately placed within the stratigraphic column. Most of the brachiopods at this location occurred within the last 20 metres of the massive reefal limestone. However, within the reefal limestone, there were areas which showed diagenetic alteration in the form of vugs and veins filled by sparry calcite. In addition, some brachiopods appeared to be completely recrystallized. These were not sampled. Other fossils found at the outcrop include bivalves, trilobite fragments, tabulate corals and some bryozoans.

The second outcrop is located 2 km west of the village Tabulska, two hundred metres off the trails. The exposure is small, approximately 20 metres long and a few metres high. This outcrop is lithologically similar to the first location, with massive reefal and coarse layered grey limestone. This location also contains what local geologists consider to be a neptunian dyke, a fine mud unit which appears to extrude through the limestone. Fossils include massive corals, brachiopods, gastropods, crinoidal stalk segments and bivalves. Brachiopods, while not as abundant as at the first outcrop, are dispersed throughout the layered limestone unit. The reefal limestone unit does have rare brachiopods but they were very difficult to remove. In addition they also appeared altered.

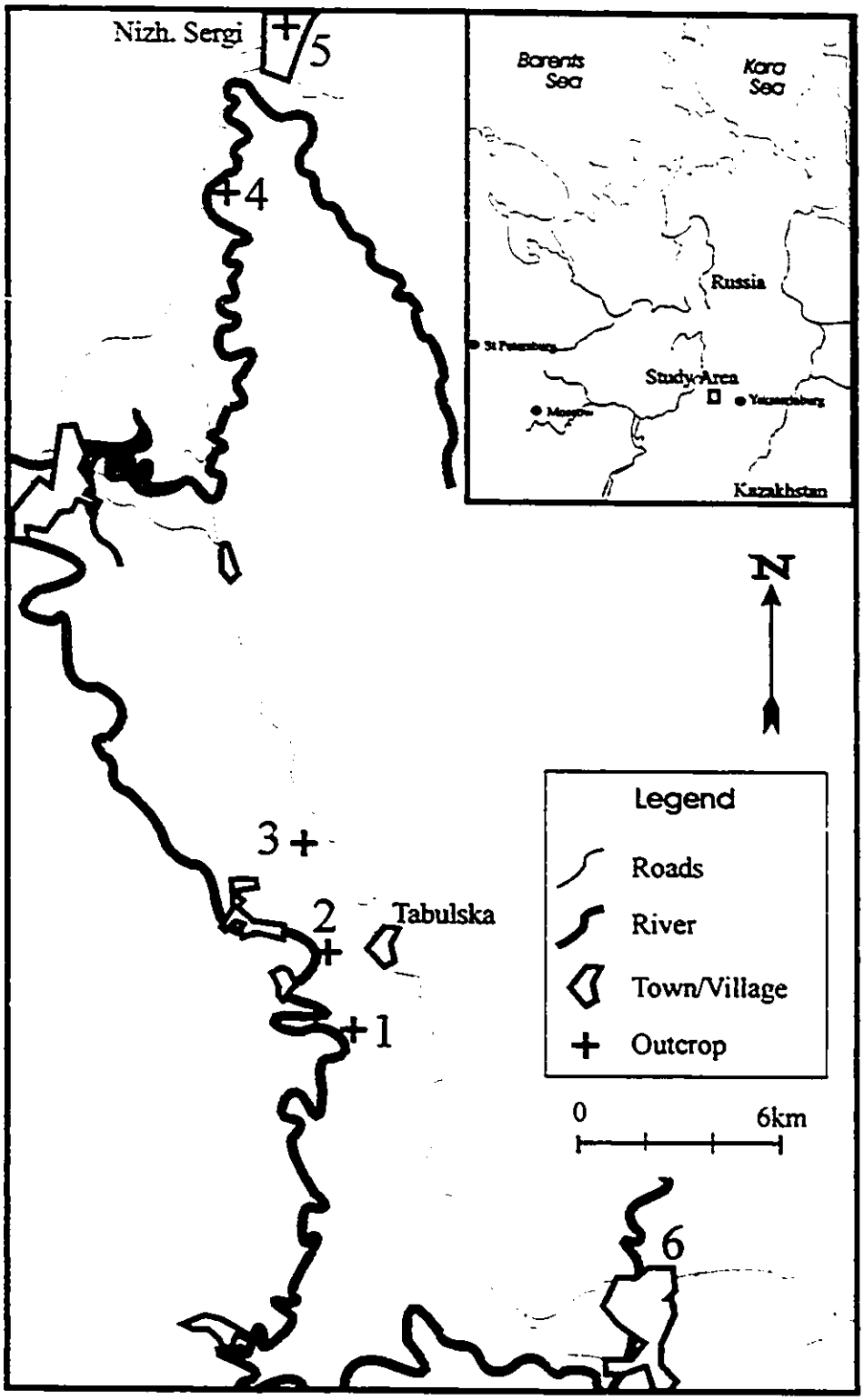

Figure 2-7. Location map of outcrops sampled on the western slopes of the Ural mountains, Russia.

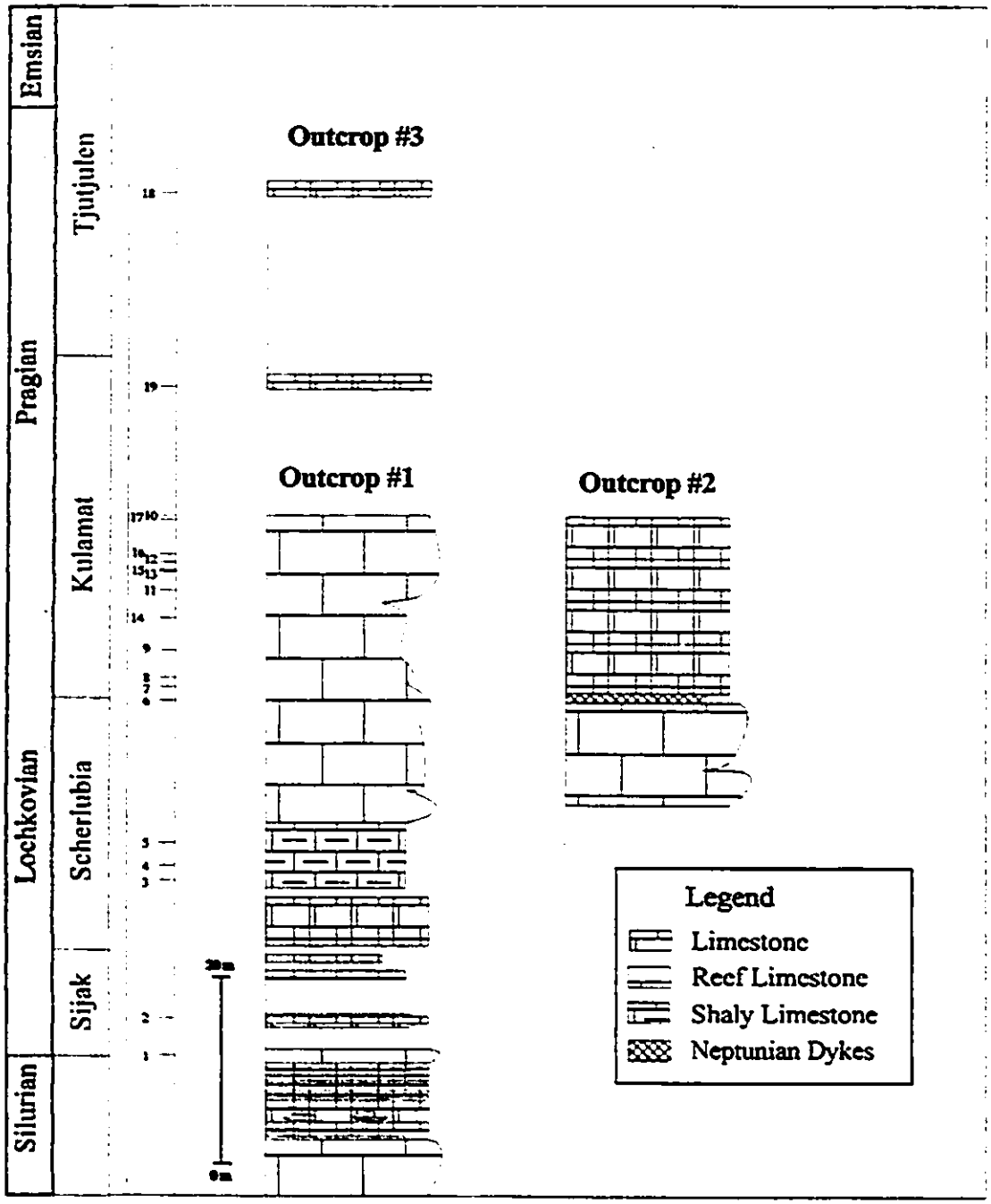

Figure 2-8. Composite stratigraphic section for the Russian Ural mountains (Pragian). Stratigraphy by Alexander Bikbaer (unpublished).

The fourth outcrop sampled is located 2.5 km south of the town of Nizhnij Sergi on the east bank of the Ufa river. A boat is required to reach the outcrop since the river is deep and flows swiftly. The outcrop was composed of massive reefal and layered grey limestone, with the latter somewhat dolomitized, that had very few brachiopods, often with signs of alteration. Only two relatively good samples were collected and even these only poorly placed stratigraphically. As a result, they were placed in the middle of their conodont biozone (figure 2-8, samples 18 and 19).

Outcrops 3, 5 and 6 (figure 2-7) were not sampled due to abundant dolomitization and few brachiopods. In addition, the stratigraphy of these outcrops was poorly constrained. Strata from these outcrops were only weakly correlated with the regional biozonal system.

2.4. Leon and Asturia region, northern Spain (Emsian)

Sixty-four samples from four outcrops spanning the Emsian were sampled over 6 days, May 15-21, 1994 (figure 2-9). Three outcrops yielded well-preserved brachiopods, while the coastal outcrop (No. 1) produced abundant but predominantly altered samples. The study areas are easily accessible by car and well exposed along roadways and coastal cliffs. Outcrop number one is located on the rocky east coast of Santa Maria del Mar Bay, approximately 10 km, or 15 minutes drive, from the town of Gijon. This location is the type locality for the La Ladrona Formation which is exposed as a low cliff best sampled at low tide. The second outcrop is located just east of the village of La Vid, approximately 20 km or 20 minutes north

of the town of La Robla. In order to reach the outcrop, it is necessary to drive east through the village and head uphill for about 2 km until a large road cut, exposed on the left, is reached. This outcrop is the type locality for the La Vid Group. Outcrop number three is a road cut exposed along the side of a factory on the outskirts of the village of Santa Lucia. The latter is located approximately 15 minutes north of La Robla, off highway 630. Access to the lower one third of the outcrop requires permission from the manager of the plant. This outcrop is the type location for the Santa Lucia Formation. The fourth outcrop is located approximately 40 km east of La Robla in the village of Collé. It is exposed on a low hill directly below the village church.

2.4.1. Geology

The geology of the Leon and Asturia region of the Cantabrian Mountains of northern Spain is structurally complex. The Devonian is exposed only as a small Variscan axial depressions and outcrops in small uplifts surrounded by the Late Paleozoic and Mesozoic strata (Carls, 1988). Lithology of the Devonian is typically Rhenish, composed chiefly of intertidal and shelf siliciclastic and carbonate rocks.

The Lower Devonian of the region has undergone Variscan (Asturian and also probable Sudetic) faulting and folding (Carls, 1988). The structurally complex nature of the region also caused mobilization of silica, manifested as quartz vein swarms and recrystallized fossils. Particularly true for the coastal sections (i.e. outcrop 1), this typically renders fossils from these localities useless for high resolution stratigraphy. In the interior, the effect is not as pronounced

due to generally low to moderate metamorphism, with most sedimentary structures and fossils well preserved. This is especially true for the second to fourth outcrops, with little to no apparent metamorphism and with fossils showing no obvious alteration features. A composite stratigraphic column for the sampled Emsian of Spain can be seen in figure 2-10. For a more complete description of geology the reader is referred to Carls (1988), Alonso et al. (1991) and Garcia Alcalde (1992).

La Vid Group

The La Vid Group can be divided into four distinct formations (Felmin, La Pedrosa, Valporquero and Coladita). The middle two were sampled at the type locality (outcrop 2) and the Coladita Formation at Collé (outcrop 4). The Felmin Formation, which covers the Pragian and Lochkovian, is also present but it is completely dolomitized. It was therefore not sampled. At the type locality, the beds strike east-west at an average dip 60° north. At Collé, the beds are much flatter, striking close to east-west at a dip of 5-10° north.

The La Pedrosa Formation is 89 metres thick and is composed of coarse interbedded limestones and shales. The limestone beds range in thickness from 5 cm to approximately 1 metre. A thin brittle fault runs through the La Pedrosa Formation at the La Vid location, causing a vertical displacement of approximately 10 metres. Fossils are abundant ranging from brachiopods, bryozoans, bivalves, crinoids, gastropods, nautiloids, conodonts, and corals.

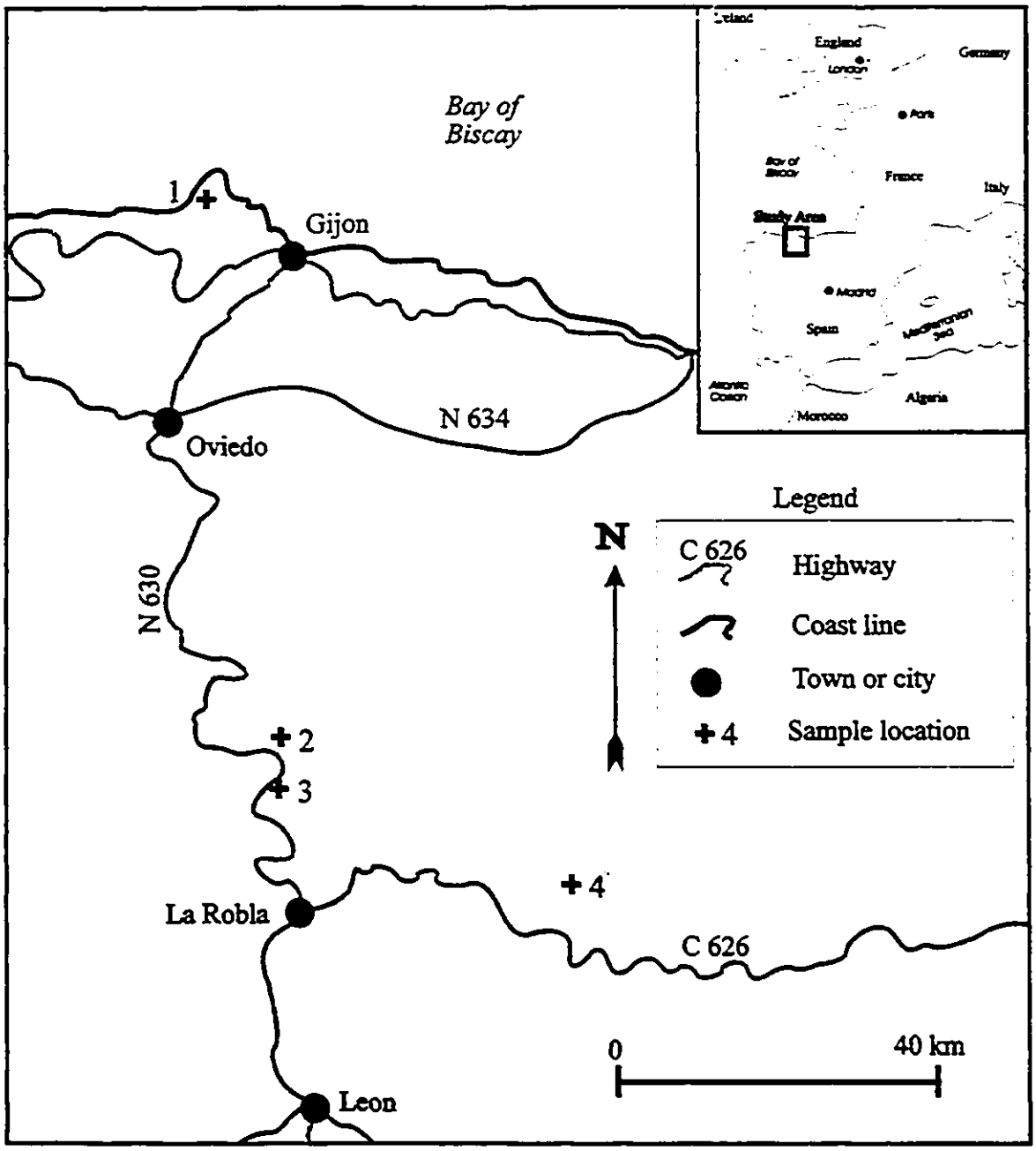

Figure 2-9. Location map for Emsian sample localities in northern Spain.

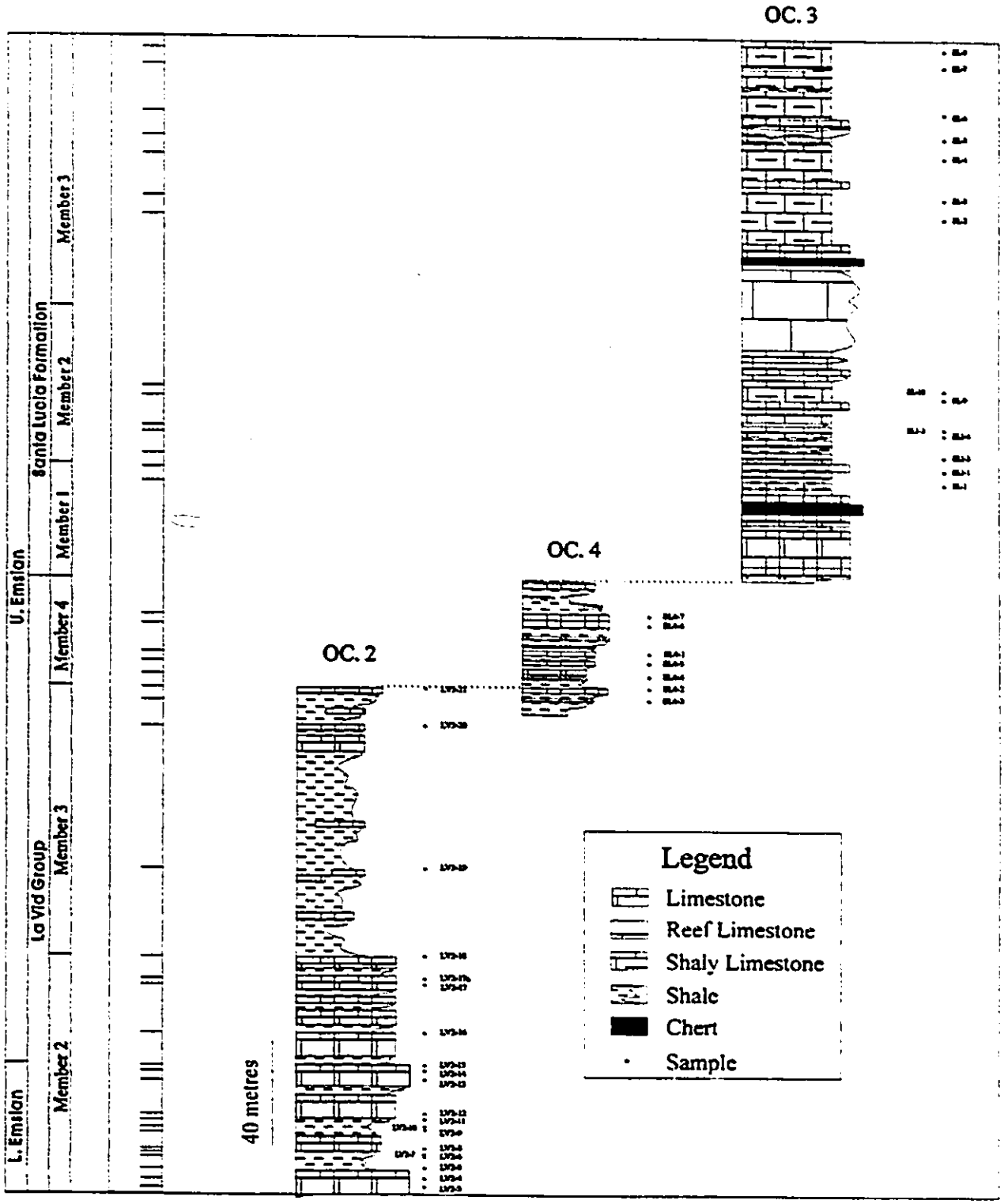

Figure 2-10. Composite stratigraphic log for the Emsian of the Leon region, Spain. Stratigraphy for OC.2 and 4 by Garcia Alcalde (1986), OC.3 by Menendez-Bedia (1976).

At the type locality the Valporquero Formation is 100 metres thick and is characterized by its high shale content and a regressive, crumbly nature. More resistant limestone lenses and thin beds, while present, are not common but they tend to focus fossil accumulation. Dominant fossil groups include brachiopods, crinoids, bivalves, trilobites, gastropods, nautiloids and conodonts.

The Coladita Formation at the village of Collé (outcrop 4) is 41 metres thick and is composed of interlayered coarse grained crinoidal limestone beds, up to 1 metre thick, and of shale. Generally, the regressive nature of the shale results in only more resistant limestone beds being present at the surface. A characteristic feature of this formation is its reddish rust colour. Fossils are very abundant, with some beds considered coquina. Fossil groups include corals, brachiopods, bivalves, crinoids, blastoids, gastropods and conodonts. At the Collé location, a digitate rugosan biostrome occurs 23 metres below the top of the formation. This location is also noted for its exceptionally well preserved and common blastoids.

Santa Lucia Formation

The Santa Lucia Formation can be divided into four members, all present at the type location (outcrop 3). Fossil are not as common as in the La Vid Group. In addition, the frequent massive nature of the formation often makes sampling difficult. The first three members fall within the Emsian while the last member is of Eifelian age. The Santa Lucia Formation strikes consistently east-west with an average dip of 80° north. Also present at this location is part of

the uppermost portion of the Coladita Formation, but it contained no brachiopods.

The first member is composed of dark grey coarse grained crinoidal and massive limestone beds with uncommon shale layers near the contact with the second member. A chert layer is present in the middle of the member. The thickness of this member is 44 metres and its dominant fossil groups include corals, brachiopods, trilobites, bivalves, bryozoans and conodonts.

The contact of the first and second member is gradual, with shaly limestone beds slowly giving way to massive biohermal limestones. The thickness of the second member is 60 metres, with the last 26 metres capped by a distinctive massive biostrome. Fossils found in the lower half of the member include mostly corals and stromatoporoids, with some brachiopods, crinoids and conodonts. The capping biostrome is mostly monospecific, composed chiefly of tabulate corals. Brachiopods were not observed in this part of the member.

An abrupt transition characterizes the contact of the second and third member of the Santa Lucia Formation. The third member is composed chiefly of coarse grained limestone with rare shale layers in the upper half. A chert layer is located near its base. This member is approximately 80 metres thick at the type locality. Lithologically, crinoidal limestone dominates, but in some beds crinoids are subordinate to tabulate corals. Other fossil groups include brachiopods, bryozoans, bivalves and conodonts.

The Eifelian contact is located at the border of the third and fourth member. The contact is abrupt, with shaly coral rich limestone passing upward into massive crinoidal limestone. For the upper 25 metres, dolomite dominates. Crinoidal stalks make up the majority of the fossils. Brachiopods, while present, are typically small and very difficult to extract. No samples were analysed from this member.

3. METHODOLOGY

Diagenesis is the single most important post-depositional factor influencing the isotopic and trace element composition of brachiopod shells. Many optical and chemical techniques have been developed to determine shell preservation, often being used in conjunction in order to obtain the most reliable information. For a detailed description of the procedures performed on the samples in this study the reader is referred to Appendix A.

3.1. Separation of shell material

The first step is to isolate shell material from the host rock in order to remove possible contamination from the matrix. There is a plethora of methods used today to achieve this, with three of the more common being: 1) Removal of the matrix material manually under a microscope utilizing stainless steel dental burs. Once the visible material has been removed, the sample is cleaned in an ultrasonic bath with deionized water and then placed in a solution of diluted HCl (15%) in order to remove any remaining foreign material (Brand, 1989a; Wadleigh and Veizer, 1992); 2) The second method involves placing approximately 10 kg of material into an organic solvent for 24 hours, followed by soaking in tap water for 24 hours. Any remaining material is sieved through two sieves of mesh 850 and 125 μm (Grossman et al., 1993). This may be the best method for extraction of small brachiopods, although the increased chemical treatment jeopardizes the potential for trace element and isotopic studies; 3) The third method involves crushing small blocks of material to 1-2 mm sized fragments. Material from

the secondary layer of the shell is then manually removed and cleaned in 250 ml. of distilled water (Diener et al., 1996). This may be the best method and it was used in this study. Methods that use micro drilling have been shown by Diener et al. (1996) to often include some contaminated material, probably from the inadvertent incorporation of matrix and/or of altered material.

3.2. Optical techniques

Optical criteria used to determine shell preservation include optical microscope, scanning electron microscope (SEM), and cathodoluminescence (CL) techniques. Under standard microscopes and SEM an unaltered shell should show distinctive internal shell fabrics (see section brachiopod shell structure). If the second fibrous layer is not present or not well preserved, or its sections appear recrystallized, then the pristine nature of the sample should be questioned. If the sample does show good internal structure then the sample may be tested under CL to see weather any of its domains show luminescence.

Textural preservation of the shells was checked using a standard binocular microscope. Secondary checks were done using both SEM and cathodoluminescence. For the SEM work, samples were coated with an Anatec Ltd. spatter coater set in order to cover the sample with 100 Angstroms of a gold/palladium dust mixture. The SEM instrument was a JEOL 6400 digital scanning electron microscope at the Department of Geology, Carleton University. Samples were scanned at 3000X magnification and at a setting of 15 kV. The best samples were photographed

using a Polaroid camera. In addition, the same images were digitized and imported into Corel Photoshop. Video images were also taken. A Nikon Technosyn cold cathode luminescence microscope, model 8200 MK II at the Department of Geology, University of Ottawa was used for cathodoluminescence on a few samples. Thin sections were polished to 30 micrometers.

3.3. Chemical techniques

Chemical techniques commonly used to determine secondary shell preservation are microprobe, atomic absorption spectrometer (AAS), and inductively coupled argon plasma atomic emission spectroscopy (ICP) analysis. Microprobe analysis is done using specially prepared thin sections. AAS and ICP techniques require micro sampling of the shell or its splinters have to be powdered.

The instrument used for the carbon and oxygen isotope analysis in this study was a Triple collector VG SIRA 12 mass spectrometer at the Department of Geology, University of Ottawa. Routine precision (2σ) on pure carbonate was 0.10‰. The reference gas used in the analysis was calibrated against the international calcite standards NBS-18 and NBS-19. CO_2 was generated by reaction of sample with 100% phosphoric acid. The ^{18}O fractionation factors used for carbonate-H_3PO_4 recalculations is α=1.01025 (Sharma and Clayton, 1965; Friedman and O'Neal, 1977).

The ICP machine used for the major and trace element analysis was the Thermo Jarrell

Ash ATOMSCAN 25 spectrometrer, an inductively coupled argon plasma (ICPA) spectrometer. Internal standard run with the samples were LMS1-3. Internal instrument standards were WATMET, CA500 and WATMAJ.

Precision was calculated as (2 X standard deviation) whereas, accuracy (Accuracy= $[ICP_{results(ave)}-XRF_{results(ave)}/XRF_{results(ave)}]$ X 100) was calculated from comparison with the recommended values for the internal standard LMS1-3 (table 1.). These recommended values were established by XRF on whole rock samples that contains 3% insoluble residue. They are therefore not directly comparable to the concentrations measured by ICP on the acid soluble portion. Since the precision for the ICP results are reasonable, I elected to accept the ICP values for Major and trace elements with the exception of Fe and Ba. The latter two elements may include contamination, probably introduced during the reaction vessel drying procedure (see appendix 1). Fe and Ba were therefore not utilized as criteria for selection of samples.

Element	Machine detection limit (mg/l) (ICP)	XRF values	LMS Average (ICP)	LMS standard deviation	Precision (+/-)	Accuracy %
Ca	0.01	38.99	39.09	0.001	0.0020	0.003
Mg	0.01	0.18	0.21	0.0002	0.0004	0.17
Ba	0.002	(18)	28	7	13	13
Fe	0.05	559	1090	166	332	95
Mn	0.002	286	331	24	48	16
Sr	0.002	436	500	27	54	15

Table 1. Detection limit, precision and accuracy for major and trace element measurements on ICP. Ca and Mg measurements in percent, Ba, Fe, Mn and Sr measurements in ppm unless otherwise stated in column heading. The XRF value for Ba is in the vicinity of the detection limit of the technique.

Strontium isotopes were analysed following procedures developed by Buhl et al. (1991). Samples were analysed on a Finnigan MAT 262 5-collector solid source mass spectrometer at the Institut für Geologie, Ruhr University. 0.5 to 1 mg of samples were dissolved in 5 ml of 2.5 N supra pure HCl. The samples were left to evaporate for a minimum of 2 hours at 25 ° C. Strontium extraction was accomplished using quartz glass exchange columns filled with Bio Rad AG50Wx8 ion-exchange resin. Strontium was flushed from the columns using 2.5 N supra pure HCl, dried, then loaded on single Re filaments after Birck (1986). The average total blank never exceeded 8.5 X 10^{-3} ng/g Sr. Standard reference material included NBS 987 and USGS EN-1. The average of 550 NBS 987 measurements over the 4.5 years interval was 0.710231 ± 3.8 X 10^{-5} (1 standard deviation) and for 130 measurements of EN-1 it was 0.709145 ± 3.2x 10^{-5} (1 standard deviation). The results were not corrected for Rb. $^{87}Sr/^{86}Sr$ ratios were normalized to $^{86}Sr/^{88}Sr$ of 0.1194. The 2σ (mean) error for a single sample was within 6-40 X 10^{-6} range, with an average of ± 9 X 10^{-6}. Each run was normalized to the long term mean for NBS 987 of 0.710231 (Diener et al., 1996).

4. THE COMPLETENESS OF THE STRATIGRAPHIC RECORD

At a glance, the distribution of sedimentary rocks on the Earth surface is not uniform. Some areas are covered by thousands of metres of sedimentary rocks while others have very little or no coverage. In addition, a correlation exists between calculated outcrop area and the age, with older rocks covering lesser area than the younger ones (Figure 4-1). Uniformitarian principles assume that physical, chemical and biological laws operating today were also in effect in the past and that the rates and intensities of geological processes were constant with time. Using this approach, early researchers arrived at incorrect dates of between 19 Ma and 1.5 Ga for the age of the Earth (Schoch, 1989). Most modern researchers realize that uniformitarian principles cannot be applied in this crude way. While physical, chemical and biological laws probably have held true through time, rates and intensities have varied.

In order to quantify the stratigraphic record, it is first necessary to understand sedimentation and the various controls influencing both deposition and syn/post depositional erosion. In addition, the effect of diagenesis must be assessed. The history of a given sequence, from sediment deposition through non-deposition and erosion to diagenesis must be determined in conjunction with resolution effects (acuity) and human biases. Only with a complete picture will geologists be able to approach with confidence the absolute completeness of a given sequence. Such a detailed account is not yet possible, and probably will not be for the foreseeable future, but with improvements in methodology and an increased understanding of the principles the gap between the calculated and actual completeness of a section may be

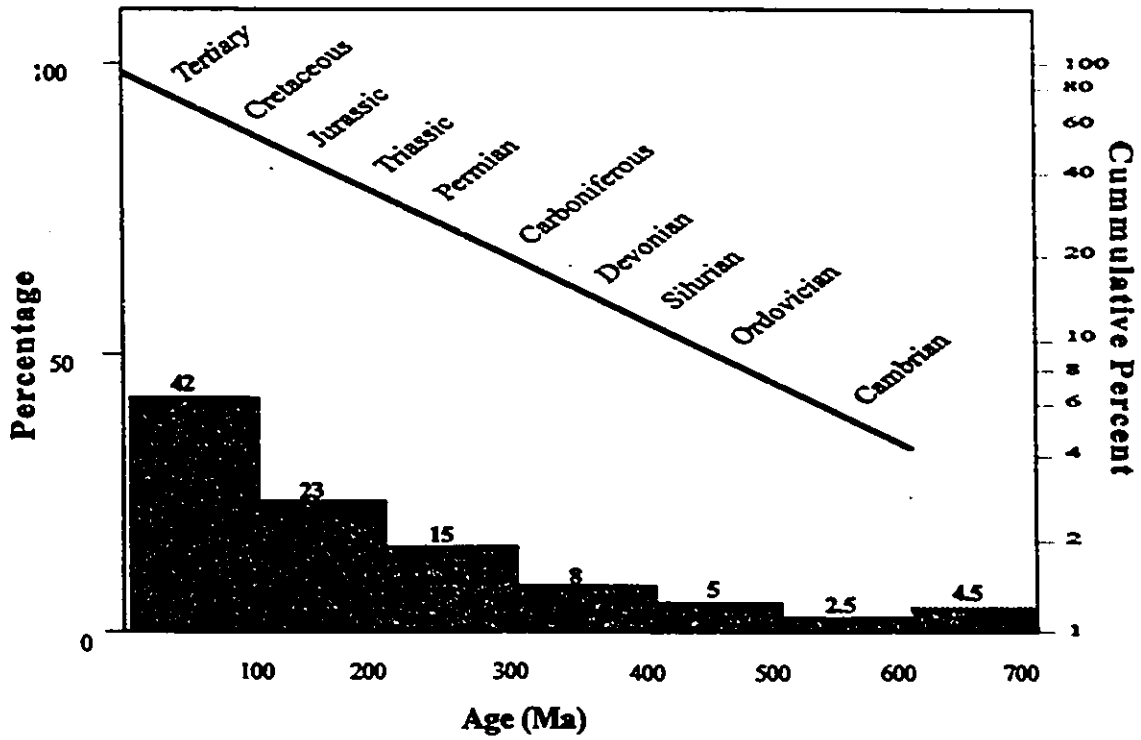

Figure 4-1. Relationship between sedimentary rock age and amount of outcrop area. Adapted from Blatt and Jones (1975).

closing.

This chapter will focus on the dynamics of sedimentation and diagenesis and how these complex processes influence the completeness of the geological record. Limitations for the most common methods used to define and correlate sedimentary sequences will also be discussed.

4.1. Measured rates of sedimentation

Stratigraphic incompleteness is primarily the result of the episodic (Markovian) nature

of sedimentation (Schindel, 1982). Sedimentation is a discontinuous process related to climatic and tectonic fluctuations as well as to the dynamics of the depositional process (Sadler, 1981; Schindel, 1982; McShea and Raup, 1986). In most environments, periods of sedimentation are balanced against periods of sediment removal. If net deposition is greater than net removal, then sediment will accumulate to eventually become sedimentary rock. On the other hand, if the reverse is true, then erosion will occur.

In figure 4-2, a comparison of sedimentation rate versus the time span of observation is shown for seven environments. What immediately becomes apparent is that the various

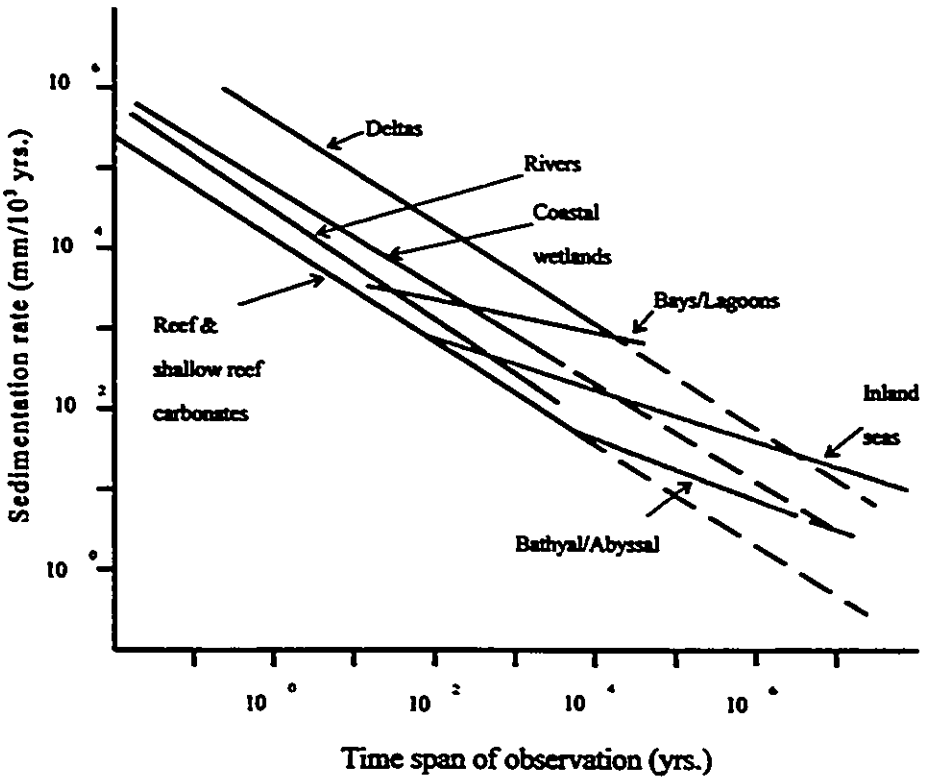

Figure 4-2. Log-log plot of sedimentation rates versus the time span of observation over which each rate is calculated. Dashed lines are extrapolated total ranges. Modified from Schindel (1982).

environments fall into two groups, each with similar slopes. These slopes represent the completeness retaining ability of each environment, with the lesser slopes corresponding to a greater retention ability. In other words, bays, lagoons, inland seas, and deep ocean, which are low energy and relatively stable environments, will in general have a greater chance of preserving a more complete record. In contrast, high-energy, typically shallow water environments, such as deltas, rivers, and reefal complexes have a relatively steep slope. These environments are less likely to preserve the sedimentation record. Another feature of figure 4-2 is that the two groups fall within characteristic time spans of observation, in part due to the sedimentation rate for each environment.

Superimposed on this record is an overprint. In some environments, rare (hurricane) and/or cyclic (seasonal floods) events dominate sediment deposition. These events typically redistribute the "every day" sediments, overprinting them with these higher energy events. For example, in some sequences, storm deposits have accumulated into formations of 10's to 100's metres thick, destroying the temporal slow "day to day" accumulation signal and replacing it with uncommon or rare high yield events. These may occur at any given location once or twice a year or, as in the instance of hurricane deposits, on the order of once every three thousand years (Sadler, 1981). This non-uniform sediment accumulation with time and place has a serious repercussion when determining the long term accumulation rates. Only in environments where there is stability in the geomorphic and environmental processes does sedimentation approach a continuous process. In some deep sea pelagic environments, where deposition proceeds very slowly and erosional and non-depositional processes are less frequent,

there is the potential for sedimentation to proceed undisturbed for what may become geologically significant periods of time (Ager, 1981). However, even in these rare stable environments the resulting sequence will probably not be complete. Post-depositional increases in pressure and temperature will produce loss of material through physical and chemical diagenesis.

Sedimentation is not only a temporal non-uniform process, but can also vary laterally within a given sequence. Most deposition appears to nucleate at one or a series of points and tends to build out sideways to form wedges, such as deltas (Sadler, 1981). The end result is that the accumulated thickness may vary markedly for a given time period (figure 4-3). Depending on the location, sedimentation rate may also vary dramatically within a given sequence, often resulting in a non-uniform thickness to the unit that is not due to erosional processes. This implies that any accumulation will vary markedly in space and time (Meshea and Raup, 1986) and that the range in accumulation rates can vary by several orders of magnitude even within the same environment and sediment horizon.

Measured rates based on active sedimentation have obvious limitations because these rates are often determined syn-depositionally and therefore do not take into account the effect of compaction and benthic mixing (bioturbation). In addition, rate measurements are based on radiometric dating which has unsystematic associated errors, the latter decreasing precision.

4.1.1. Human biases

The way geologists choose to measure accumulation rates has a direct effect on how stratigraphic completeness is perceived. Typically, accumulation rates are measured by one of four ways. These are: a) continuous observation, b) reoccupation of survey stations, c) radiocarbon dating, d) by biostratigraphic techniques coupled with K/Ar radiometric dating, each with its own associated errors (Mcshea and Raup, 1986). This is apparent in figure 4-4 where a compilation of 25 000 rates versus time spans were plotted (Sadler, 1981). The black regions represent the four techniques researchers use to collect data. Continuous observation (a) is characterized by short duration, whereas biostratigraphy coupled with radiometric dating (d) can only be useful for rates with time spans controlled by the resolution of the method. The data on accumulation rate is in essence being moulded by the observation technique and not by nature. If figure 4-4 reflected natural processes, then the diagram, while retaining the same slope, would not show patchy black regions but instead be characterized by a single sloping patch which decreases concentrically towards the periphery.

Determining the sampling scale has important repercussions on the perceived completeness of a section. Scales are typically artificially derived by the researcher and do not accurately represent the true nature of the record. The finer the time scale, the more accurate and less complete the section will be perceived to be regardless of the geological period. On the other hand, Anders et al. (1987) felt that sampling on fine scales was prone to too much accumulation rate variability. At larger scales, completeness is more likely to be achieved,

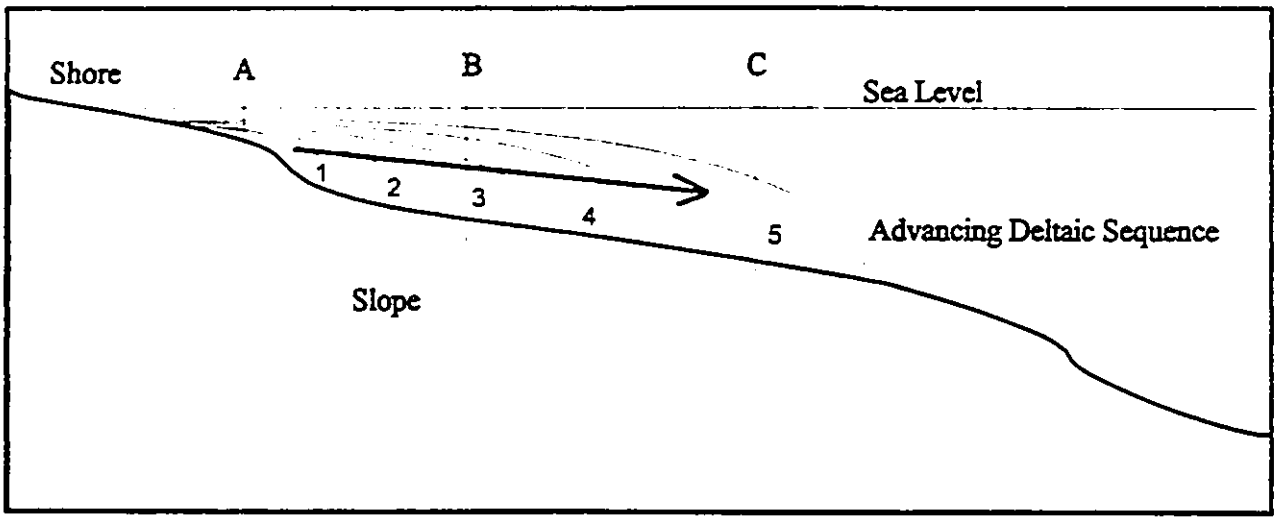

Figure 4-3. Schematic diagram representing a hypothetical detaic sequence. Notice thickness fluctuations across the transverse from A to C.

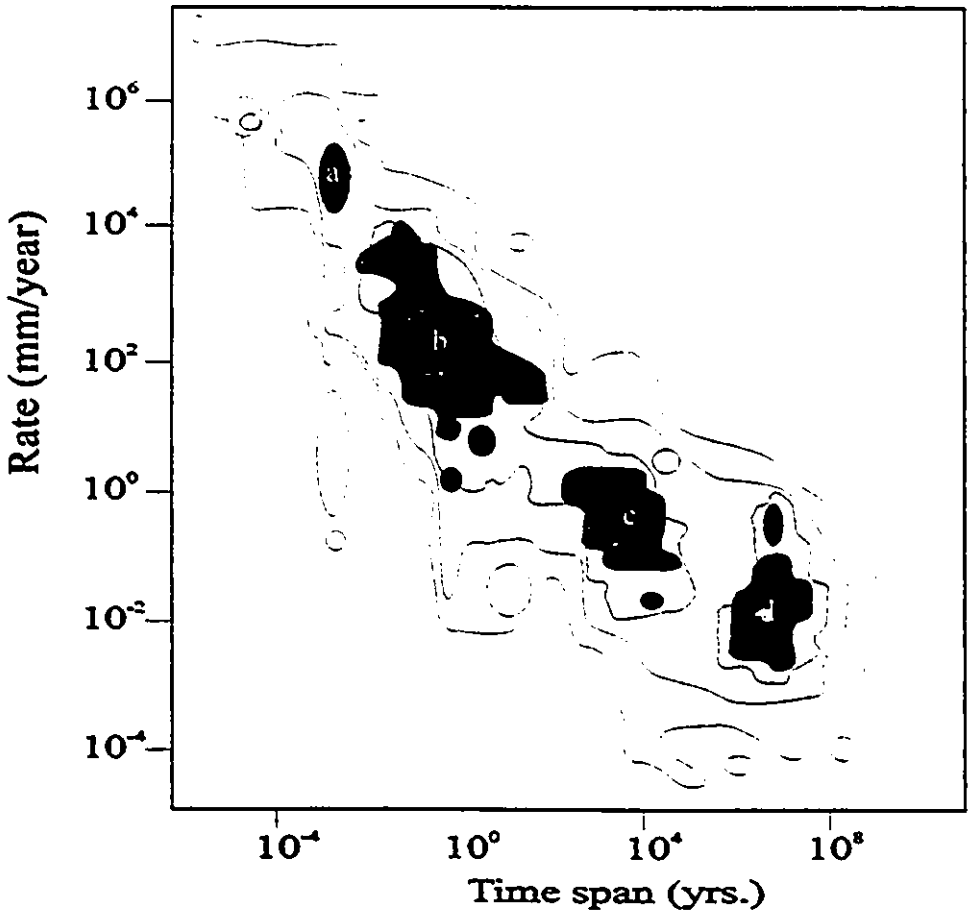

Figure 4-4. Plot of accumulation rate versus time span of observation with 25000 data points taken from geological literature. Modified from Sadler, (1981).

albeit, with loss of accuracy. Ideally, all rates from the smallest grains to the largest accumulation events should be equally represented for each time span. In practice, this is impossible with the end result being that small scale hiatuses will be overlooked, resulting in completeness of the stratigraphic record to be overestimated.

4.2. Completeness of the sedimentary record

It is fairly safe to assume that any given stratigraphic section only intermittently records the passage of geological time (Dingus, 1984). On a global scale, as one views the total volume of sedimentary rock, it becomes immediately apparent that there is a general decrease in rock volume with age (figure 4-1). This suggests one of two things. Either the rate of deposition for a given environment has progressively decreased with age or the record has become progressively less complete with time, the remaining rock forming some fraction of the whole that represents deposition versus net removal from both erosional and diagenetic sources (Sadler, 1981). If the former holds true, then the uniformitarian principles which geologists hold true are wrong and some, if not all, of our physical laws have changed with time. This is unlikely, therefore the problem lies with the second possibility. This section delves into some of the more common characteristics of this second possibility.

4.2.1. Hiatuses

Within any sedimentary sequence, there are hiatuses which represent periods of non-

deposition, erosion and/or diagenesis (Sadler, 1981). Stratigraphic sections spanning greater temporal extents have a greater opportunity of incorporating more hiatuses and hiatuses spanning longer periods of time (Sadler, 1981; Korvin, 1992). The end result is a progressive decrease in the completeness of the stratigraphic record with increasing age.

Determining the stratigraphic position and duration of a hiatus within a section is often problematic. In situations where erosional contact is matched by abrupt facies (and sediment) change, hiatus location is typically easily achieved, albeit, hiatus duration even in these situations is still difficult to determine. Another source of easily recognizable hiatuses are bedding planes (Ager, 1981). Considering the abundance of these "mini-conformities" in a stratigraphic section, the potential for loss of record is immense.

In general, sequences have erosional or non-depositional contacts which are impossible to identify from lithological parameters alone. In these situations, biostratigraphy, absolute dating and magnetostratigraphy are often utilized. For example, if a sequence containing layers with graptolites is overlain by a lithologically undistinguishable layer containing ammonites a hiatus can be deduced since these two fossil groups evolved at very different geologic times. Unfortunately, there are limitations on the effectiveness of each method (see section 4.3.). Presently, the highest resolution can be achieved with biostratigraphy, with a resolution limit rarely better than 0.5 Ma and more often on the order of one or more million years. As a result, the upper limit for using this method for hiatus identification can never be better than 0.5 Ma. In addition, bioturbation can effectively homogenize sediments in the upper 10-15 cm, rendering

any stratigraphic resolution method meaningless at scales less than 15 cm (Anders et al., 1987). If sediment accumulation is slow, then the effect of bioturbation on the resolution may become geologically significant.

The temporal extent of hiatuses is inversely proportional to the relative error size. As the size of a hiatus decreases, the percentage of variance between the temporal extent of hiatuses and error size increases.

4.2.2. Diagenesis

A problem inherent in all stratigraphic sections is post-depositional alteration or diagenesis. This process involves both physical and chemical destruction of sediment with an end result of loss of stratigraphic record.

Physical diagenesis, the result of overburden pressures associated with burial produces compaction. The extent of compaction is largely dependent on lithology, length and depth of burial. For example, clays have the potential of up to 90 percent loss of volume while sands generally do not loose more than 40 percent. Sediments with high water content or abundant porosity are more likely to be compacted greater than sediments with lower porosities because water can migrate easily and can take up a large volume of the rock. Water produces a ready path of least resistance for compaction to proceed. Length and depth of burial can have a great effect on the degree of compaction. Generally these two factors are related since increased

length of burial is usually but not always the result of increased depth. Rock may be buried shallowly for a geologically significant period of time and undergo only a little compaction because of the lack of pressure, albeit, temporal extent can, in the long run, approximate burial at depth and increased pressure. On the other hand, shallow burial often will not have the same degree of pressure solution (especially for chemically stable rocks such as arenite) as burial, the latter involving high pressure. The processes responsible for compaction are understood to such an extent that the percentage of rock removal due to compaction can be calculated (Boggs, 1987).

Chemical diagenesis can also be responsible for the removal of sediment, especially, but not limited to chemically unstable sediments (i.e., carbonates). The solubility of the rock type is controlled by a multitude of variables (figure 4-5). For a stratigraphic column, there is potential for removal of many metres of rock due to dissolution. However there is no simple equation to determine quantitatively how much rock was removed. If the pressure is high enough, then even arenites can undergo pressure solution. This generally takes the form of fused sand grains which, while not great can have a perceivable effect on the completeness of a section. Stylolites, often associated with carbonate buildups, have a greater impact on the completeness of a section. They represent dissolution of material due to pressure solution at depth. Potentially thick sequences of rock can be reduced to a thin seam composed of the remaining chemically stable minerals. The pressure solution process can be enhanced by increasing the concentration of impurities in the host rock (Bogg, 1987), although the reason for this is still not clearly understood. In addition, the geothermal gradient of a region can also be

an important contributing factor. Increasing temperature produces increased reactivity of the ground waters which may result in increased dissolution of some rock types but have the opposite effect on others (Boggs, 1987). For carbonates, this is partly due to the control temperature has on pCO_2. Unlike compaction, determining the extent of dissolution is in most situations impossible. However, what is apparent is the need to consider lithology as well as the length and the depth of burial in tandem when considering the extent of diagenesis.

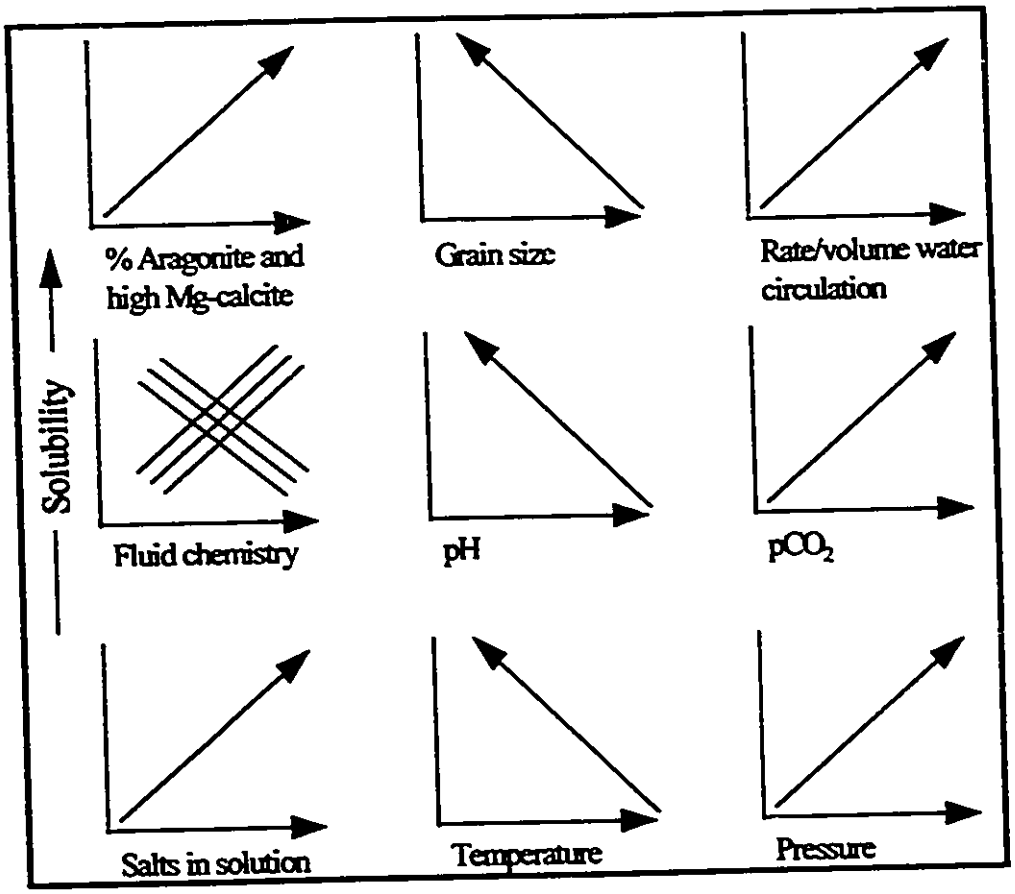

Figure 4-5. Effect on carbonate solubility of mineralogy, grain size, and diagenetic environmental factors. The arrows indicate the direction of increased values. (From Longman, 1982).

4.2.3. Acuity

Modern stratigraphers define a complete section as one which has no gaps larger than each time unit of a specific scale (Anders et al., 1987). As the resolution improves (corresponding to shorter time scales), there is a corresponding decrease in the perceived completeness of the section (figure 4-6). Therefore, improved sampling accuracy will result in

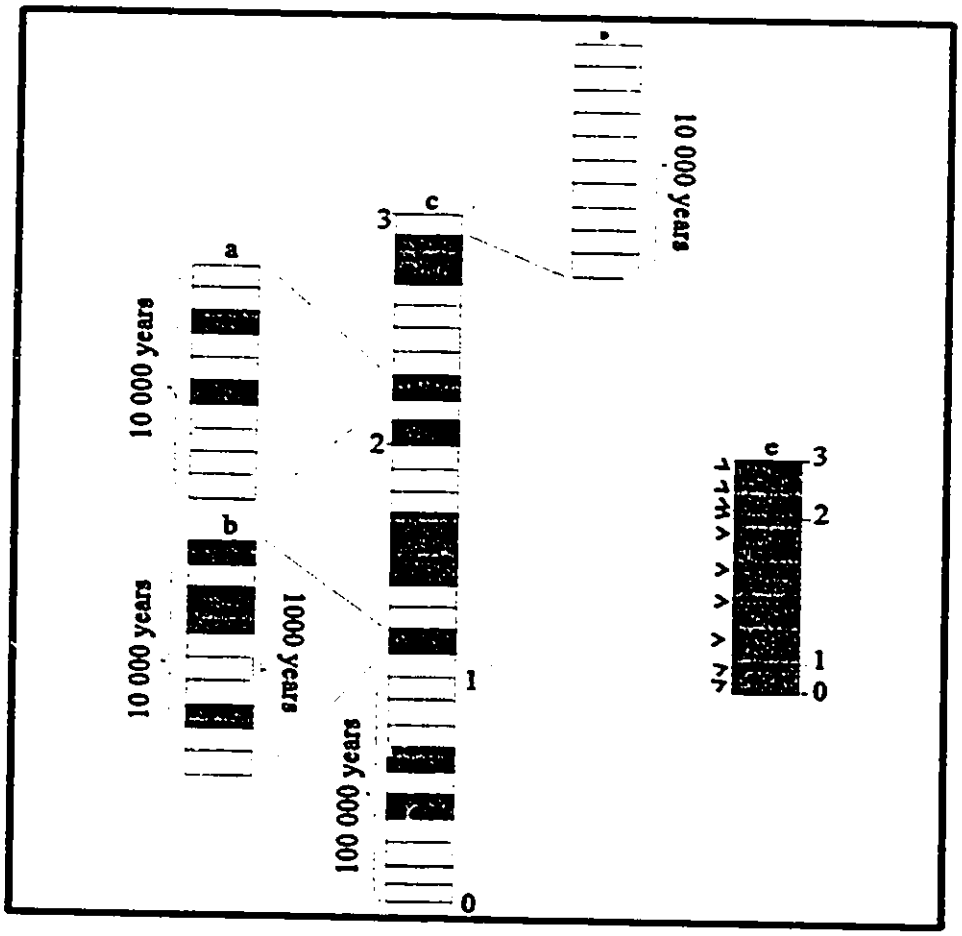

Figure 4-6. Hypothetical representation of a stratigraphic column (e) with 10 000 year markers 1,2 and 3. The other columns represent absolute age (a, b, c and d). Modified from Anders et al. (1987).

an overall decrease in the perceived completeness of the stratigraphic section (Dingus, 1982; Schindel, 1982). In fact, this relationship helps to demonstrate the incompleteness of the stratigraphic record. Ager (1981) suggested the analogy of the fishnet. In it he relates the stratigraphic record to a fishnet in which the netting material represents the stratigraphic record and the gaps between the netting represent hiatuses. If anything, this analogy is conservative with the remaining stratigraphic record actually being even less complete (Korvin, 1992). On average, it is estimated that approximately 1/30th of the record is represented in a stratigraphic section (Miall, 1994)

Time units are artificial measures and do not accurately represent time and how time effects the completeness of the record. As resolution improves, there will be a decrease in the perceived completeness, representing the increased quantity of smaller scale hiatuses. In other words, the assessment of the completeness of a stratigraphic section will decrease until such a time that all hiatuses at all time scales are accounted for.

4.3. Methods of stratigraphic resolution and correlation

The modern stratigrapher has a large arsenal of tools available for work on stratigraphic resolution and correlation, each with its own strengths and weaknesses. The most powerful and commonly used methods include biostratigraphy, radiometric dating, sequence stratigraphy, magnetostratigraphy and isotope stratigraphy.

4.3.1. Biostratigraphy

Biostratigraphy can be defined as the branch of stratigraphy that is concerned with spatial and temporal mapping of fossil units in rocks (Ludvigen et al., 1986). The fundamental biostratigraphic unit is the biozone, which is defined by its fossil content. Alcide d'Orbigny (1802-1857), a french paleontologist classified a biozone or stage as an assemblage of index fossils, some of which have a global distribution. This unit was used to define a period of time. A good index fossil should be: 1) easily recognizable, 2) restricted to a narrow temporal range, 3) have a wide geographical distribution, and 4) occur in a wide range of environments. Unfortunately, ideal index fossils are rare. Typically, fossils which covered a large geographic range also occurred in numerous environments and were evolutionary successful, therefore having a large temporal range. There is also a potential for confusing juvenile animals as a separate species to their adult phases. For some species, the juvenile and adult habitats differ. This could result in a species with a potentially good geographical range to be classified as two separate species with smaller ranges.

Throughout the Phanerozoic, some of the best index fossils have been pelagic (conodonts, foraminifers, diatoms) while others have been benthic (trilobites, brachiopods). This is surprising for benthic animals, because these are often restricted to shelf or shallow slope environments where they can find food. One possible explanation for their success as index fossils may be partly due to their juvenile stages, which for some species are pelagic (i.e. brachiopods). This would greatly increase the degree and speed of geographic distribution and

allow for species expansion to regions which are inaccessible to strictly benthic species. The rate of decline may also effect the perceived temporal range of an index fossil. A fossil which originally was a good index fossil may, while on its decline, find a localized niche where it will continue to be successful. Globally the species will become all but extinct except for that one restricted environment, the end result being a misrepresentation of the temporal range of that species. There are examples of brachiopod species becoming extinct in Europe up to one million years before they became extinct in North America (Ziegler, 1979).

Sampling resolution may also be problematic. The resolution of the biostratigraphic section will depend upon the frequency of sampling throughout the section. If only a small percentage of the strata are sampled, then the resolution will suffer. Rare taxa may be missed and the lower and upper limits on a species range misrepresented, causing a decrease in the stratigraphic resolution of the section. The rate of sedimentation will be important when determining an adequate sampling interval. In areas with high accumulation rates, short time intervals will correspond to large sediment accumulations whereas in areas with low accumulation rates. large time intervals will correspond to a small accumulation quantity. If an arbitrary sampling resolution of one sample every 10 cm is used through a sequence which has variable accumulation rates, the resulting biostratigraphic resolution will also correspondingly fluctuate.

On the other hand, biostratigraphy is still probably the best method now available for correlation and stratigraphic purposes. For some index fossils the resolution approaches one

half million years or even better. This is still better than any other method, albeit methods such as isotope stratigraphy are closing th gap and may soon approach or even surpass biostratigraphy.

4.3.2. Radiometric Dating

In the latter part of the twentieth century numerous methods of absolute dating were developed, utilizing various radiogenic isotopes. The theory behind their use is that each nuclide produces daughter products according to a decay constant and each has a characteristic half-life. Meaning that the decay rate is constant, independent of temperature or pressure and therefore should represent a cumulative nuclide/daughter ratio from the time of the sample formation. The closing temperature of any radioisotope system varies greatly. Unfortunately, there are complications inherent to radiometric dating. There are some sampling and analytical problems inherent in this method whose additive effect put into question the accuracy and therefore use of radiogenic dating (Odin, 1982).

Historically, decay constants varied depending on the laboratory where the tests were done, producing results which varied substantially even for the same sample. This problem was partially resolved in 1976 with the agreement for a set of international constants. This meant that laboratories could calibrate their equipment according to these constants, increasing the potential instrument precision. Due to instrumental limitations, absolute accuracy can never be achieved, but with modern instruments accuracy now approaches one percent (Blatt et al., 1991).

Another potential problem is with post-emplacement isotopic movement and resetting. For example, the temperature at which the K-Ar system closes is about 350°C. For other systems it may be even lower. Since the temperature of many intrusive bodies is much higher than 350°C when they are emplaced, the setting of the isotope system will not occur until the intrusive body cools to the appropriate temperature. Since many of these bodies cool very slowly, there can be a large difference in the emplacement age and the inferred age at the time the system cooled to the closing temperature (Blatt et al., 1991). Also, if at any time the temperature of the intrusive rock surpasses the closing temperature of the isotopic system, the system will be reset. The end result being that the sample will indicate the latest time the rock surpassed the closing temperature for that isotopic system and not the initial time of emplacement.

Much of the radiogenic dating of sedimentary rocks is based on superposed intrusive rocks. Therefore, the enclosing sediments can only be given a minimal age. Where igneous rocks are truncated by sediments, only the maximum age can be determined. In the case where sediments are sandwiched between two igneous bodies, a time bracket can be established. Using minerals found in the sedimentary rocks can also prove to be difficult. Zircons, common in many clastic sediments can only be used to give the maximum age of the sediment because this mineral retains its original radiogenic signature set when it was an igneous or metamorphic rock. Authigenic minerals such as some clays are sometime used for K-Ar and Rb-Sr dating, provided that the isotopes will not be reset by a temperature increase which is greater than the closing temperature.

The development of isotope/radiometric dating methods in the twentieth century produced the concept of "absolute age". This terminology has since been recommended to be dropped by the North American Commission on Stratigraphic Nomenclature (NACSN) (1983). Instead, the term "isotopic age" should be used for any determinations based on isotopic ratios and "numerical age" for age determinations from any quantifiable approach, including isotopic/radiometric methods (Schock, 1989). NACSN also recommended that the Geological Time Scale calibration be based on chronostratigraphic boundaries, not numerical ages. It may be more accurate to refer to a chronostratigraphic unit than to give it a numerical age (e.g., Lower Devonian versus approximately 408.5-386 Ma)(Harland et al., 1990). The numerical age can only be an approximation because of the generality of the method as well as human and instrumental errors. In addition, these errors increase with increasing age. Nonnumerical chronostratigraphic units do not have errors because they refer to sequential temporal units and not to "absolute ages". Finally, there are differences between the various numerical systems used globally. For example, with the American system, a billion equates to 10^9 years whereas in the British system, a billion equates to 10^{12} years. For chronostratigraphic units, this is not a problem because units are qualitative as opposed to quantitative.

Although the use of "numerical age" has many pitfalls, they can be useful in chronocorrelation in sequences where other means of correlation do not work. For example, in barren sequences where all other methods of stratigraphic correlation are inadequate.

4.3.3. Sequence stratigraphy

The main theory behind sequence stratigraphy as described by the Exxon school is that the main global stratigraphic architecture is controlled primarily by eustatic sea-level changes with episodicity in the range of 1-10 Ma. These eustatic events are global, hence correlatable between sections. In other words, a global master curve can be developed based on "correlative conformities" bound by unconformities (Miall, 1994). The problem with utilizing an unconformity as a chronostratigraphic boundary is that a hiatus represents a finite period of time that is bound to be represented by a sequence somewhere (Heldberg, 1976). In addition, hiatuses often represent a complex history bounded by two surfaces which may vary in age considerably from place to place. One may thus get a large difference in time depending upon which surface and location it is measured.

Sequence stratigraphy has also other errors. For example, there is the potential for confusing a sequence boundary with ravinement surfaces, channel scours and marine erosion surfaces, all which are represented by hiatuses but the do not necessarily represent an eustatic sea level change and therefore are not a sequence boundary. Other unconformity features which can be confused with a sequence boundary include, boundaries formed by submarine erosion, "drowning unconformities", the generation of erosional surfaces during falling sea levels and psuedo-unconformities from seismic reflection records (Miall, 1994). In addition, the nature of the transgressive-regressive cycle can create offsets of up to half a cycle. Does one take the start, middle or the end of the transgression as the boundary? Any of these features can produce

boundary placement errors which can represent time periods of 10-100 Ka or more (Miall, 1994).

4.3.4. Magnetostratigraphy

A characteristic of the Earth's magnetic field is that it periodically reverses. Magnetic oxide grains, such as magnetite which occur as a trace mineral in many sediments and magmas, are affected by the Earth magnetic field often aligning themselves to the poles. These oriented grains are preserved at the Curie point (approximately 500-600°C) and are retained for geologically long periods of time unless the temperature of the rock exceeds the Curie point, resulting in resetting of the magnetic oxide grains. When the poles reverse polarity, the magnetic grains are equally affected. This effect is global and is known as palaeomagnetism. The basis behind utilization of magnetic polarity reversals as a stratigraphic tool is based on identification of these reversal patterns and correlating them to radiometric absolute dates as first developed by Cox (1973), Glen (1982) and Mcdougall (1977). The modern magnetostratigraphic sequence is linked also to the seafloor magnetic anomaly record, because the latter is continuous, albeit difficult to date accurately (Boggs, 1987).

Magnetostratigraphy is of limited use to stratigraphers, because the magnetic polarity record is accurate and useful as a stratigraphic tool only for the last 5-7 Ma (Boggs, 1987). The older record up to approximately 200 Ma lacks the detail necessary for accurate stratigraphic work. For sediments older than 200 Ma, the magnetostratigraphic sequence has yet to be

developed. The 200 Ma limit corresponds to the oldest known oceanic crust. This renders magnetostratigraphy useless for Paleozoic strata and for the lower part of the Mesozoic. In the future, the record may improve for the Lower Mesozoic and it is also probable that the record will be extended into the Paleozoic, because magnetic signatures have been found in terrestrial samples. On the other hand, it is doubtful that it will ever approach the resolution achievable with other stratigraphic methods, including biostratigraphy and isotope stratigraphy. Since magnetic anomalies are linked to absolute dating, magnetostratigraphic sequence will automatically incorporate the errors associated with absolute dating. As a benefit, paleomagnetic data is an important tool for paleogeographic reconstructions.

4.3.5. Isotope stratigraphy

The basic principle behind isotope stratigraphy is that the ratios of various isotopes in past seawater have not been constant and these fluctuations may have been recorded in fossils and sediments. If the samples have not undergone any alteration and were not affected by biogenic fractionation, then they can reflect the isotopic composition of coeval seawater. Matching the isotopic records from various stratigraphic sections to the global curve may thus provide an accurate method for stratigraphic correlation.

Using modern techniques, strontium can be accurately measured to five decimal places and is usually written as a ratio (0.7XXXX). It can also be expressed in delta notation as

$$\delta^{87}Sr = \{ (^{87}Sr/^{86}Sr_{sample} / {}^{87}Sr/^{86}Sr_{sea\ water}) - 1 \} \times 10^5$$

For example, the strontium isotope ratio for modern marine seawater is 0.7092 whereas the average ratio for river water is 0.7111. For O and C isotopes, the standard technique is to compare the ratios to a standard.

$$\delta^{18}O_{(PDB)} = \left\{ \frac{(^{18}O/^{16}O)_{sample} - (^{18}O/^{16}O)_{standard}}{(^{18}O/^{16}O)_{standard}} \right\} X\ 1000$$

and

$$\delta^{13}C_{(PDB)} = \left\{ \frac{(^{13}C/^{12}C)_{sample} - (^{13}C/^{12}C)_{standard}}{(^{13}C/^{12}C)_{standard}} \right\} X\ 1000$$

This has typically been the V-PDB (Vienna convention *Bellemnitella americana*) from the Cretaceous Peedee Formation in South Carolina for carbonates (McCrea 1950) and to Vienna Standard Mean Ocean Water (V-SMOW) for ocean water (Craig 1961). Conversion between V-SMOW and V-PDB can be achieved using the equation:

$$\delta^{18}O_{V\text{-}SMOW} = 1.03091 \times \delta^{18}O_{PDB} + 30.91$$

and

$$\delta^{18}O_{PDB} = 0.97002 \times \delta^{18}O_{V\text{-}SMOW} - 29.98$$

The question arises to what extent the curves for many isotopes represent global curves and to what extent they only reflect the regional seawater chemistry (Grossman et. al. 1991).

If localized, these isotopic techniques would only be useful for regional correlations of two stratigraphic sections. It has also been suggested that the reference curves reflect global trends on which regional variations are superimposed. For example, the terrestrial biomass explosion during the Devonian-Permian could have resulted in a characteristic global signal in the carbon isotope curve (Brand 1989a).

Strontium isotopes may represent one of the most likely methods for an accurate global curve, since the Sr isotopic ratio is globally homogeneous in seawater at time scales in excess of 1000 years (Broecker, 1963; Goldberg, 1963). This isotope has been used successfully by many researchers and the resolution of the strontium isotope reference curve is improving with the increased database. The decay of ^{87}Rb to ^{87}Sr could contaminate the isotopic ratio for some samples with high clay content. Such radiogenic Sr may be incorporated into the measured sample during acid leaching of the clays at the time of laboratory digestion. Proper handling and selection of study material is therefore a necessary precondition.

Carbon isotopic composition of sea water is influenced by factors which may or may not be of global significance. Some features, such as the terrestrial biomass "explosion" during the Devonian-Permian interval is a global trend and should show in the δC^{13} global record. Short term or regional fluctuations, such as seasonal changes or evaporation, cannot be correlated globally and may not show up on a global curve. This invalidates utility of C isotopes as a stratigraphic tool for all but the most general time-scales. Carbon isotopes can therefore be used for regional stratigraphic correlation only when environmental conditions of stratigraphic

sections are similar. On the other hand, they do provide a powerful means of constraining global and regional environmental events.

As for carbon, the use of oxygen isotopes as a global stratigraphic tool is laden with pitfalls. Oxygen isotopes are strongly influenced by temperature that is very variable globally. Consequently, any global oxygen curve will have to take into account seasonal, depth and latitudinal temperature variability. In other words, the oxygen isotopes will reflect, at least in part, environmental change. As a consequence, oxygen isotopes can only be used regionally for stratigraphic correlation or as an environmental indicator.

5. LOWER DEVONIAN STRATIGRAPHY

The Lower Devonian spans a time interval of 22.5 Ma. (Harland et al., 1990) and has been subdivided into three stages based primarily on work initiated by Dumont (1848) in the Rhenish Mountains of Germany. These stages are the Gedinnian, Siegenian, and the Emsian. In the 1950's, Chlupáč developed a parallel system of classification based on Hercynian magnafacies located in the Czech Republic (Chlupáč, 1953). This second system divides the Lower Devonian into four stages, including the Lochkovian, Pragian, Zlichovian and Dalejan. For the most part the two classifications have similar boundaries although some discrepancies exist, particularly for the Lochkovian/Pragian boundary, the upper Emsian boundary and the Hercynian equivalent of the upper Dalejan boundary. Recently, the International Commission for Devonian Stratigraphy has been attempting to standardize the Lower Devonian stages utilizing parts of both systems. They recommended that the Lower Devonian be divided into three stages including the Lochkovian (408.5-396.3 Ma), Pragian (396.3-390.4 Ma) and the Emsian (390.4-386.0 Ma) (Harland et al., 1990) (figure 5-1).

The Lower Devonian was originally defined on the basis of lithostratigraphic parameters (Dumont, 1848) and only later was there an attempt to incorporate biostratigraphy. However, this was a transitional period for some of the more important biostratigraphic fossil groups which caused problems with subsequent biostratigraphic correlation. Graptolites were on the decline, last occurring in the lower Emsian while ammonites were still in their infant stage. As

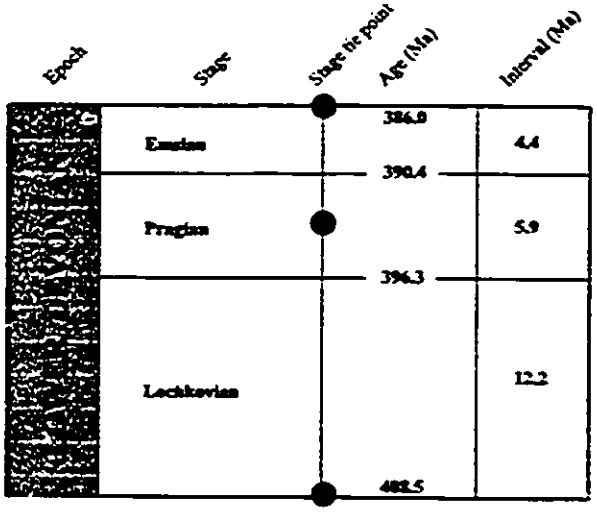

Figure 5-1. Time scale for the Lower Devonian. (From Harland, 1990).

a result, biostratigraphic correlations were only partly successful, relying, at least until recently, on benthic assemblages (brachiopods and trilobites) and on graptolites. In the 1960's, with the advent of microbiostratigraphic correlation, pelagic conodonts and dacryoconarids took the forefront of biostratigraphy, while the use of brachiopods declined (Dineley, 1984). Even then there were discrepancies as to how many faunal zones there were in the stratigraphic ranges of these zones.

The Lower Devonian can be presently subdivided into nine conodont zones, nine dacryoconarid zones, eight graptolite zones, and one ammonite zone (figure 5-2). The spirifers *Acrospirifer* and *Paraspirifer* are also important although generally they are more important for regional stratigraphy due to their mostly endemic nature. Conodonts, being the most commonly used and detailed group, were utilized in this study.

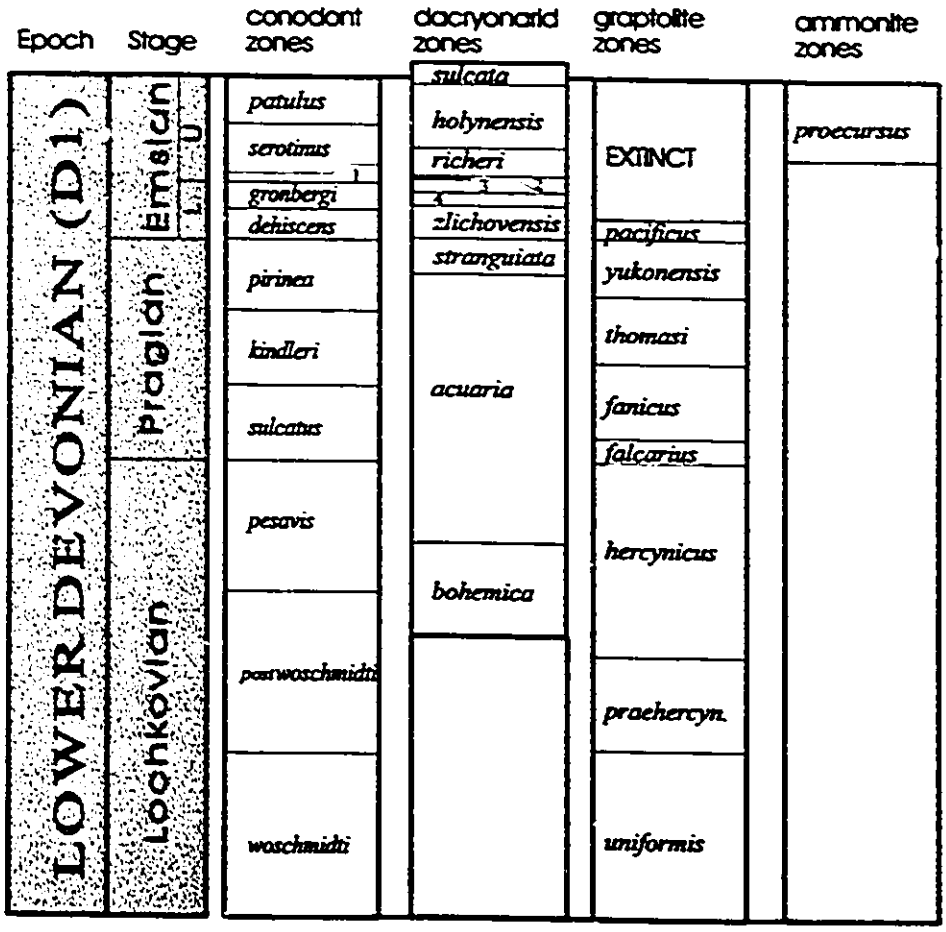

Figure 5-2. Lower Devonian conodont, dacryonarid, graptolite and ammonite biozones. Conodont biozones from Harland et al. (1990) and Carls (1988), dacryonarid, graptolite and ammonite biozones from Dineley (1984). 1= *laticosti*, 2= *cancellata*, 3= *elegans* and 4= *barrandei* biozones. Complete conodont names as in figure 2.2.

5.1.1. Lochkovian stage

The latest data has the Lochkovian covering a time interval of 12.2 Ma (Harland et al., 1990). The base of this stage is marked by the first appearance of the graptolite *Monograptus uniformus*. It can be subdivided into four zones based on conodonts and three zones based on

graptolites. It also spans the dacryonarid *bohemica* and part of the *acuaria* zone. The Pridoli/Lochkovian boundary is also the location of a stage tie point (Harland et al., 1990).

5.1.2. Pragian stage

The Pragian covers a time interval of 5.9 Ma (Harland et al., 1990). The boundary between the Lochkovian and the Pragian is lithologically defined, corresponding to the Pragian base at its type section. It is only poorly defined biostratigraphically, the result of poor faunal representation. The Pragian encompasses three conodont zones. The top of the dacryonarid *acuaria* and all of the *strangulata* zone is also present. During this stage graptolite use decreases due to rapid faunal decline, with only three poorly represented zones present. The middle Pragian is the location of a stage tie point (Harland et al., 1990).

5.1.3. Emsian stage

The Emsian covers a time interval of 4.4 Ma (Harland et al., 1990). It is also stratigraphically the best understood Lower Devonian stage (Ziegler et al., 1977). In Europe, the boundary between the Pragian and Emsian is best defined by the extinction of the brachiopod *Acrospirifer primaevus* and the first introduction of *Arduspirifer arduennensis antecedens*. In Germany a twofold subdivision is used (Lower and Upper Emsian). The boundary between the Lower and Upper Devonian is based at the first occurrence of the brachiopods *Arduspirifer a. arduennensis* and *Eurospirifer paradoxus* along with the

disappearance of the conodont *Pedavis granbergi*. Since Lower Devonian brachiopods typically show great provincialism, other fossil groups are generally used for global correlation. Lower Emsian conodont biozones include the *Polygnathus dehiscens* zone and *Polygnathus gronbergi* zone. The Upper Emsian conodont biozones include *Polygnathus laticostatus*, *Polygnathus serotinus*, and lower *Polygnathus patulus* zones. Based on dacryonarids, both the Lower and Upper Emsian can be subdivided into three zones. The rare goniatite *anetoceras* zone encompasses all of the Emsian and the upper part of the Pragian. The Emsian/Eifelian boundary is the location of the final stage tie point (Harland et al., 1990).

5.2. Lower Devonian sequences and stratotypes

Since the first introduction of the Lower Devonian by Dumont in 1848, two classical marine type successions have been recognized (Table 2). The first is located in the Rhenish Mountains of Germany (Rhenish magnafacies). Here a series of type sections for the Gedinnian, Siegenian and Emsian were developed. The rocks are characterized by shallow clastic and carbonate facies. Later in the Barrandian area of the Czech Republic, the Lower Devonian Hercynian type sections were developed for rocks of Lochkovian, Pragian, and Zlichovian-Dalejan stages. These rocks differ greatly from Rhenish magnafacies, being characterized by predominantly deeper offshore carbonate facies (Boucot et al., 1969). These two classical successions are typical of many global Lower Devonian marine sequences.

Unfortunately, the Rhenish magnafacies, while having abundant benthic fossils, does

not have as many conodonts or graptolites. This can make global correlation difficult. In contrast, the Hercynian magnafacies has many conodonts and graptolites and this enables much easier correlation over large distances. It is in part due to these reasons that the International Commission for Devonian Stratigraphy dropped the use of the Gedinian and Siegenian in favour of the Lochkovian and Pragian, while retaining the Emsian which is well characterized in terms of resolution and correlation capabilities.

RHENISH MAGNAFACIES	HERCYNIAN MAGNAFACIES
Lithofacies Characteristics	**Lithofacies Characteristics**
- Sediment 'impure': conglomerates, greywackes, sandstones, quartites, quartzitic shales, ect. - Calcium carbonate content low or absent	- Sediments 'pure': Mostly pure limestones and argillaceous shales. - Calcium carbonate high as a rule.
Biofacies Characteristics	**Biofacies Charateristics**
- Corals -Solitary corals almost absent. -Tabulate corals rare or absent. -*Pleurodictyum* typical.	- Corals -Very common and typical. -Very common and typical (*Favosites, Chaetetes, Heliolites*). -*Pleurodictyum* absent
- Brachiopods -Strongly strong ribbed forms predominate -Smooth and rounded forms rare. -Ribbed spirifers with long 'wings' are typical and very frequent.	- Brachiopods -Considerably less common. -Typical (pentamerids, meristids, ect.) -Smooth rounded spirifers are typical and frequent.
- Bivalvia -Cardiocoochs nearly absent -*Conocardium* rare. -*Hercynella* absent -Typical: *Grammysia, Phthonia, Leptodomus,Sphenotus, Limoptera,Dechenia, Modiomorpha*, ect.	- Bivalvia -Present and typical (*Pawenka, Kralowna, Buchiola*, ect. -Sometimes very common. -Present and typical -All absent or very rare.
- Tentaculitida -*Tentaculites* predominant -All absent or rare.	- Tentaculitida -Nearly absent. -*Nowakia, Guerichina*, and *Styliolina* frequent and typical.
- Cephalopoda -Nautiloidea rare. -*Arthrophyllum* present. -Bratritida always present. -Goniatites as rare exception only.	- Cephalopoda -Very frequent and numerous. -Absent -Present and typical -Present and typical.
- Arthropoda -Ostracods generally sculptured -Trilobites mostly poor in number of genera and individuals. -Typical: *Asteropyge* and related genera. *Homalonotus* and related genera	- Arthropoda -Nearly always smooth -Rich in number of genera, species and individuals.

Table 2. Distinguishing features of Rhenish and Hercynian magnafacies. (From Dineley, 1984).

6. LOWER DEVONIAN PALEOGEOGRAPHY

Paleogeographic reconstruction using paleomagnetic signatures is an especially powerful tool. It should be noted, however, that many sources of error exist, particularly for Paleozoic rocks such as the Lower Devonian. Such errors include: i) lack of reliable pole positions, ii) samples having more that one component of magnetization, each with uncertain ages, iii) samples with poor biostratigraphic ages (i.e. red beds), iv) absence of a continuous ocean floor due to the missing oceanic crust, except for some rare ophiolitic fragments, and finally v) deformation of a significant percentage of the Lower Devonian continental crust. The end result is that discrepancies in positioning of continents enable differing paleogeographic reconstructions (Livermore et al., 1985). The general landmass distribution appears to be, for the most part, consistent between models, but some discrepancies exist as to their location with respect to the paleoequator (Boucot, 1985; Morel and Irving, 1978; Scotese et al., 1979; Livermore et al., 1985; Scotese, 1994), depending on whether the reconstructions were based on paleomagnetic, lithostratigraphic or biogeographic criteria.

The first two stages of the Lower Devonian were periods of predominantly eustatic regression. Following the low point in the Pragian, there was a rapid transgressive event that extended into the Middle and Late Devonian (Dineley, 1984; Boucot, 1985). This transgression may have been a consequence of growth and rapid plate spreading at MOR's (Dineley, 1984). Average estimates of landmass area suggest that approximately 13 percent of the total planetary surface was covered by land during the Lower Devonian. This subsequently

increased to approximately 21 percent for the remainder of the Devonian (Ronov et. al., 1980).

Most data suggests that there was a well developed Lower Devonian climatic gradient which gradually declined during the Middle Devonian (Boucot, 1985). However, no evidence suggests sea level glaciation. This would rule out glaciation as a possible controlling mechanism of marine regression. At mid-latitudes of the southern hemisphere, there is strong evidence for broad arid belts characterized by abundant marine evaporites and calcretes (Boucot, 1985).

Two main oceans existed during this period. The Paleotethys covered most of the planetary surface and the Hercynian ocean formed a 3000 km long trough between Laurentia and Gondwanaland (figure 6-1). Various smaller basins and seaways developed at low latitudes between the continental and micro-continental landmasses. These basins and seaways were important to the development of many faunal sub-provinces in the Old World realm. Such seaways could have produced complex currents that could restrict movement of some pelagic species, or of the pelagic juveniles of some benthic species, such as the brachiopods.

The Silurian through Lower Devonian saw the continental landmasses migrating southward while Gondwanaland rotated counterclockwise. This caused sub-continent segmentation that eventually would result in the closure of the Hercynian Ocean and in the formation of Pangea in the Late Paleozoic. Morel and Irving (1978) suggested a short period of continental collision between Laurussia (Laurentia and Baltica) and Gondwanaland during

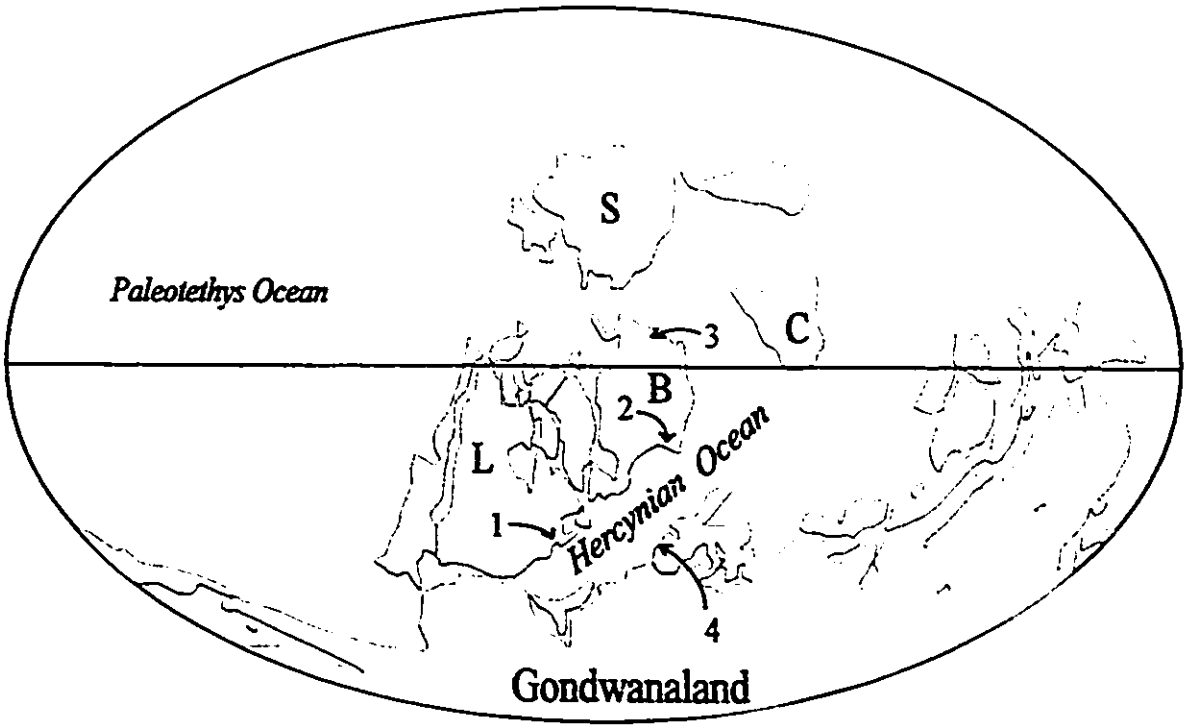

Figure 6-1. Paleogeographic reconstruction of the early Emsian. Field areas: 1) New York State, 2) Podolia, Ukraine, 3) western Ural Mountains, Russia and 4) northern Spain. L= Laurentia, B= Baltica, C= China and S= Siberia. Simplified from Scotese (1994).

the Late Devonian. While Scotese and others (1979) agree with the formation of Laurussia during the Late Devonian, they question an earlier collision with the Gondwanaland. Some research suggests that the closure of the Hercynian ocean was gradual, culminating in continental collision in the Permian (Scotese, 1994). It is apparent that more accurate data set for this time period is needed in order to specify the location of landmasses and their movement. It should be noted that the Lower Devonian was, for the most part, orogenically dormant interval, with the possible exception of the Silurian-Lower Devonian transition that was characterized by some isolated orogenic activity (Boucot, 1985). For example, the Tasman and the Acadian Orogenies fall into this time interval.

The globally high climate gradient, in addition to the Lower Devonian paleogeographic changes, is also an important factors to be taken into consideration when explaining biogeographic characteristics (see chapter 7.4.1. for more details).

One paleogeographic model (Scotese, 1994) suggests that the landmasses comprised the supercontinent Gondwana, the continents of Laurentia and Baltica, and some microcontinents, such as Siberia, Kazakhstania and China (figure 6-1). Gondwanaland, located around the south pole, was composed of a conglomerate of cratons that included Africa, Antarctica, Australia and South America. Laurentia, located at low latitudes, was composed of Central and North America, as well as sections of eastern Siberia and Greenland. Baltica, adjacent to Laurentia, was made up of Scandinavia and most of northern Europe. The micro-continents were located near the paleoequator and north of Baltica, probably in close proximity to each other because of floral and faunal similarities. There is some discrepancy as to the location of a portion of southwestern Europe. In Scotese's model, Spain, France and Italy are located within Gondwana, just north of the African craton. In contrast, in the model of Morel and Irving (1978), Spain and France are placed on the other side of the Hercynian Ocean, in southern Laurentia.

7. BRACHIOPODS

7.1. Brachiopod ecology

Brachiopods originated in the Lower Cambrian and have been around in various quantities ever since. More than three thousand fossil genera are known with about 100 living today (Clarkson, 1993). They have undergone numerous extinction/expansion episodes, but showed most diversification during the Paleozoic (figure 7-1).

Brachiopods are marine organisms, mostly sessile, benthonic, epifaunal, suspension feeders. This mode of life appears to have been characteristic throughout geologic time. Juveniles appear to have been pelagic, although some adult species may have led epiplanktonic lifestyles. Other species appeared capable of filter-feeding and although unconfirmed, some researchers feel that a few species may have been limited carnivores (Moore, 1965). Brachiopods are found in a plethora of environments but most are found attached to rocks or shells. Some species appear also capable of anchoring and even lying free on a soft substrate. Often they cluster together forming broods of one or more species, with successive generations using previous generations as a substrate base.

Salinity is an important factor controlling brachiopod location and distribution. All modern, and probably fossil, brachiopods are extremely sensitive to salinity and are found only in normal marine conditions (Moore, 1965; Boucot, 1975; Clarkson, 1993). There are no known

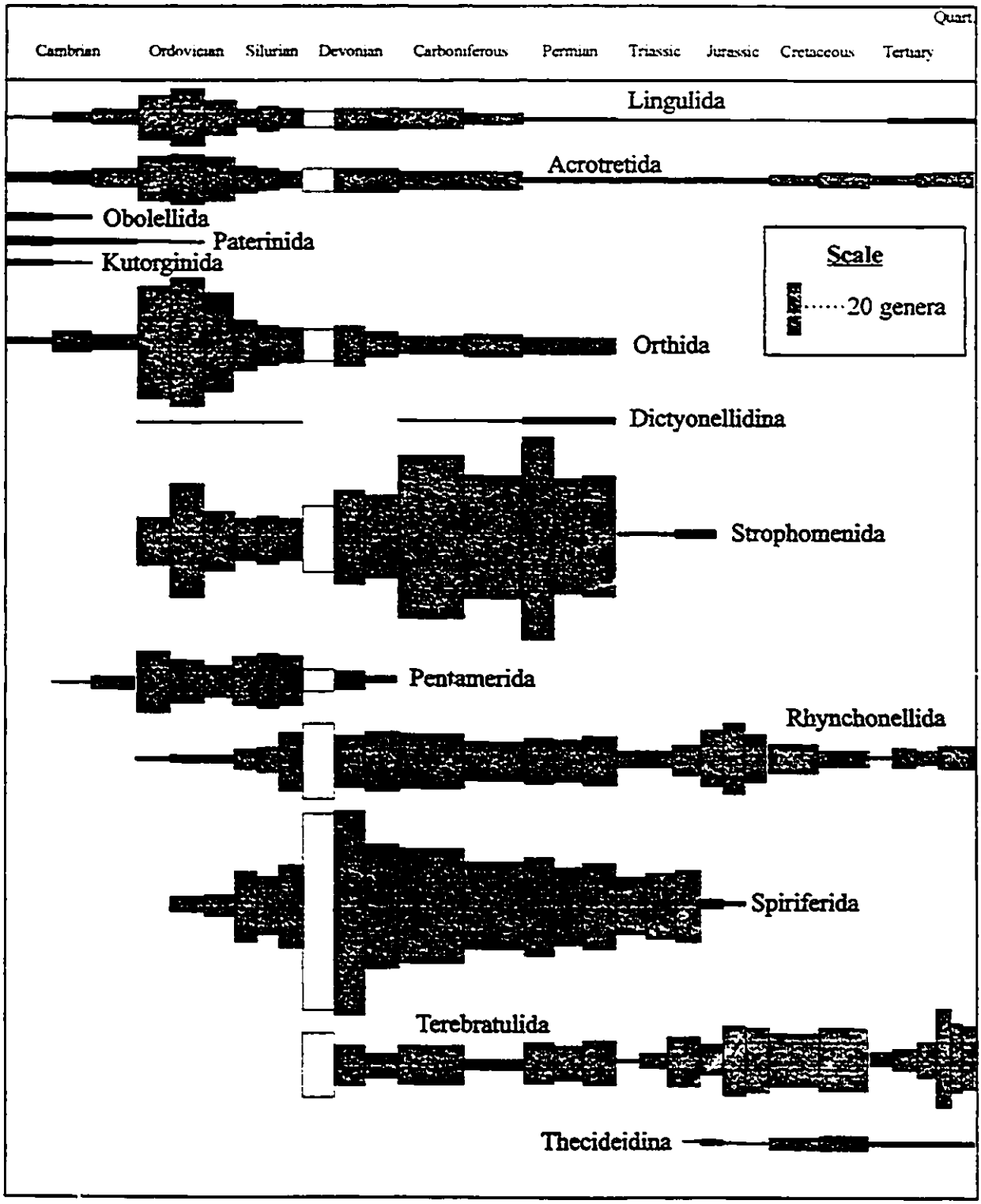

Figure 7-1. Stratigraphic distribution of brachiopod orders and sub-orders with proportionate number of genera. Lower Devonian highlighted light grey. Modified from Moore (1965).

species of articulate brachiopods which can handle even slightly brackish or freshwater conditions. Only inarticulate ligulids can survive in brackish water, and then only for a very short time. On the other hand, since only a fraction of brachiopod species has survived into modern times, it is naive to conclude that some extinct brachiopod families could not have survived at different salinities. The fossil record suggests that brachiopod distribution was far greater than it is today.

Brachiopods also require well-oxygenated water (Moore, 1965), although a few isolated fossil examples from black shales do exist. Examples have been found also in the modern equivalent, anoxic black organically rich muds. It has been, however, hypothesized that ancient specimens found in black shales are allochthonous or from epipelagic species (Moore, 1965).

Modern brachiopods occur mostly in cool temperate waters, with semitropical and tropical examples found in progressively deeper waters, although a few species do live in warm water. Paleodepth data indicates that this was not always the case. Many Paleozoic species seemed to have preferred shallow warm water. This apparent dichotomy can be possibly explained through a gradual evolutionary preference for cooler water, although this is unsupported (Moore, 1965). Another view is that the past mass extinction events preferentially killed off the near surface species. The deeper water species would have been buffered from rapid environmental changes and had a better chance of survival.

The modern consensus is that brachiopods appear capable of living in a wide range of

temperatures and depths, from a few metres to abyssal depths of more than 3600 metres. But at the species and even family rank level there is noticeable stratification. Some researchers have attributed this stratification to temperature gradient, but the data is still inconclusive (Boucot, 1975). Others have shown that the quantity of food may have played a role, with the more advanced orders, such as the Pentamerida and Spiriferida, capable of living in deeper waters with lower food supply. In contrast, Rhynchonellida with their primitive lophophore apparatus were capable of surviving only in shallow near-shore environments (Fürsich and Hurst, 1974). It is probable that a combination of both depth and food supply controls brachiopod distribution.

7.2. Brachiopod shell morphology

Brachiopods characteristically have two valves of different sizes, symmetrical about a median axis (Clarkson, 1993). They typically are attached to some type of substrate by a pedicle, although some species are attached by cementation or through their spines. A few species are free lying on the ocean floor.

Living and extinct brachiopods can be subdivided into inarticulate and articulate classes, each with its own characteristic shell structure and composition. Most inarticulate brachiopods have an outer organic periostracum which is underlain by a primary layer composed of alternating lenses of organic and phosphatic material. There are no secondary layer and no punctae (Clarkson, 1993).

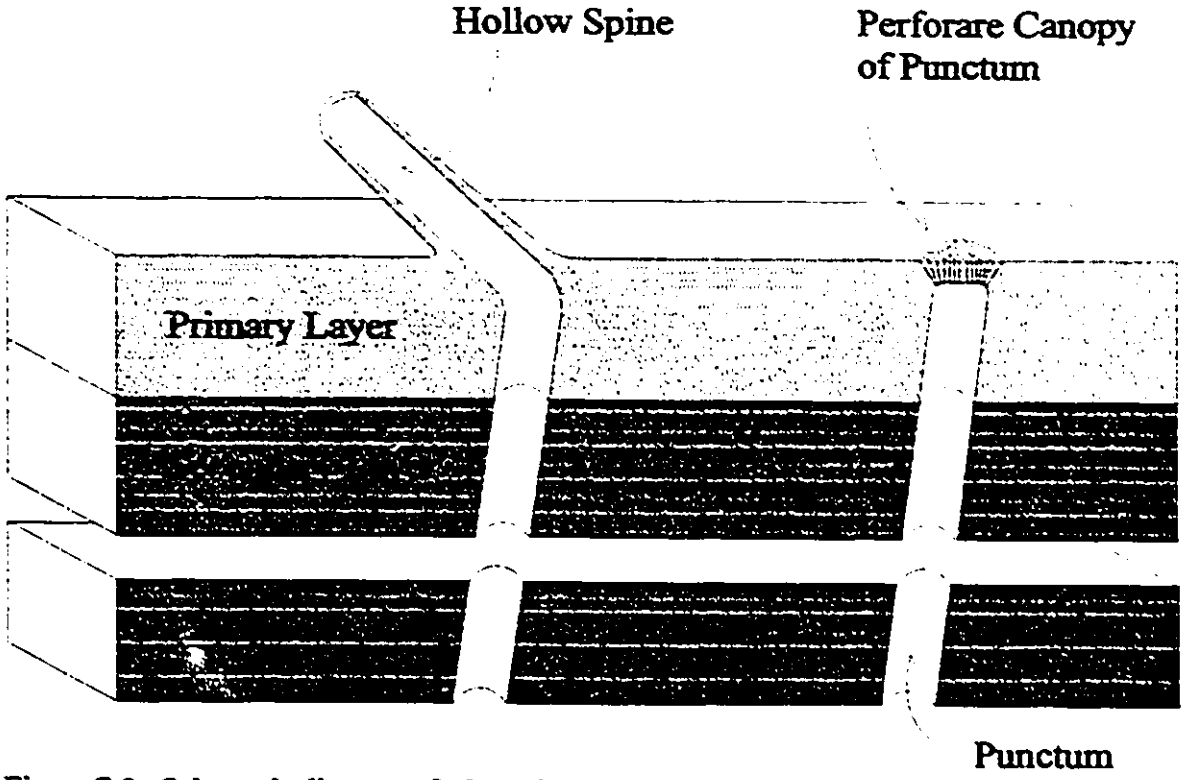

Figure 7-2. Schematic diagram of a brachiopod shell. From MacKinnon (1974).

The majority of brachiopods and the ones most often used for isotope geochemistry are rticulate brachiopods (figure 7-2). These brachiopods have a greater shell complexity than inarticulate ones, sometimes having complex ornamentation, such as ribs or spines. Like inarticulate brachiopods, the periostracum of articulates is a thin triple organic layer responsible for perimeter shell growth. While this structure is present in modern species, it is not preservable and therefore not found in the fossil record. The thin primary layer is difficult to detect except in well preserved unaltered specimens. It is composed of cryptocrystalline low magnesium calcite (LMC) and its thickness is typically consistent throughout, except where the development of ornamentation produces predictable thickness variations. The thicker secondary layer is distinguishable from the primary layer by being composed of oblique (approx. 10^{o} to

the primary layer) fibrous LMC. This layer generally thins towards the growth edge of the shell, with the thickest fibres found towards the middle near the umbones where the shell is oldest (Clarkson, 1993). In cross-section, the secondary layer is characteristically trapezoidal. A tertiary layer can also be found among the orders Pentamerida and Spiriferida. In species where a tertiary layer is produced, it forms a distinct but compositionally similar prismatic LMC lenses (Moore, 1965; Williams, 1968).

Articulate brachiopods may or may not have punctae or punctae-like structures. Punctae are numerous "caecal evaginations" which penetrate the calcareous layers of the shell, emanating from the periostracum (Moore, 1965). Species where they do develop are referred to as endopunctates on. Pseudopunctate articulates have caecal-like structures but these structures do not penetrate the entire shell layers. Impunctate articulates have no perforations within the shell structure.

7.3. Major and trace element chemistry of the shell

Brachiopod shells can chemically be divided into two main groups based on whether the shell is mostly composed from calcium phosphate, as is the case for most inarticulate brachiopods, or from calcium carbonate, such as for articulate brachiopods. Some major and trace chemical features are similar for both types of brachiopods, but overall each type has its characteristic chemical signatures. This section deals with the major and trace element chemistry of brachiopods.

The dominant feature distinguishing inarticulate from articulate brachiopods is the major element chemistry of their shells. Inarticulate brachiopods are composed generally 50-75 percent from inorganic calcium phosphate. They also contain a small percentage of calcium carbonate, typically from 1 to 8.6 percent and almost always minor amounts of $MgCO_3$, Al_2O_3, Fe_2O_3 and SiO_2 (Moore, 1965). Trace elements common to inarticulates include Sr, Cu, Ba, Ti, F, Al, B and Zr Fluorine, toxic to many animals, may represent removal of this element from the brachiopod body by fixation (Moore, 1965). Many of these elements are essential to the shell, while others are solely a characteristic of the brachiopod environment without affecting the animal one way or the other (i.e. Al and B). The organic periostratum of inarticulate brachiopods also contain inorganic compounds, commonly iron with concentrations as high as 10 weight percent in some species.

Organic material also makes up a significant portion of an inarticulate shell. Generally 25 to 52 percent of the shell of inarticulates are organics. The typical organic components are chitin, proteins and some lipids.

By far, the majority of brachiopods are articulates, composed typically of 94.6 to 98.6 percent calcium carbonate. In addition, there is typically a small percentage of phosphate, approaching 0.5 percent as in the case of *Crania*. Minor oxides and trace elements present in articulates are similar to those found in inarticulates. Organic material, while present in articulate brachiopods, generally does not exceed 0.9 to 4 weight percent. These are typically proteins and lipids. Articulate brachiopod periostratums, while containing protein, does not

contain chitin, a molecule associated with inarticulates. The formation of chitin is associated with phosphate (Moore, 1965).

7.4. Lower Devonian brachiopods

The Lower Devonian saw the introduction of the order Terebratulida while many of the other orders were undergoing a period of stasis or decline. The orders Spiriferida and Rhynchonellida were at or near their greatest diversity. The only existing order to diversify during the Lower Devonian was Strophomenida (figure 7-1)(Moore, 1965; Clarkson 1993).

While most groups of articulate brachiopods can be found in the Lower Devonian, the majority are genera from the orders Spiriferida, Rhynchonellida and Strophomenida. The orders Terebratulida, Pentamerida and Orthida are also present, albeit in lesser quantities. Only the orders Lingulida and Acrotretida are inarticulate brachiopods. Morphological descriptions for genera can be found in Moore (1965).

7.4.1. Lower Devonian brachiopod bioprovinces

During most of the Silurian, brachiopod communities were generally cosmopolitan. Holdover fauna crossing the Pridolian/Lochkovian boundary made up the majority of the faunal groups, although its importance progressively declined, with only the odd Silurian holdovers found in the Emsian. Changes in the Lower Devonian produced provincial faunal communities

which reached their greatest geographic range in the Emsian. As a result, three brachiopod bioprovinces developed, some with their own sub-provinces. Each province and sub-province showed its own characteristic faunal assemblages (Boucot et. al., 1969; Johnson and Boucot, 1973; Johnson, 1979). For a more complete summary of brachiopod zoogeography see Boucot et al. (1969).

During the Lochkovian stage, developing provincialism from eustatic regression produced land mass barriers that influenced the development of the Appalachian and Old World provinces. These provinces were well defined, with Appalachian fauna restricted to eastern and southern North America. Old World fauna dominated the western and arctic North America as well as all other marine environments. Two sub-provinces, definable within the Old World realm, were the Tasman and the Rhenish/Bohemian sub-provinces. These were developed primarily due to climatic variations and due to additional physical barriers (Johnson, 1979).

Increased endemism during the Pragian stage saw expansion westward of the Appalachian province. At the same time, the Old World province continued to segment. This saw the introduction of the Ural and Cordilleran sub-provinces. The beginning of this stage saw marine transgression which by itself was insufficient to overcome existing barriers.

The Emsian was the period of greatest Devonian provincialism and saw the development of a third province (figure 7-3) and the introduction of the Productid family. Although the Dalejan saw the beginning of another eustatic rise, it was again insufficient to

decrease the numbers of bioprovinces. The Malvinokaffric province developed in cold waters and is present in Emsian rocks from Patagonia, South Africa and Antarctica. This stage also saw the commencement of retreat of the Appalachia Province from western North America. The Old World province continued to divide into more sub-provinces with the introduction of the New Zealand and Kazakhstan. These sub-provinces are considered unusual in that they are composed of fauna from two provinces (Johnson and Boucot, 1973). The New Zealand sub-province is composed of fauna from Malvinokaffric and Appalachian provinces, while the Kazakhstan sub-province is composed of Appalachian and Old World fauna.

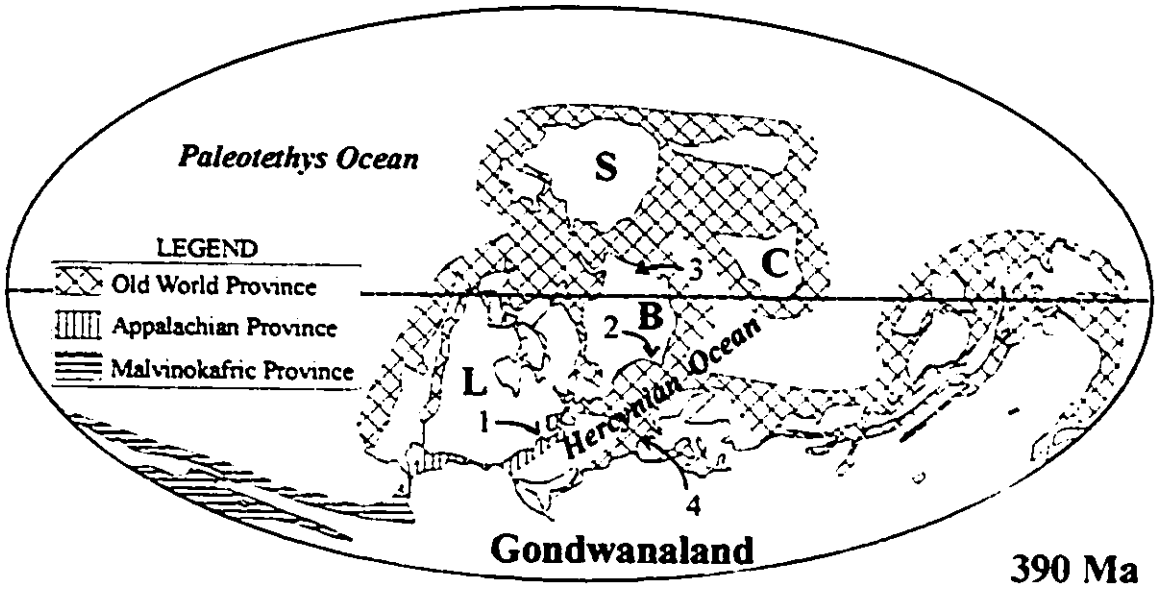

Figure 7-3. Early Emsian brachiopod provinces plotted on a paleogeographic reconstruction with field areas. 1) New York State, 2) Podolia, Ukraine, 3) western Ural Mountains, Russia and 4) northern Spain. L=Laurentia, B= Baltica, C= China, and S= Siberia. Paleogeography from Scotese (1994). Brachiopod bioprovince data taken from Johnson and Boucot (1973).

7.4.2. Stratigraphic resolution of Lower Devonian brachiopods

Until the introduction of conodont biostratigraphy in the 1960's, brachiopods were considered the primary index group for the Devonian (Johnson, 1979). This is because they were at their greatest diversity during the Lower Devonian while other groups traditionally used for biostratigraphy (trilobites, graptolites) were on the decline or had not developed sufficiently (goniatitic cephalopods) to be used in biostratigraphy. Unfortunately, the Lower Devonian was also a period of great brachiopod provincialism. This produced great diversity and rapid extinction rates (endemism), but also retarded geographic distribution. As a result, most zonal assemblages are only useful on a regional scale (Johnson, 1979; Boucot, 1975). When attempts are made to correlate over long distances, care must be taken. For example, comparing the stratigraphic range of the genus *Paraspirifer* from American and German sites, a discrepancy exists. The German *Paraspirifer* stratigraphic range commences lower (older) in the column than the American *Paraspirifer*. This may suggest that the genus migrated from the Old World to the Appalachian bio-province. On the other hand, at regional level, brachiopods have successfully shown resolution to the stage level or better (Ziegler, 1979).

8. ISOTOPIC EVOLUTION OF SEA WATER

Isotopes provide researchers with a powerful tool for deciphering the chemistry of past oceans which, in turn, can be utilized for constraining the paleoenvironmental variables. Carbonate minerals incorporate many of these isotopes (i.e. strontium, carbon and oxygen) from a parent solution, thus reflecting its chemistry. In other words, elements precipitated from sea water can ideally be used as a proxy for the isotopic chemistry of ancient oceans.

This chapter delves into the general theory behind utilization of strontium, carbon and oxygen isotopes as a proxy for ancient sea water composition throughout the Phanerozoic and discusses also some of the pitfalls, weaknesses and strengths inherent in the techniques.

8.1. The isotopic evolution of strontium in sea water

During the Phanerozoic, the isotopic composition of sea water strontium defines a trough with a minimum in the Jurassic and with superimposed higher order oscillations (Peterman et al., 1970; Burke et al.,1982; Stille et al., 1992)(figure 8-1). These higher order fluctuations reflect primarily the input of Sr from riverine, ground water, and hydrothermal sources (Veizer and Compston, 1974; Stille et al., 1992).

The residence time of Sr in sea water is on the order of 2-5 X 10^6 years and the oceanic mixing time is about 10^3 years. It is therefore reasonable to assume that the $^{87}Sr/^{86}Sr$ ratio is

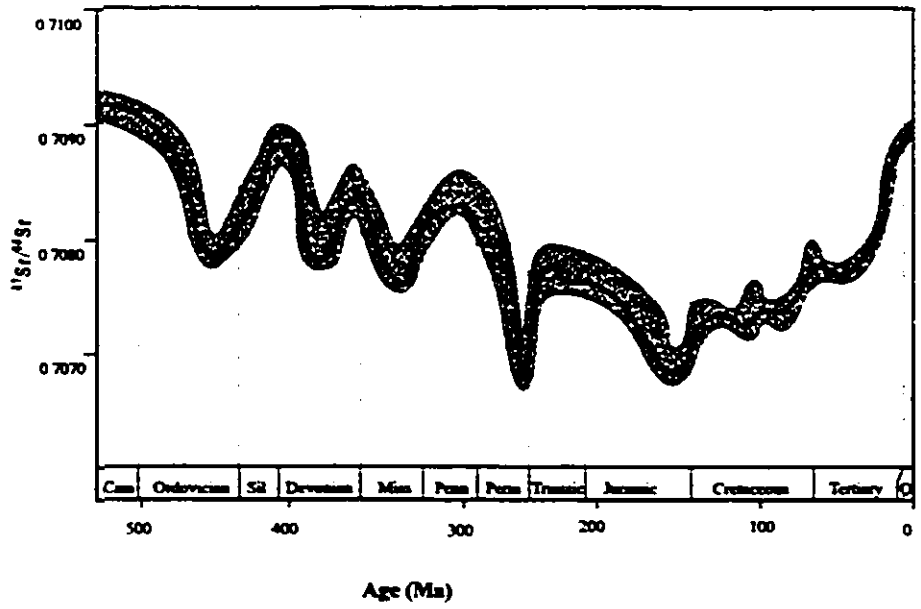

Figure 8-1. The variations of $^{87}Sr/^{86}Sr$ during the Phanerozoic. Modified from the original data of Burke et al. (1982).

uniform in sea water for any given time (Veizer and Compston, 1974; Burke et al., 1982; Stille et al., 1992). Temporal $^{87}Sr/^{86}Sr$ fluctuations of the magnitude of 10^{-4} are theoretically feasible for time intervals of 10^5 to 10^6 years, even for well mixed sea water, but only if an input from one source were greatly skewed. Nevertheless, it is more realistic to assume that the inputs from weaker sources will act as a buffer against the dominant source, restricting the amplitude of any such fluctuations.

8.1.1. Strontium fluxes for the oceans

The strontium isotopic ratio in marine water is buffered predominantly by the recycling

of marine carbonate rocks. Variations in isotopic composition of sea water predominantly result from changing the proportion of Sr delivered into the marine environment by volcanic fluxes relative to continental dominated weathering fluxes (Faure, 1986; Veizer, 1989). Large rapid changes, however, may only be possible from a compound effect, such as increased continental weathering in conjunction with decreased addition of $^{87}Sr/^{86}Sr$ from volcanic sources.

Sea water is continually receiving Sr from both riverine and ground water, as well as hydrothermal sources. Riverine sources give variable (figure 8-2) but high $^{87}Sr/^{86}Sr$ ratio which reflects the predominantly sialic nature of the continents (Burke et al., 1982). Sialic rocks, such as granites, are rich in ^{87}Sr. As these ^{87}Sr rich rocks erode, the Sr becomes part of the dissolved

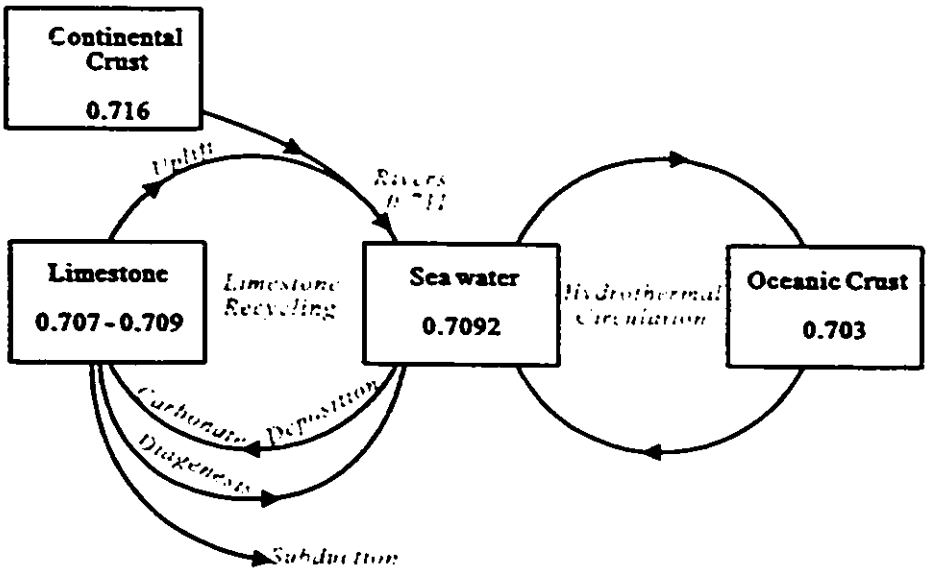

Figure 8-2. Box model for the marine geochemical cycle of strontium (modified from Palmer and Elderfield (1985), Hess et al. (1986).

load of the rivers, eventually being flushed into the ocean. However, the effect of erosion on the quantity and isotopic composition of Sr added to the aqueous system is complex. Strontium from sialic rocks is more susceptible to weathering than Rb due to the nature of their host minerals. For example, Rb is generally found in higher concentrations in weathering resistant minerals, such as mica and K-feldspars, whereas Sr rich minerals, such as plagioclase and calcite, are more prone to weathering. As a result, the $^{87}Sr/^{86}Sr$ ratio of the weathering solution is generally lower than that of the weathered rocks (Faure, 1986). The average $^{87}Sr/^{86}Sr$ ratio of the ground water flux (0.7110) is very similar to that of the riverine flux (0.7111), the consequence of a common sialic source, although this ratio in the latter can vary from 0.7045 to 0.943 (Veizer, 1989). Additional $^{87}Sr/^{86}Sr$ gets incorporated into the system through weathering of continental mafic and sedimentary rocks. The riverine signature is often dominated by the recycled sedimentary strontium, particularly from the dissolution of carbonates.

Hydrothermal sources within the ocean system strongly effect its $^{87}Sr/^{86}Sr$ ratio. The mantle derived Sr that is incorporated into the sea water via hydrothermal alteration at vents and by marine subaqueous weathering has low $^{87}Sr/^{86}Sr$ ratios. While the strontium concentration in sea water is not strongly effected by its circulation at Mid-Oceanic Ridges (MOR)(Palmer and Elderfield, 1985; Wadleigh and Veizer, 1992), the relative concentrations of each isotope is affected (Burke et al., 1982; Stille et al., 1992; Veizer, 1992). Plumes of hydrothermal waters near hydrothermal orifices show $^{87}Sr/^{86}Sr$ ratios that tend towards the "basaltic" value of 0.703 (figure 8-2). Sub-aqueous weathering may also decrease the Sr isotopic ratio of sea water. This

is due to the predominantly mafic nature of the ocean floor. In contrast, carbonate sediments and rocks formed within the oceans will generally incorporate Sr in equilibrium with sea water , thus not affecting the $^{87}Sr/^{86}Sr$ ratio during its reincorporation.

Atypical fluctuations may reflect localized $^{87}Sr/^{86}Sr$ values associated with hydrothermal activity, with proximity to a river mouth, or reflect localized restricted circulation in basins adjacent to continents (Clauer, 1981; Burke et al., 1982; Stille et. al., 1992). However, due to the fact that Sr concentration in sea water are almost 3 orders of magnitude higher than that of meteoric waters, most brackish waters with have the $^{87}Sr/^{86}Sr$ ratio of open marine sea water (Faure and Powell, 1972).

8.2. Isotopic evolution of carbon in sea water

The carbon isotope record for the Phanerozoic, based on carbonates, shows that the average carbon isotope ratio of sea water varied within a 3.0 per mil band. In the course of the Paleozoic, the isotopic record shows a strong ^{13}C enrichment trend, followed by a depletion during the Mesozoic and Cenozoic (figure 8-3). Superimposed on this are small second order fluctuations. Veizer (1992) felt:

> "These oscillations are probably caused by the relative proportions of C sequestered into carbonates and organic matter, respectively."

Added to this are possible local depositional, salinity, and paleogeographic factors affecting isotopic ratios. Additional mechanism that can cause the carbon isotope ratio to vary in the carbonate sample relative to sea water is vital effect that causes isotope fractionation during biotic precipitation of the shell.

8.2.1. Controls of carbon fluxes and temporal oscillations

The two dominant reservoirs of exogenic C are carbonate rocks and organic matter (Schidlowski et al., 1976; Veizer et al., 1986). Although these two reservoirs differ isotopically they are intrinsically linked. Photosynthesis preferentially absorbs ^{12}C resulting in a ^{13}C increase in sea water (Grossman et al., 1991). Carbonate rocks will generally incorporate the isotopically heavy C in equilibrium with sea water although the degree of enrichment will depend on the precipitated polymorph (Rubinson and Clayton, 1969). Aragonite will be enriched in ^{13}C relative to calcite. Some calcareous secreting organisms (particularly if their growth is rapid) will precipitate aragonite or calcite in disequilibrium with the dissolved carbonate of sea water, incorporating dissolved organic carbon (DOC) with its characteristic ^{13}C depleted signature (Goreau, 1977; McConnaughey, 1989; Gagan et al., 1994). Positive deviations in sea water $\delta^{13}C$ may reflect biomass expansion and burial of organic C. For example, strong $\delta^{13}C$ increase observable in the Devonian-Permian samples may reflect a rapid biomass growth associated with its expansion from a marine to a terrestrial environment (Brand, 1989a). Conversely, a decreases in oceanic $\delta^{13}C$ may reflect a decrease in biomass production. Gradual and abrupt environmental changes, such as glaciation may cause biomass fluctuations. Bolide impacts, causing mass extinction, may be another cause of such

rapid fluctuations, causing a $\delta^{13}C$ decline, as claimed for the Cretaceous-Tertiary (KT) boundary (Joachimski, 1993).

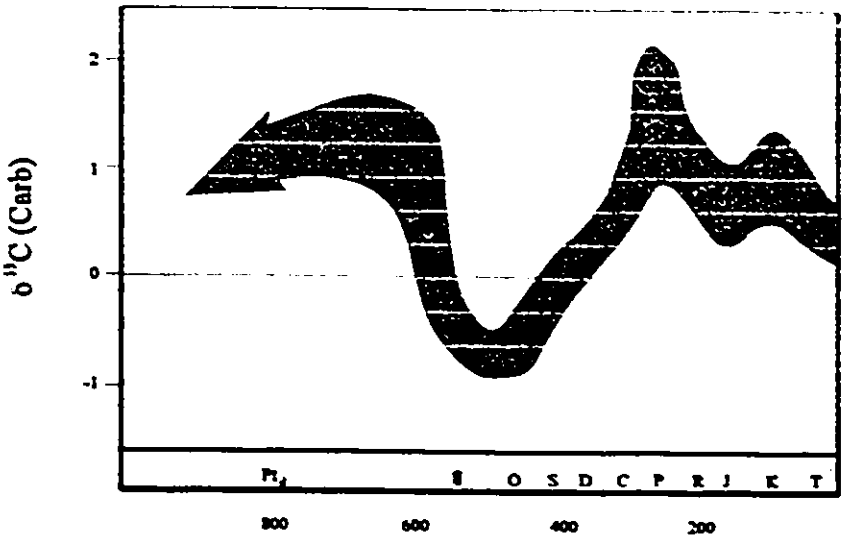

Figure 8-3. Secular variation of $\delta^{13}C$ (carbonate) through geological time. Modified from Veizer et al. (1980).

8.2.2. Spatial distribution

Studies of pelagic and benthic organisms suggest that the oceanic $\delta^{13}C$ ratios of DIC vary both vertically and horizontally (figure 8-4). These gradients are probably produced through evaporation, biogenic fractionation and organic matter fallout. However, it should be noted that the $\delta^{13}C$ ratios generally are fairly homogeneous within the wave base because of rapid mixing.

Evaporation causes preferential removal of ^{12}C in the water column causing the near surface

layer to be enriched in ^{13}C. This process is probably more important for horizontal gradients because evaporation is a surface feature. It may also be of importance for semi-restricted and restricted basins, such as the Red Sea.

Organic matter fallout is the most important process generating vertical gradient. This vertical gradient appears to be linked to the oxidation of organic matter as it settles through the water column (Grossman et al., 1991). Such process releases ^{12}C into sea water, causing ^{13}C dilution. As a result, sea water near the surface generally is isotopically heavier than the average and water at depth lighter (figure. 8-4)(Craig and Gordon, 1965; Kroopnick et al., 1972). In modern oceans, the production of cold, salty, and dense O_2 rich waters at high latitude produces density

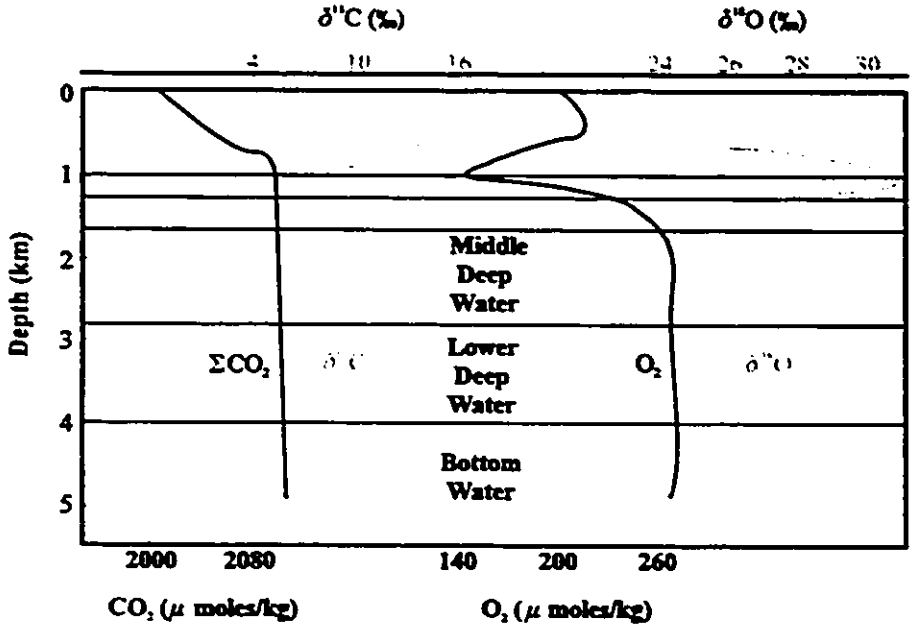

Figure 8-4. Changes in $\delta^{13}C$ of TDC (CO_2) and $\delta^{18}O$ of dissolved O_2 with depth for the North Atlantic Ocean. $\delta^{18}O$ in SMOW, $\delta^{13}C$ in PDB. From Kroopnick et al. (1972).

currents which migrate south (Kroopnick et al., 1972). As this water ages it collects more and more organic matter which oxidizes, releasing the ^{12}C and generating the ^{13}C depleted nature of the total dissolved carbon (TDC). In ancient oceans, the ocean dynamics may have differed. At times, dense waters may have formed by evaporation processes. Such stratified oceans would eventually turn over, bringing the deep, O_2 poor, water to the surface (Railsback, 1990). This would produce an anoxic environment which would hinder production of organic matter and therefore ^{12}C intake. It would also retard the flux of organic matter to the new deep dense water. However, it should be noted that this is only a model and may not represent a real ancient ocean dynamics.

In near shore locations, or in semi-restricted basins, subaerial weathering of outcrops may cause ^{12}C enrichment due to reintroduction of old organic carbon into marine ecosystems (Joachimski and Buggisch, 1993). Riverine fluxes rich in DOC will cause locally lighter waters in areas near the mouth of rivers or in areas where circulation is restricted. Grossman et al. (1991), comparing stratigraphically equivalent Pennsylvanian brachiopods, noticed a definite decrease in $\delta^{13}C$ values from Texas to New Mexico and finally Kansas. This was interpreted as being due to localized shifts in the DOC inputs, as a result of changes in ocean circulation during the formation of Pangea.

8.2.3. Vital effects

For all organisms secreting calcareous shells, metabolic CO_2 may be incorporated into $CaCO_3$. This may result in biogenic fractionation of C isotopes (figure.8-5). For instance,

photosynthetic calcareous algae are always depleted in ^{13}C, the result of photosynthesis which preferably incorporates ^{12}C into the $CaCO_3$ structure. Only a few organisms (brachiopods and foraminifers) are considered to precipitate $CaCO_3$ at or near equilibrium with sea water (Lowenstam, 1961, McConnaughley, 1989), but even for these organisms internal isotopic variations do exist (Veizer, 1992; Prasada and Green, 1993), probably a result of seasonal environmental changes in the carbon input. During spring runoff, increased DOC input from riverine sources may temporariiy decrease the ^{13}C content of near coastal waters which may be reflected in the C isotope ratio of the shell. Since the photosynthetic symbiotic algae preferentially incorporate ^{12}C, with the degree of incorporation dependent on the photic level (Goreau, 1977), many modern scleractinian corals have slightly heavier $\delta^{13}C$, because the ambient carbon pool is isotopically depleted by algal photosynthesis. This will also have an effect on other local metazoans. Since photosynthesis is seasonal for many regions, some observed $\delta^{13}C$ fluctuations may be seasonal. Research by Gagan et al. (1994) on modern corals suggests that annual coral mass spawning has a strong positive effect on the $\delta^{13}C$ signature. This annual ^{13}C spike could be reflected in the shells of other calcareous secreting organisms. Over the year, the $\delta^{13}C$ can fluctuate on the order of 1.5‰, producing a scatter across the growth rings of the shell.

The view that brachiopods precipitate their shells near equilibrium with ambient sea water is not universally held. There are well documented cases which suggest that brachiopods do fractionate C isotopically and that this biogenic fractionation is not consistent at the family or even genus level (Wefer, 1983; Popp et al., 1986; Veizer et al., 1986; McConnaughey, 1989; Rush and Chafetz, 1990; Carpenter and Lohmann, 1995). If true, then brachiopod utility for isotopic studies

is best contemplated at a single species or genus level (Veizer et al., 1986). Other researchers question the importance of vital effect, feeling that biogenetic fractionation is insignificant compared to lithologic and/or environmental induced variations (Brand, 1989a, b; Grossman et al.,

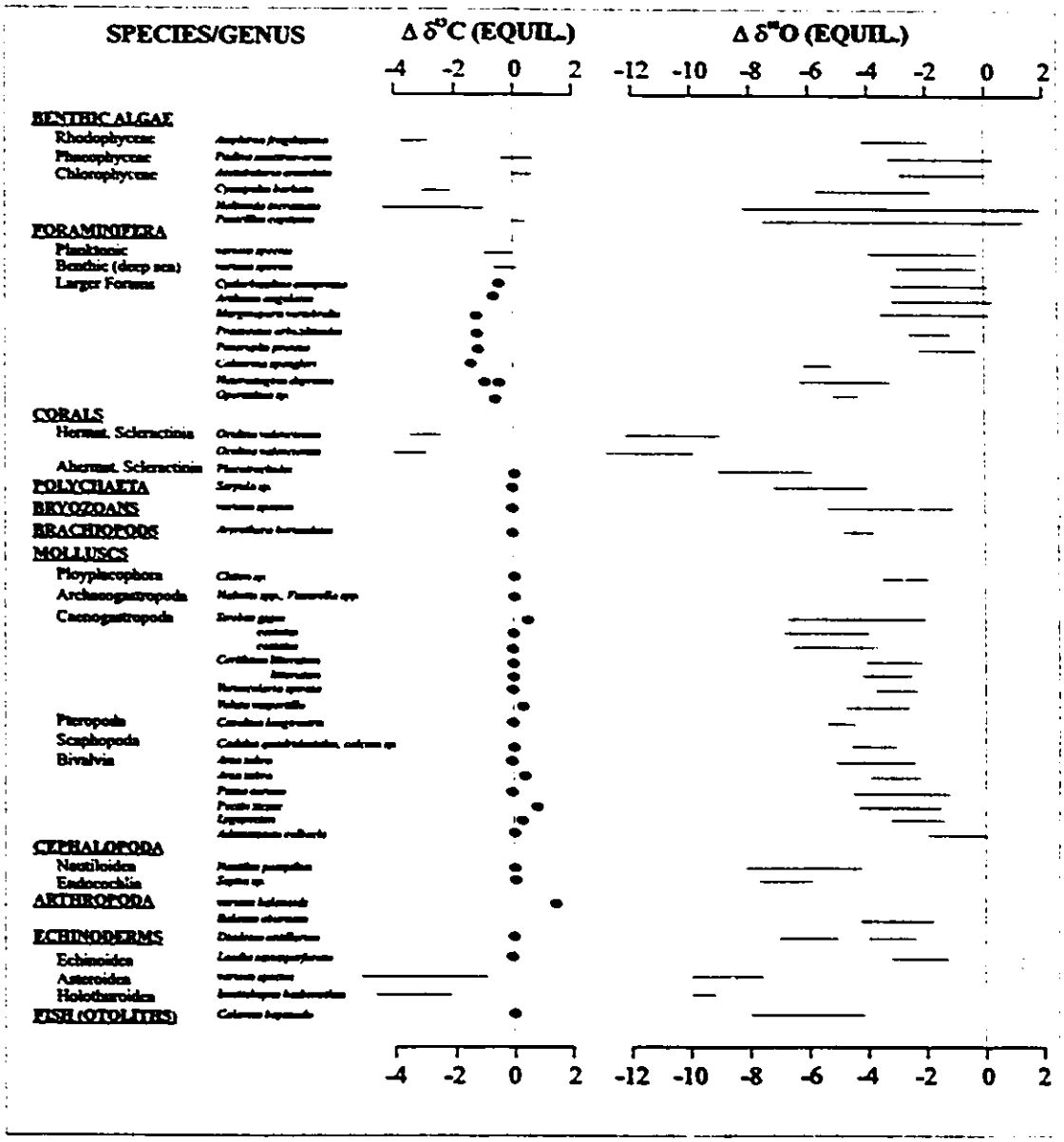

Figure 8-5. Summary graph of vital effects for various organisms secreting calcareous shells. Modified after Wefer (1985).

1991, 1993). In recent studies of Pennsylvanian brachiopods from Kansas, New Mexico and Texas, Grossman et al. (1991,1993) proposed that the observed isotopic differences were the result of habitat variability rather than of vital effects. They suggested that infaunal species incorporated carbon from pore-waters rich in DOC, while epifaunal varieties incorporated bottom water with a heavier isotope signal. Semi-faunal species had intermediate $\delta^{13}C$ values.

8.3. Isotopic evolution of oxygen in sea water

Oxygen isotope ratio in sea water typically varies both with depth as well as in response to temperature changes during freeze and thaw, to salinity gradients, and to kinetic effect during meteoric precipitation. The riverine input, and water mass interactions may also influence the $\delta^{18}O$ makeup of sea water (Craig and Gordon, 1965). As a result of influence by so many variables, the $\delta^{18}O$ values of all major marine and lacustrine bodies of water can vary greatly.

Isotopic data from $CaCO_3$ of the shells suggest that, in general, the $\delta^{18}O$ of the shells becomes more ^{18}O depleted with their increasing age; a trend particularly visible for the Paleozoic (figure 8-6)(Popp et al., 1986; Veizer et al., 1986; Lavoie, 1993). Superimposed on this general trend are higher order fluctuations due to local factors or, in some cases, perhaps to global events.

8.3.1. Dependency on temperature and salinity

Oxygen isotopes are very sensitive to fractionation by both chemical and physical processes.

In sea water, the most important factor controlling the evolution of oxygen isotopic ratios appears to be tectonic evolution (Walker and Lohmann, 1989). In other words, the water-rock interactions due to hydrothermal activity will increase the $\delta^{18}O$ value in the water, whereas weathering on continents or on the seafloor will deplete its $\delta^{18}O$ signature. This could explain the first order trend through the Phanerozoic, with the possible rates of change on the order of 1‰ per 10^8 years.

The temperature dependency of oxygen isotopes plays an intrinsic part in the process of isotopic fractionation. For example, a strong $\delta^{18}O$ increase in sea water can be generated at times of glaciation when ^{16}O is preferably sequestered into ice during freezing. The $\delta^{18}O$ of progressively colder water increases at a rate of approximately 1 per mil per 4° C (Adlis et al., 1988). However,

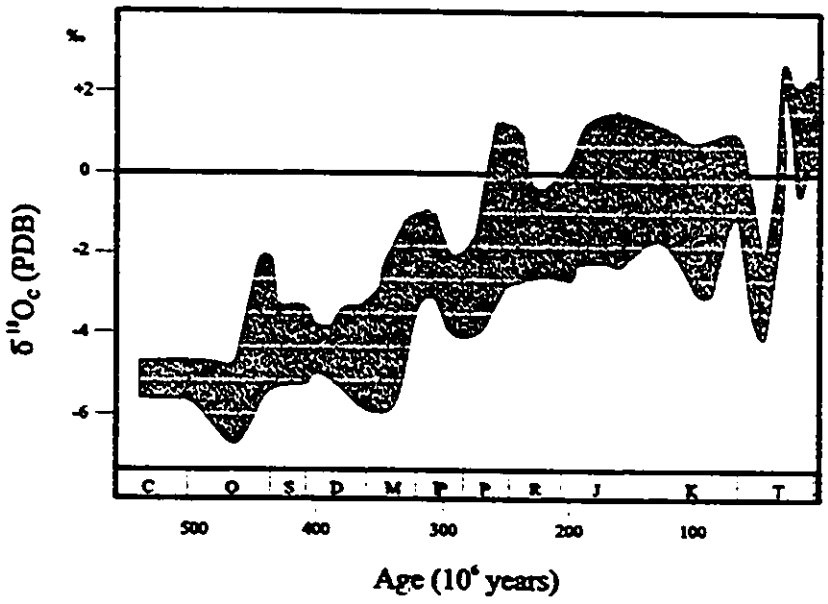

Figure 8-6. Range of oxygen isotopic composition of well-preserved marine macrofossils. Summarized from Hudson and Anderson (1989).

the rate is dependent on the mineralogy of the precipitate, with aragonite being enriched in ^{18}O of up to 1‰ relative to calcite (Tarutani et al., 1969).

Mixing above wave-base homogenizes $\delta^{18}O$ in near surface waters. However, the $\delta^{18}O$ values generally increase below the mixed layer to a point just below the oxygen minimum zone (O^{min}). Above the O^{min} zone, ^{16}O consuming bacteria produce a relative sharp increase in $\delta^{18}O$ levels. Below, the concentration of bacteria drops drastically to the level in stabilized deep and bottom waters (figure. 8-4)(Kroopnick and Craig, 1976). It should be noted, that these depth profiles do vary slightly, depending on the ocean and profile location, but overall the trends persist. Large discrepancies, however, can be observed in semi-restricted basins, such as the Mediterranean, where strong evaporation can produce a sharp spike in the $\delta^{18}O$ of near surface waters (Thunell et al., 1987). These profiles may perhaps serve as approximate analogs to some ancient oceans where deep water circulation might have been driven by evaporation processes.

During evaporation and precipitation, $^{18}O/^{16}O$ fractionation follows a process known as Rayleigh's Law.

$$R_t = R_o f^{(x-1)}$$

Where R_t is $\delta^{18}O$ at time t, R_o is initial $\delta^{18}O$, f is the fraction of vapour remaining in the cloud, and x is the fractionation factor. As evaporated ^{16}O rich water vapour rises, it cools and begins to condense into clouds, producing reverse equilibrium fractionation. As the water droplets form, they preferentially incorporate the heavy ^{18}O, increasing the already ^{16}O rich nature of the residual water

vapour. This process continues as the clouds rise. This produces a gradient which is steeper over continents than over the oceans due to land-mass topography that forces clouds to rise and cool more rapidly (Gat, 1980; Hays and Grossman, 1991). In the ocean, the remaining water is enriched in ^{18}O and also has a higher salinity. The salinity caused $\delta^{18}O$ enrichment effect can approach 8‰ in some hypersaline waters, the general relationship being 0.1‰ $\delta^{18}O$ per 1‰ increase in salinity between 0 and 80‰ (Ferronsky and Brezgunov, 1989; Anati and Gat, 1989).

Precipitation incorporated into runoff and ground water regimes shows the ^{18}O depleted nature of the water vapour. Runoff incorporated into riverine and lake systems eventually returns to the oceans, potentially causing the sea water to be locally ^{18}O depleted.

The $^{18}O/^{16}O$ ratio of the ocean water is partly related to global ice volume. As already discussed, ice preferentially incorporates ^{16}O, resulting in an isotopically heavier composition of the remaining sea water. During warm periods, ice will melt producing less saline and isotopically light melt waters (Prasada and Green, 1993). This, in turn, may result not only in localized $\delta^{18}O$ fluctuations, but can also generate global changes in $\delta^{18}O$ of sea water during transition from glacial to interglacial periods. For example, during the Pleistocene glaciation, the $\delta^{18}O$ of sea water was lighter by as much as 1‰ (Fairbanks and Matthews, 1978), if compared to today. Note also that inputs of large quantities of glacial melt water will also result in sea level rise and transgressions (Grossman et al., 1991).

8.3.2. MOR interactions

Water typically becomes isotopically heavier when it interacts at high temperature with silicate rocks during hydrothermal processes on the seafloor (Veizer et al., 1986; Walker and Lohmann, 1989; Lavoie, 1993). From model considerations, the rate of change of 1 per mil for 10^8 years has been proposed by Walker and Lohmann (1989). Others (e.g. Muehlenback and Clayton, 1976), argue that sea water $\delta^{18}O$ is perpetually buffered by such phenomena at ~0‰ SMOW. Regardless of the model, the observed sharp $\delta^{18}O$ fluctuations cannot be accounted for by hydrothermal interactions alone. It does seem likely therefore that a combination of hydrothermal interaction of sea water at MOR's, temperature and salinity is required to explain the $\delta^{18}O$ fluctuations throughout the Phanerozoic.

8.3.3. Causes of the secular trend in $\delta^{18}O$ of paleoseawater

Four main theories attempt to explain the $\delta^{18}O$ secular trend observed in marine sediments. These are: 1) diagenetic reequilibration (Degens and Epstein, 1962; Killingley, 1983), 2) warmer Palaeozoic oceans (Knauth and Epstein 1976; Karhu and Epstein 1986), 3) secular variation in the oxygen isotopic composition of sea water with time (Popp et al., 1986; Veizer et al., 1986; Veizer, 1992; Wadleigh and Veizer, 1992); and 4) formation of a stratified ocean (Railsback, 1990).

In a study of Tertiary foraminifers, Killingley (1983) felt that diagenetic overprinting coupled with changes in ocean water temperature and by ice-buildup, were the most important

factors controlling the $\delta^{18}O$ of sea water. He argued that reequilibration with pore-water, while not completely destroying the primary signal, could account for many of the short term abrupt $\delta^{18}O$ fluctuations.

One model, based on coexisting chert and phosphates, suggests that the secular isotopic variation are mostly reflecting past climatic fluctuations. Temperatures of up to 52°C for the Precambrian, and 40°C for portions of the Palaeozoic, have been proposed by Karhu and Epstein (1986). They felt that rapid $\delta^{18}O$ changes, of up to 3-5 per mil, could not have been caused by changes in isotopic composition of sea water. On the other hand, it is hard to justify such high temperatures for global oceans at times of widespread glaciations. Furthermore, despite the fact that some simple procaryotes and protozoa can survive of temperatures of 40° C and higher, complex metazoans cannot. A probable upper limit for aquatic vertebrates is likely 38°C (Brock, 1985). Finally, considerations based on radiation balance suggest that a more likely upper limit for sea water temperature is approximately 31°C (Newell and Dopplick, 1979).

One of the most widely held views is that the O isotopic composition of sea water varied with time. Temperature, salinity, and tectonic activity are just some possible factors which can result in $\delta^{18}O$ variations of the type seen in (bio)chemical sediments. For example, abrupt shifts in $\delta^{18}O$ at the end of the Palaeozoic correspond to similar shifts in carbon isotope ratios (Brand, 1989a). In a similar manner, the observed ^{18}O enrichment in high latitude Permian samples from Tasmania suggest possible localized glacial cold water influx (Prasada and Green, 1993).

A relatively recent hypothesis developed by Railsback (1990) suggests that during times of interglacial warm seas, strong evaporation could result in salinity/density turnovers. Since most of the sampling to date has occurred only at shallow depths, and therefore represents only a small portion (approx 6%) of the ocean volume, it is difficult to evaluate the overall trends from such a restricted database. This is definitely a hypothetical model, developed from relatively few data that should be taken with great reservation.

9. DIAGENETIC ALTERATION OF BRACHIOPOD SHELLS

Diagenesis is the single most important post-depositional factor influencing the isotopic and trace element composition of brachiopod shells.

9.1. Major and trace element alteration

Brachiopods are composed of low-Mg calcite, the most stable calcite polymorph and therefore the most resistant to alteration. However, diagenetic alteration of shell material is a common feature of fossils. It is therefore important to understand its effect on the chemistry of the shell. Most brachiopod shells typically have some luminescence which may signify diagenetic alteration. Often the primary layer is luminescent while the secondary and tertiary layers may or may not show luminescence, suggesting that the primary layer is more susceptible to diagenetic alteration. Mn is often enriched during meteoric water diagenesis and it is this enrichment which causes the luminescence. At the same time, a high Fe content masks the luminescence (Meyers, 1974). There is now evidence suggesting that luminescence is controlled by complex trace element patterns and not just by Fe-Mn interactions (Popp et. al., 1986).

Elemental Ca, Fe, Mg, Mn, Na, S and Sr concentrations can be used as additional constraints on shell preservation (Brand, 1989a). According to research done by Brand and Veizer (1980), Sr, Na, and possibly Mg concentrations should decrease, while Fe and Mn concentrations should increase in the course of diagenetic alteration (figure 9-1). The

determining factor controlling the direction and magnitude of change is the nature of the pore waters and the duration and depth of burial. This was briefly touched upon in chapter 4.2.2.

It should be noted that variations in lithology and paleoenvironmental factors may also influence the concentration of various elements within brachiopod shells (Brand, 1989a). Some samples which would normally be inferred altered due to high trace element concentrations may in fact just represent coeval environmental control.

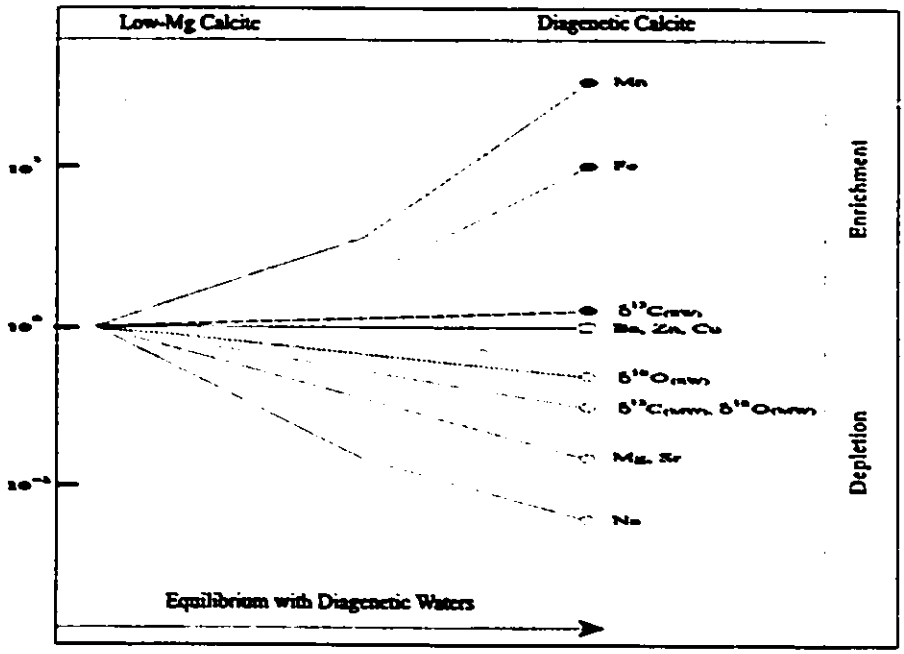

Figure 9-1. Summary of direction and magnitude of elemental and isotopic change with progressive post-depositional alteration. (SW)= sea water, (MW) = meteoric water. From Veizer (1983).

9.2. Preservation of the isotopic signal

9.2.1. Diagenetic effect on strontium

Diagenesis will normally deplete the Sr concentration in samples but either increase the $^{87}Sr/^{86}Sr$ ratio or leave it unaffected (Veizer and Compston, 1974; Burke et al., 1982). This is dependent on the source of the diagenetic fluid, usually of meteoric origin (Veizer, 1992). Such meteoric solutions will have incorporated ^{87}Sr from Rb rich sialic rocks and this will result in the diagenetically altered material becoming enriched in ^{87}Sr.

Sea water derived diagenetic fluids, on the other hand, generally effect the isotopic ratio little because the sources of the diagenetic fluid and of the solution that originally precipitated the shell are similar, but the subsequent post-depositional isotopic shift may be of variable magnitude. As the ratio of meteoric water/sea water in the intervening pore space increases, there will be an associated diagenetic increase in the Sr isotopic ratio of a shell.

The are rare occasions where the diagenetic fluids will decrease the Sr isotope ratio. This occurs with diagenetic solutions which infiltrate environments dominated by mafic volcanic or volcaniclastic sediments. The ^{87}Sr depleted nature of these rocks will modify the surrounding solutions. As the fluid migrates, it may subsequently affect the Sr isotope ratio of the proximal rock types.

In general, post-depositional recrystallization of the shells usually result in depletion of Sr, but the Sr isotope ratio frequently will not be affected due to the buffering effect of the recrystallizing carbonate phase (Burke et al., 1982; Veizer, 1992).

9.2.2. Diagenetic effect on carbon isotopes

Alterations which lead to trace element changes often are accompanied by $\delta^{13}C$ changes. The source of the diagenetic fluid is important when considering the direction of $\delta^{13}C$ shift (figure 9-1). Typically, the $\delta^{13}C$ of the shell is depleted when the diagenetic fluid is meteoric water that has generally high concentrations of DOC inherited from the terrestrial biomass that is enriched in ^{12}C. When diagenetic fluid is of sea water origin, the $\delta^{13}C$ shift will be only slight (Brand 1989a,b). Consequently, the magnitude of diagenetic overprint will depend upon the relative proportions and mixing of meteoric and sea water in the diagenetic solution.

9.2.3. Diagenetic effect on oxygen isotopes

Diagenetic alteration of a shell will usually result in ^{18}O depletion (figure. 9-1)(Brand, 1989a, b; Grossman et. al., 1991; Veizer, 1992). The magnitude of this depletion will depend on the textural and chemical composition of the material and the source of the diagenetic fluid. Marine diagenesis typically influences samples only at shallow depths. As samples are buried to greater depths, the influence of meteoric water will increase. The oxygen isotope ratio found in meteoric water is typically very depleted due to Rayleigh distillation processes that generate

progressively more ^{18}O depleted precipitation as the water vapour moves inland (Veizer, 1992). A concomitant increase in temperature with the depth of burial also results in ^{18}O depletion in the precipitated carbonates.

10. RESULTS OF STUDY

10.1. Transmitted light results

A total of 189 samples were collected for this project. Seventy-four of these were considered to be texturally altered from optical studies based on binocular microscope. The rejected samples included all from the Ladrona Formation in Spain and 5 samples collected in France. The remaining 115 samples, a few sampled twice, had a fibrous secondary shell layer often with a pearly luster.

10.2. Brachiopod identification

A total of 122 specimens from four orders were studied (Appendix 2, table 2). The order Rhynchonellida accounts for the 46.8 % of the shell material or 58 specimens, Spiriferida for 39.5 % or 49 specimens, Strophomenida for 8.9 % or 11 specimens and Pentamerida for 4.8 % or 6 specimens. The rhynchonellids were found at all localities, spiriferids and strophomenids were also found everywhere but the western Urals, and the pentamerids are only from the western Urals.

10.3. Scanning electron microscope (SEM) results

Fourteen samples were studied under SEM in order to evaluate the state of their textural

preservation, with particular emphasis placed on New York State samples. Random checks were applied to the other sampled regions. The usual magnification was 3000. The New York State samples showed moderate to high textural degradation (Plate 1b, c), but samples from the other regions, with the exception of RA- 9, showed moderate to "pristine" textural preservation. Sample LV4-6 from Spain showed the highest degree of textural preservation (Plate 1a).

10.4. Cathodoluminescence results

Cathodoluminescence was used as an additional test, particularly for samples from Spain, with a total of 30 samples tested. Nine of these were from the Ladrona Formation in Spain and they were rejected from further consideration because of their cathodoluminescence patterns as well as the high silicification. The luminescence in the remaining 21 samples ranged from non-luminescent to moderately dull.

10.5. Major and trace element results (Ca, Mg, Sr, Mn and Fe)

One hundred and twenty-one samples were analysed for major and trace elements (Appendix 2, table 2) calcium, magnesium, iron, strontium, manganese and barium. Calcium concentrations ranged from 36.73% to 39.49 %, with an average of 38.80%. The standard deviation for the entire population was 0.004%. Magnesium concentrations ranged from 0.07% to 0.50%, with an average of 0.22%. Trace element concentrations varied, with iron ranging

Plate 1a. SEM photo of sample LV4-6 from Spain showing well preserved textural features. Magnification 3000X at 15 kV.

Plate 1b. SEM photo of sample AH-39 from New York State showing moderate preservation. Predominant textural features are the longitudinal calcite fibres with some early, small scale dissolution features. Magnification 3000X at 15 kV.

Plate 1c. SEM photo of sample AH-11 from New York State showing poor textural preservation. The fibrous calcite has underwent dissolution to such an extent that only the vague outline of the original fibrous calcite is distinguishable. Magnification 3000X at 15 kV.

1a)

1b)

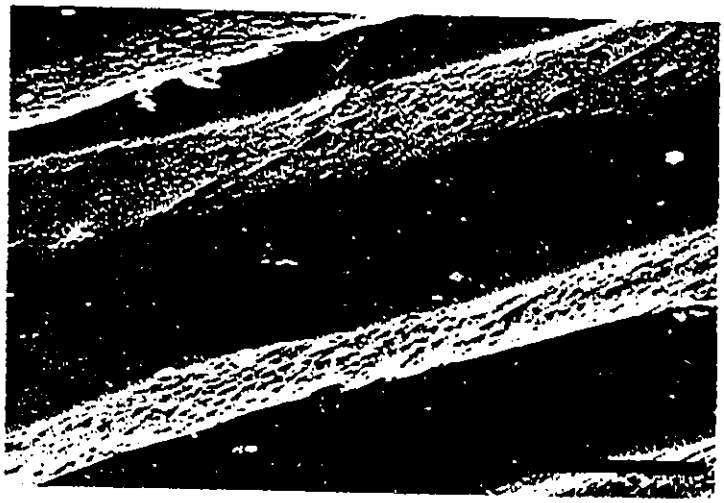

1c)

from 369 to 14139 ppm, average 1705 ppm and standard deviation 1912 ppm; strontium from 618 to 2144 ppm, average 1283 ppm and standard deviation 386 ppm; manganese from 4 to 2234 ppm, averaging 197 ppm and standard deviation 334 ppm; and barium from 16 to 376 ppm, averaging 39 ppm, and standard deviation 37 ppm.

In order to test the degree of chemical and textural preservation, strontium versus manganese concentrations were cross plotted by region and by brachiopod order and compared to modern brachiopods. The results are shown in figures 10-1, 2. By region, 86 percent had Sr and Mn results similar to modern brachiopods, as judged from the ranges proposed by Morrison and Brand (1986) and Qing and Veizer (1994). The R^2 values for each region ranged from a low of 0.01 to a high of 0.23 for samples from Russia. By brachiopod order, the R^2 values range from 0.01 to 0.42 with the R^2 values related to group the size. The larger the population the smaller the R^2 value, indicating that brachiopods do not control Sr and Mn concentrations at the order level. The data are not sufficiently numerous to test the role of vital effect at the genus or species level.

Fe results were not utilized as a selection criteria for sample preservation, due to contamination during analytical handling of the samples.

10.6. Isotope results (Sr, C and O)

Fifty-three samples were analysed for $^{87}Sr/^{86}Sr$, with values ranging from 0.70782 to

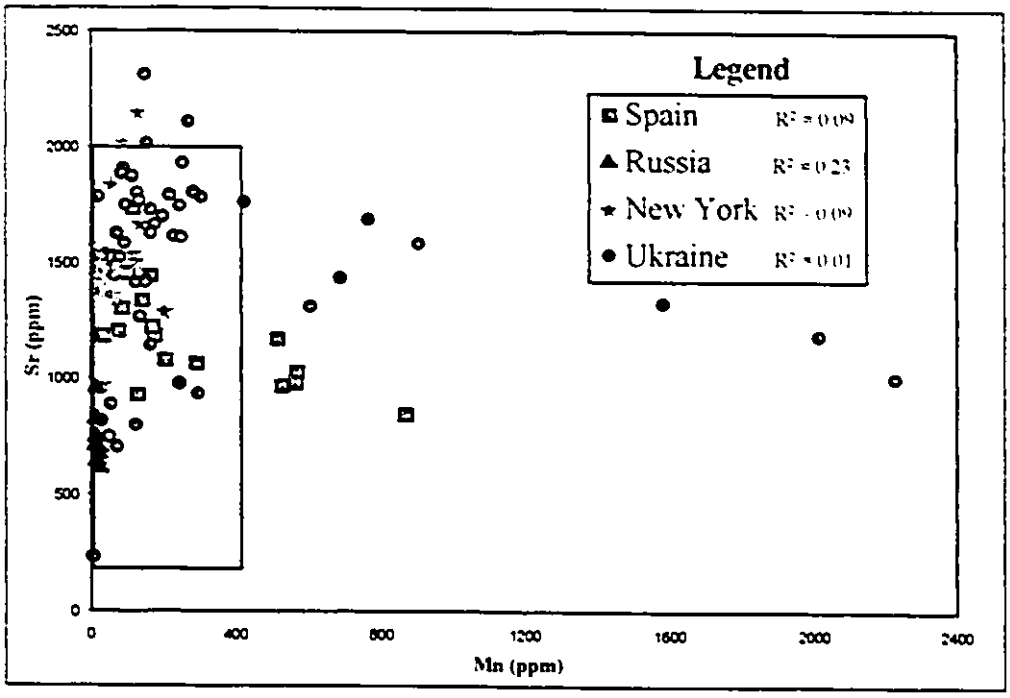

Figure 10-1. Scatter diagram of Mn versus Sr concentrations for Lower Devonian brachiopods plotted by region. 120 samples.

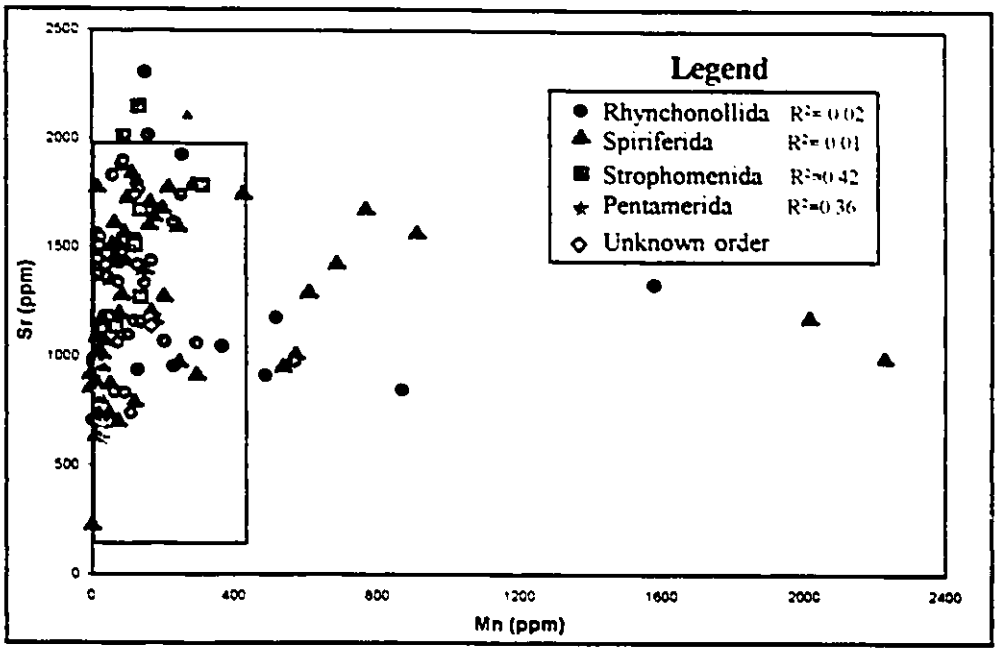

Figure 10-2. Scatter diagram of Sr versus Mn concentrations for Lower Devonian brachiopods plotted by brachiopod order. 120 samples.

0.709486 (Appendix 2, table 2). The distribution of well-preserved samples include one from the Pridoli, 29 from the Lochkovian, 5 from the Pragian and 18 from the Emsian. An average of 0.708477 and a standard deviation of $3.5X10^{-4}$ was calculated for the 53 samples. The strontium isotope trend decreases from the Pridoli to the Emsian (figure 10-3). In detail, the Pridoli and Lochkovian trend shows only minor variations around a value of 0.70870. During the Pragian, the slope steepens, followed by flattening towards the Emsian - Eifelian boundary. The three outliers in the data set were also plotted, but not used to construct the strontium isotope curve.

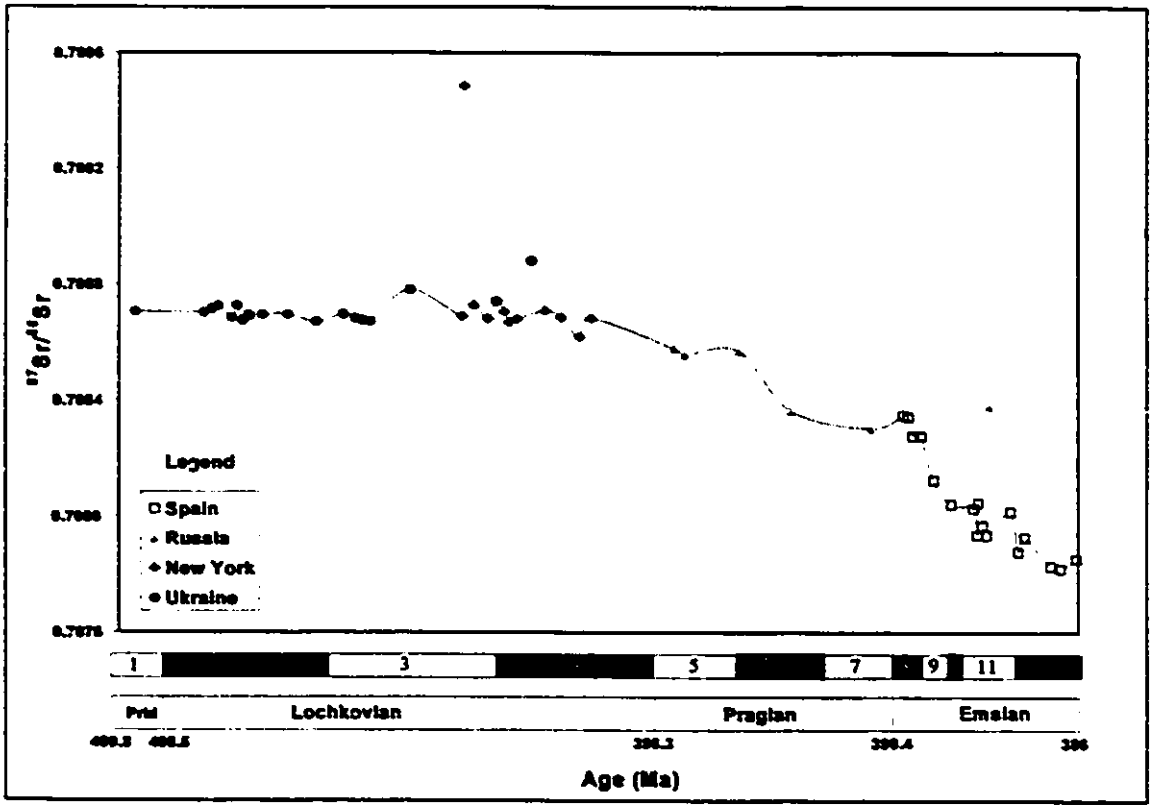

Figure 10-3. $^{87}Sr/^{86}Sr$ plot for 53 Lower Devonian brachiopod shells. Conodont biozones numbered 1-12: 1-*eosteinhoznensis*, 2-*woschmidti*, 3-*postwoschmidti*, 4-*pesavis*, 5-*sulcatus*, 6-*kindlera*, 7-*pirinea*, 8-*dehiscens*, 9-*gronbergi*, 10-*laticosti*, 11-*serotinus* and 12-*patulus*.

One hundred and ten samples were analysed for $\delta^{13}C$, with results ranging from -1.49 to 5.5 ‰ (VPDB) (Appendix 2, table 2). The population of well-preserved samples includes 2 for the Pridoli, 48 for the Lochkovian, 8 for the Pragian and 33 for the Emsian. The remaining 19 samples were altered and therefore not plotted. The samples had a calculated average of 1.48 ‰ and a standard deviation of 1.17 ‰. The carbon isotope trend (figure 10-4) through the Lower Devonian is characterized by a flat slope. The majority of the data fall within ±1.5 ‰ of the mean value.

One hundred and ten samples were analysed for $\delta^{18}O$ with results that range from -8.84 to -1.89 ‰ (VPDB) (Appendix 2, table 2). The temporal distribution of well-preserved samples is the same as for carbon isotopes. The average for all samples is -5.07 ‰ , with a standard deviation of 1.61 ‰. The oxygen isotope trend for the Lower Devonian (figure 10-5) is characterized by a relatively flat slope, with the exception of the New York State samples which tend to be more depleted in ^{18}O. The cause for this discrepancy can be either a higher degree of post-depositional alteration for the New York State samples, or it may reflect original variations in environmental parameters, such as ambient temperature. At the outset, I will utilize trace element criteria to test the degree of chemical preservation of these shells.

The plots of $\delta^{18}O$ and $\delta^{13}C$ versus Sr (figure 10-6, 10-7) show, in general, no correlation of these variables, with strontium contents comparable to values expected for calcite in equilibrium with sea water (≥ 1000 ppm, Veizer, 1983). This suggests that, as a group, the samples do not suffer from a large degree of recrystallization and the observed scatter can be

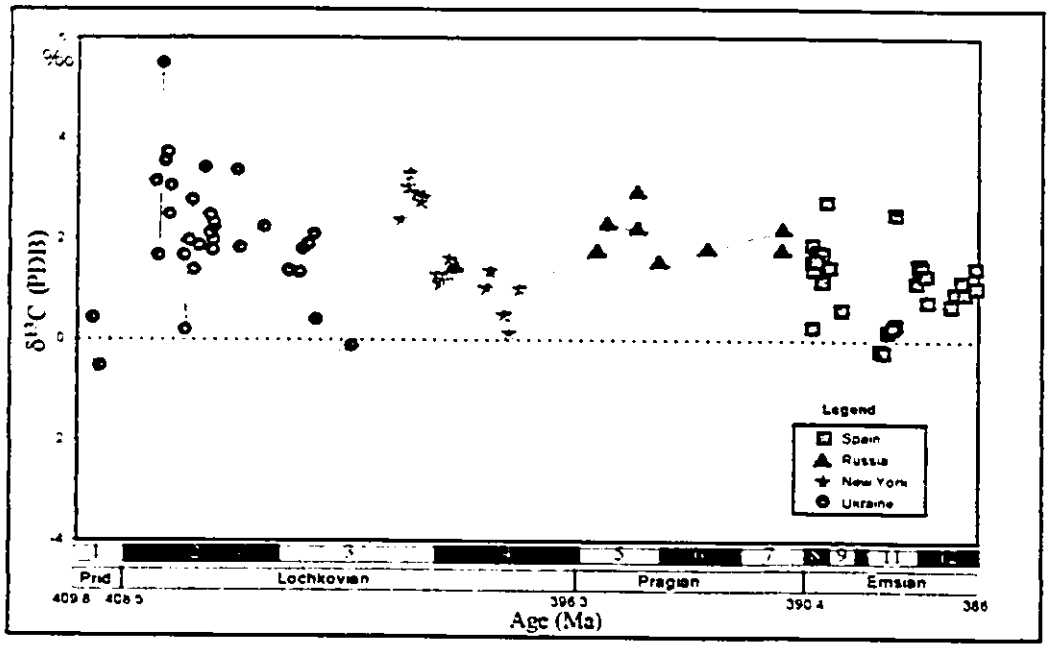

Figure 10-4. δ ^{13}C variations for Lower Devonian brachiopods (secondary shell layer). Conodont biozones the same as figure 10-3. 88 samples.

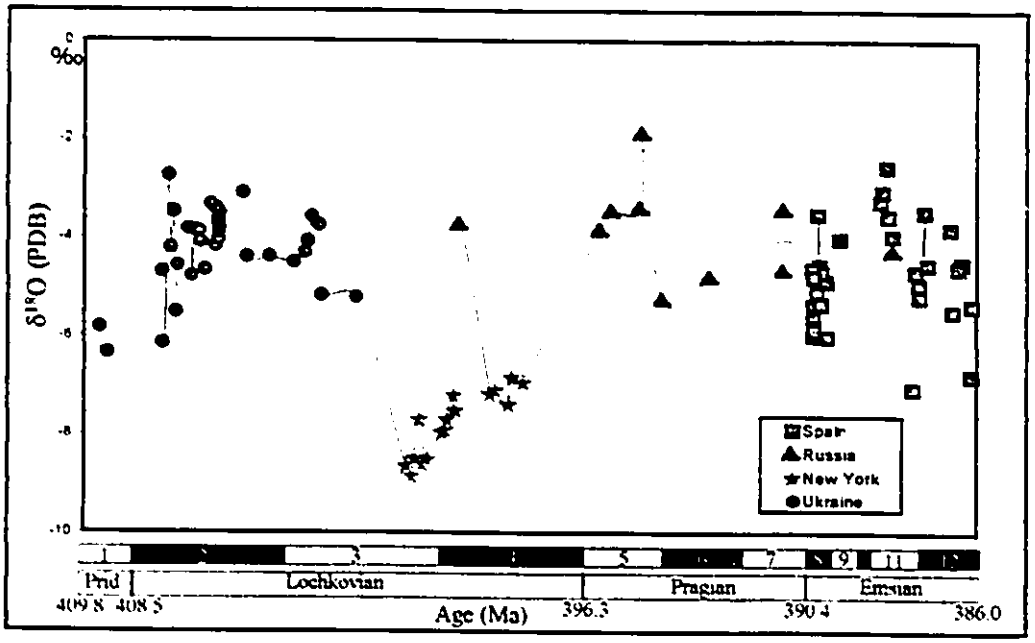

Figure 10-5. δ ^{18}O variations for Lower Devonian brachiopods (secondary shell layer). Conodont biozonation the same as figure 10-3. 88 samples.

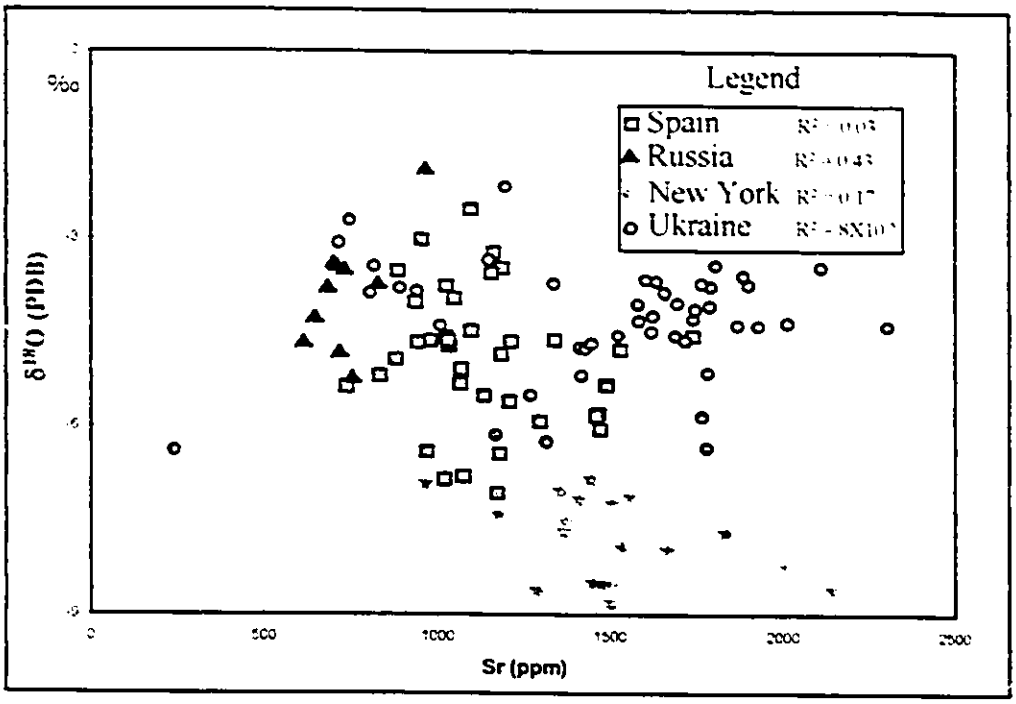

Figure 10-6. Scatter diagram of Sr concentration versus δ ^{18}O for Lower Devonian brachiopods plotted by region. 94 samples.

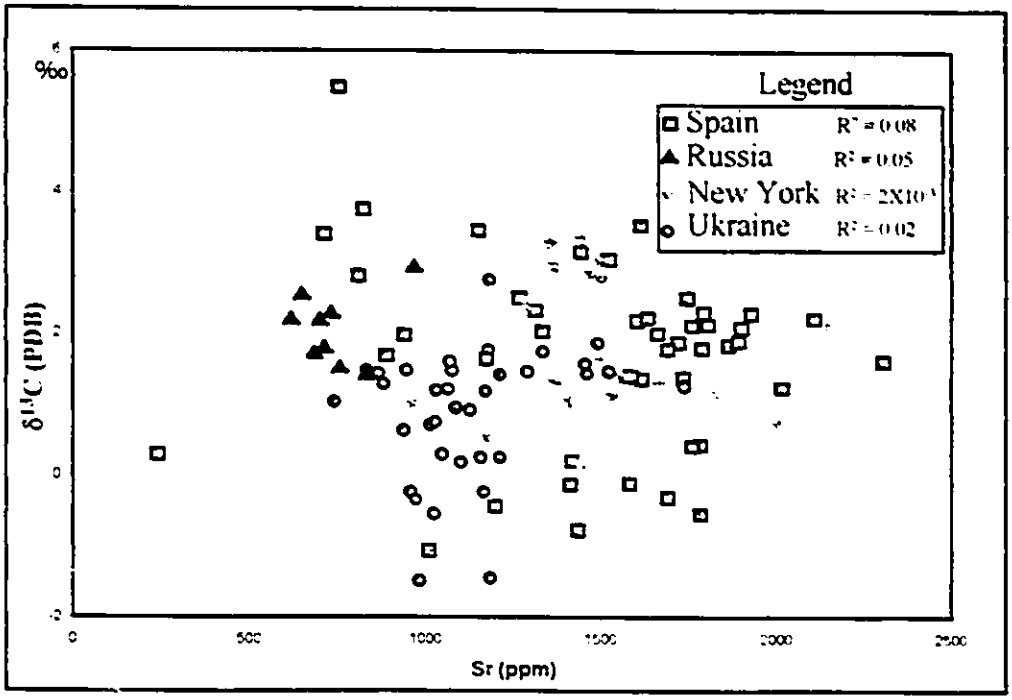

Figure 10-7. Scatter diagram of Sr concentration versus δ ^{13}C for Lower Devonian brachiopods, by region. 94 samples.

for the most part an inherited original property of the studied brachiopod population. Manganese is a more sensitive indicator of alteration than either strontium or stable isotopes, due to a large difference in Mn concentrations of sea and meteoric waters (figure 9-1) and the Mn concentrations, in some samples are in excess of expected equilibrium values for marine calcite (≥ 80 ppm) (figure 10-8), suggesting some degree of post-depositional alteration.

Overall, and in particular when larger populations are considered, there is no clear cut patterns or correlation between $\delta^{18}O$ and $\delta^{13}C$, regardless whether considered by location (figure 10-9), age (figure 10-10) or by brachiopod orders (figure 10-11). This again supports the proposition that overall the studied brachiopod population reflects the inherited scatter of the original isotope signal and indicates also that this scatter is not principally due to vital fractionation. However, this does not preclude the possibility of isotope fractionation due to vital effect at the genus or species level.

Due to this inherent scatter of data, coupled with the uncertainties of interregional correlation at resolution higher than a biozone, the temporal trends were therefore replotted as lower resolution curves (figure 10-12, 10-13). These curves represent more realistic estimates of the resolution available for global correlations. Note, nevertheless, that the bands that delineate the present data are far narrower than the ones available previously; a feature well illustrated by comparison with the Burke et al. (1982) trend.

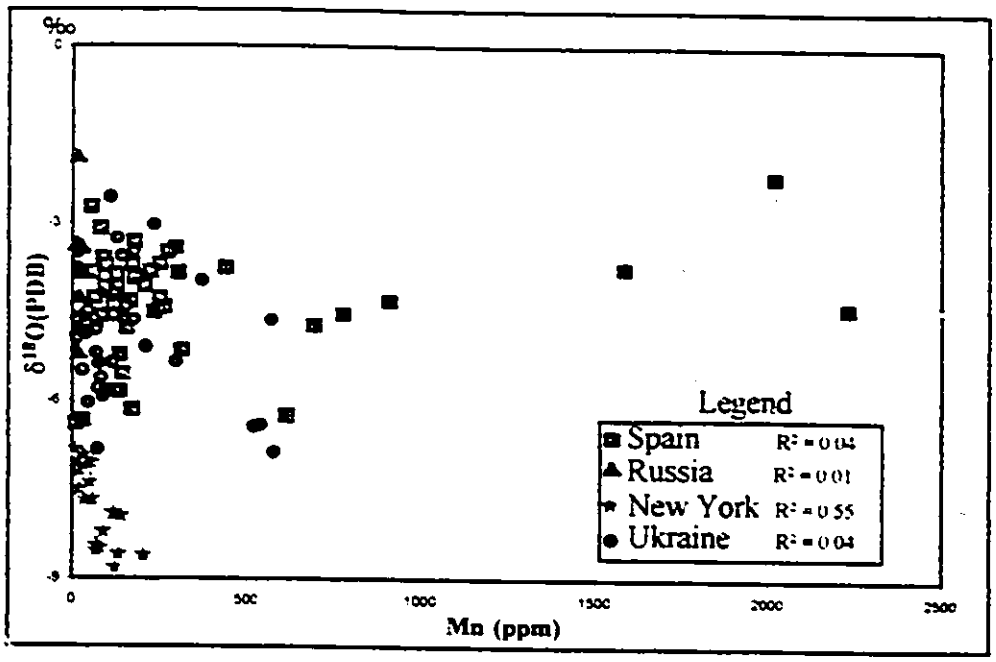

Figure 10-8. Scatter diagram of Mn versus δ ^{18}O for Lower Devonian brachiopods plotted by region. 94 samples.

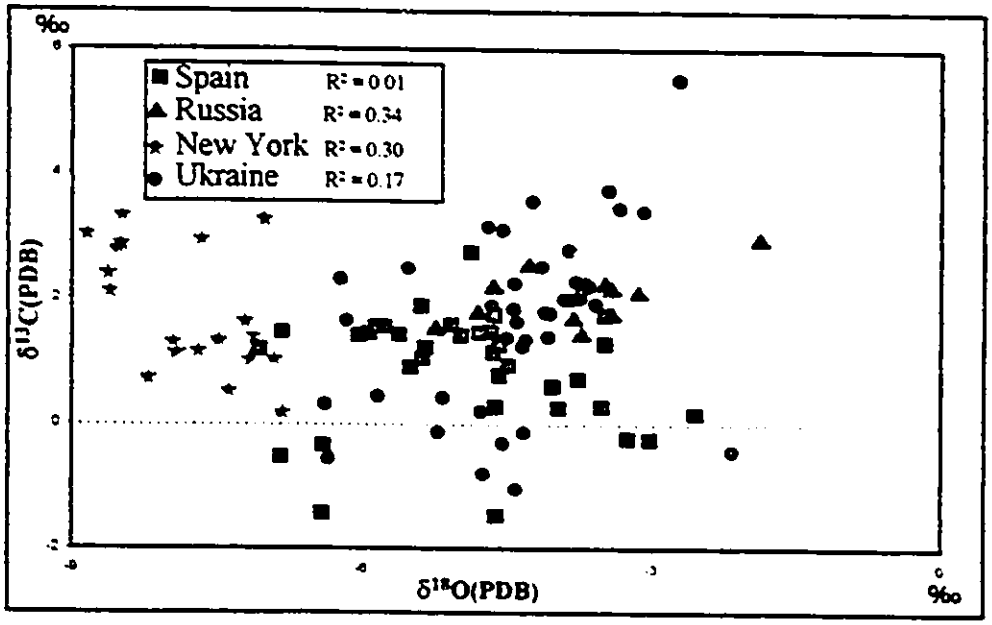

Figure 10-9. Scatter diagram of δ ^{13}C versus δ ^{18}O for Lower Devonian brachiopods plotted by region. 94 samples.

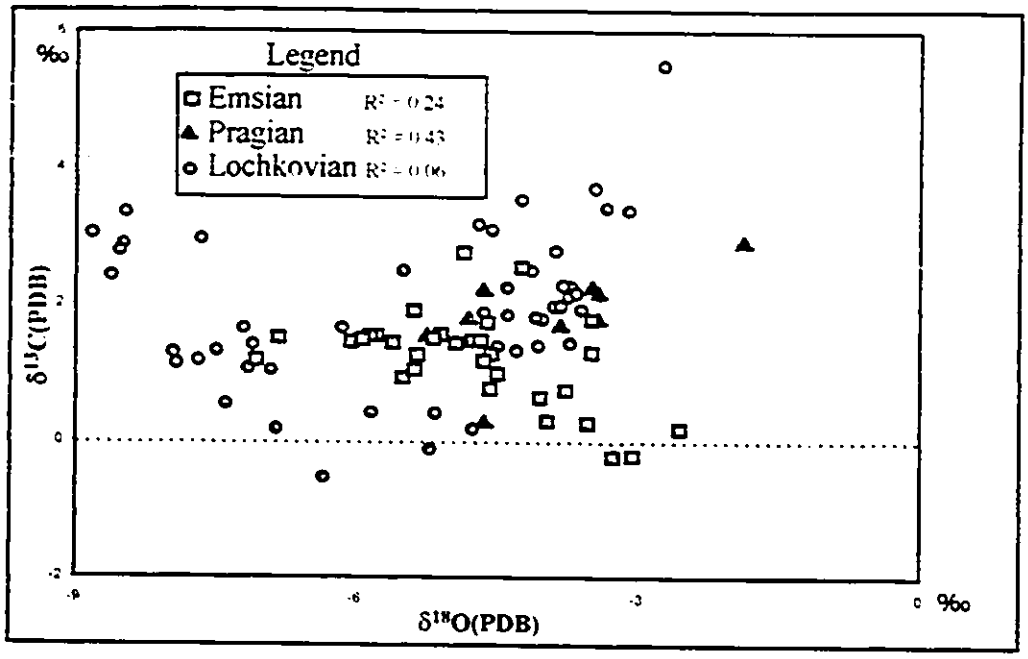

Figure 10-10. Scatter diagram of $\delta^{18}O$ versus $\delta^{13}C$ for Lower Devonian brachiopods. Plotted by stage. 94 samples.

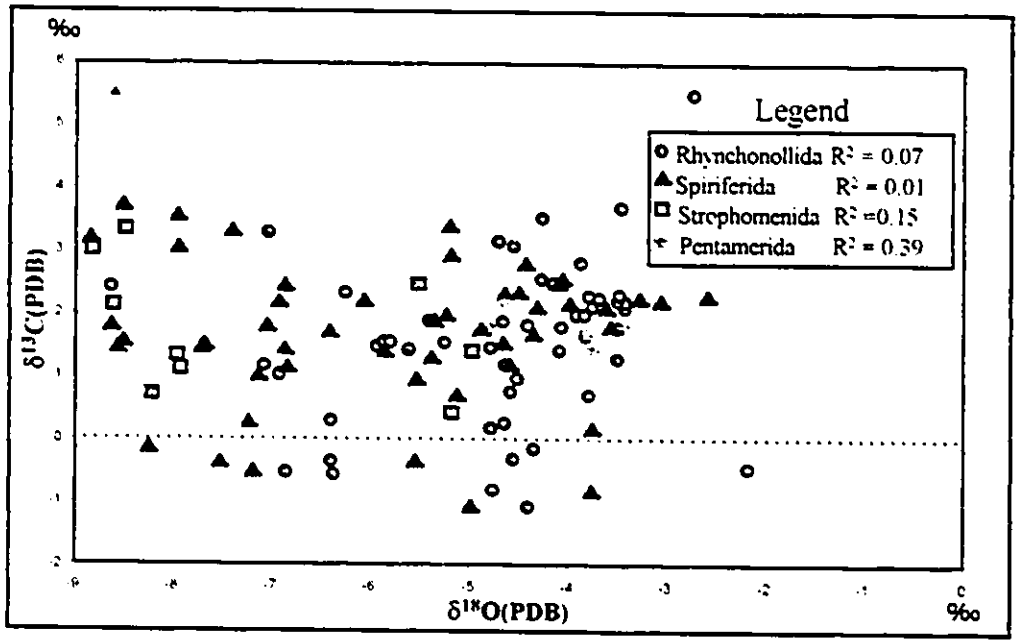

Figure 10-11. Scatter diagram of $\delta^{13}C$ versus $\delta^{18}O$ for Lower Devonian brachiopods plotted by brachiopod orders. Total 108 samples, 53 Rhynchonellida, 40 Spiriferida, 9 Strophomenida and 6 Pentamerida.

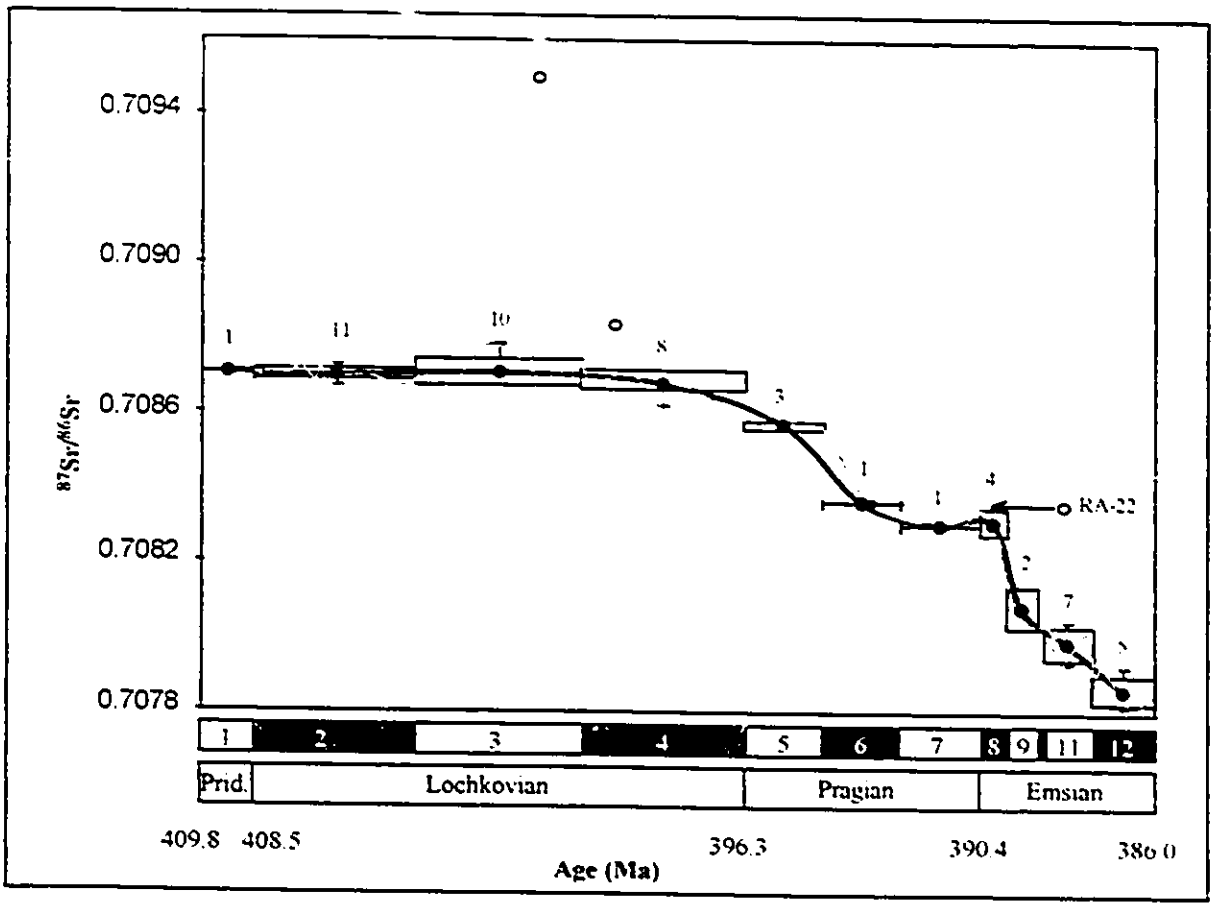

Figure 10-12. Low resolution $^{87}Sr/^{86}Sr$ scatter plot for the Lower Devonian brachiopods based on averaged isotopic data for the conodont biozones. Conodont biozones are the same the same as in figure 10-3. The box indicates 2 standard deviations for a given biozone, vertical bars the range of the data and the numbers are the number of samples. Dark line represents the mean and the grey line the high resolution curve in fig. 10-3. Outliers are indicated by hollow circles. Arrow indicates the direction and the magnitude of displacement for an outlier. Shaded band approximates the Burke et al. (1982) curve for the Lower Devonian. Absolute ages taken from Harland et al. (1990).

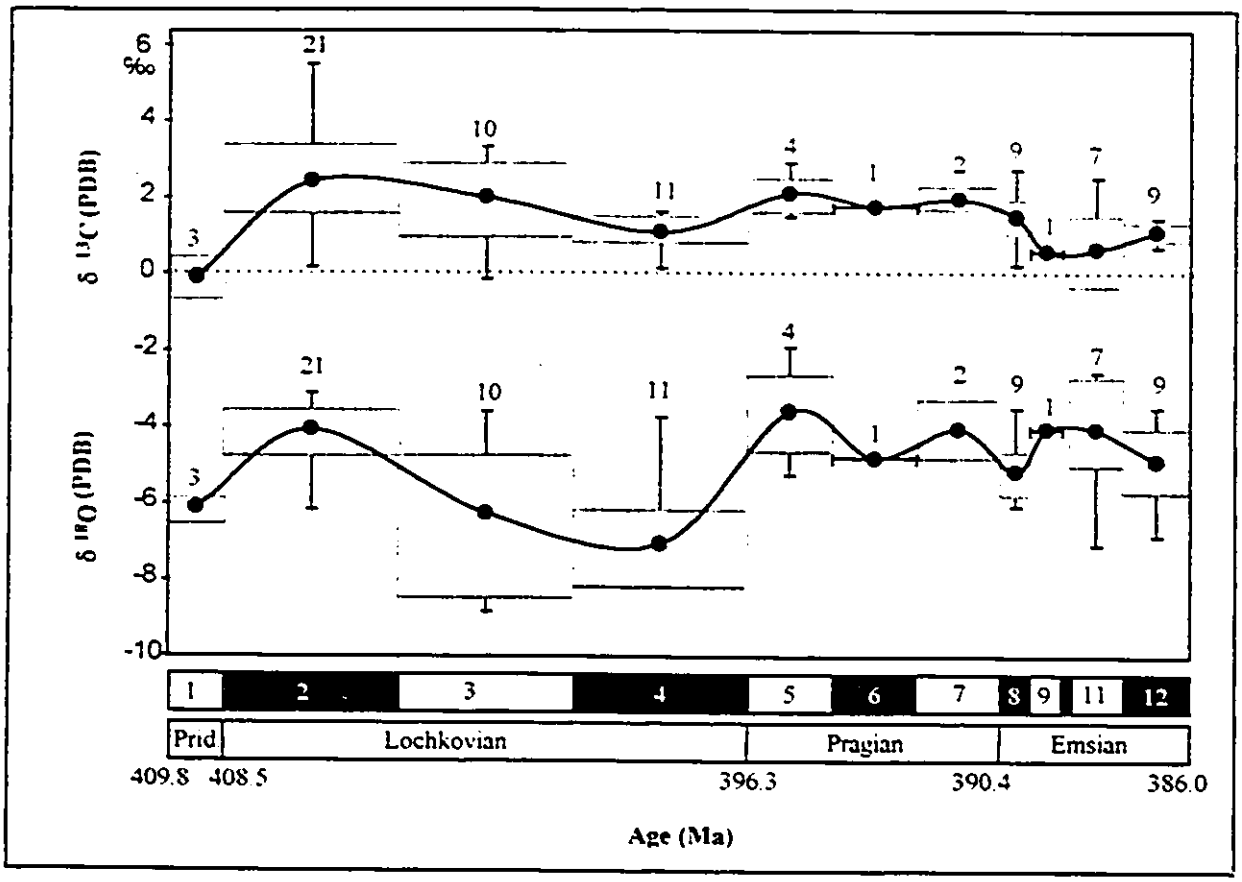

Figure 10-13. Low resolution $\delta^{13}C$ and $\delta^{18}O$ scatter plot for the Lower Devonian brachiopods based on averaged isotopic data within each conodont biozone. Conodont biozones are the same as in figure 10-3. The boxes indicate 2 standard deviations for a given biozone, vertical bars, the range of the data, and the numbers are the number of samples. Absolute ages takenfrom Harland et al. (1990). 78 samples.

11. DISCUSSION

The first question which must be asked is whether the observed isotope data sets are primary or secondary. If primary, the data must satisfy certain preconditions. First, their chemical attributes have to be comparable to those of modern brachiopod shells. For the majority of the data in this set, this appears to be the case. The few outliers were rejected from further consideration. Second, for a global signal, the data collected from disparate regions have to yield comparable results. This is clearly the case for the $^{87}Sr/^{86}Sr$ temporal trend, with the oscillations comparable to those of the previous results from coeval and near-coeval sequences (figure 10-12 and Veizer and Compston, 1974; Lavoie 1993; Diener et al., 1996). For all these reasons, I believe that the strontium isotope signal of the Lower Devonian brachiopods reliably reflects the $^{87}Sr/^{86}Sr$ of the contemporaneous sea water. The observed decline in ^{87}Sr throughout the Lower Devonian may reflect an increased influx of mantle derived Sr, a decreased influx of radiogenic Sr from the continents, or some combination of both. At this stage it is difficult to argue for a dominant cause. The Lower Devonian has been described as orogenically relatively quiet period (Boucot, 1985), but with rapid southward continental drift (Morel and Irving, 1978). Such a fast drift, related to fast spreading rates, may perhaps be a reason for the observed decline in the $^{87}Sr/^{86}Sr$ of the Lower Devonian sea water. The onset of a major transgression in the Pragian that continued well into the Middle Devonian may also be compatible with such a scenario, providing that faster spreading results in higher standing oceanic ridges, hence displacement of water masses over shelves.

The oxygen isotope values for the York State samples are depleted by approximately 2 ‰ relative to the remainder of the data. If primary, such a depletion may reflect sea water temperatures that are about 9°C warmer than in the other three areas or it may reflect mixing of seawater with a fresh water. Alternatively, this material has been subjected to some degree of or post-depositional alteration.

Visually, the textures of samples from New York compare favourably with those from the other regions, showing only minor dissolution features. Only a few samples exhibited features of complete recrystallization and they were discarded from the final set that was utilized for generation of the secular curve. Similarly, trace element data for the majority of the New York shells are similar to those of modern brachiopod shells, with some Lower Devonian samples having strontium concentrations even higher that the modern ones. R^2 values are also generally low, the only exception being $\delta^{18}O$ versus Mn which had R^2 values for the New York samples of 0.55. Isotopically, both carbon and strontium isotopes from New York fit well with the trends from other regions. All this, taken together, indicates that the New York oxygen data may reflect a primary signal, perhaps the temperatures of the near surface Hercynian Ocean, but the actual cause is difficult to discern. Paleogeographic reconstruction places the study area towards the southern end of the Hercynian Ocean (figure 6-1, location 1) and this may have been the reason for the postulated higher ambient temperatures. In modern oceans, variations of up to 10° C have been observed for water masses of comparable latitudes (Skinner and Porter, 1987). For example, the August surface temperature at 30°N for the Pacific Ocean off the coast of Baha California averages 20° C, whereas off the coast of China it is 28°C. The

paleogeography of the Hercynian ocean is consistent with a scenario of this type. The possibility that the oxygen isotope depletion reflects fresh water mixing is unlikely since the sampled Helderberg strata contain abundant crinoidal remains, a fossil group which inhabits only stenohaline normal marine environments (Clarkson, 1993).

12. APPLICATIONS

One of the most powerful applications of strontium isotopes is their utility for high resolution stratigraphic correlations. The data set plotted in figure 10-12 suggests such a potential particularly for the Pragian and Emsian, because of the high slope of the curve that yields a potential resolution of the order of 1-2 Ma and perhaps better for the early Emsian. On the other hand, the flat slope of the curve during the Lochkovian renders it unsuitable for correlation purposes.

Sample RA-22 can be utilized to illustrate the potential of such isotope correlation. Due to poor biostratigraphic control, the sample was assigned an age of 388.2 Ma (figure 10-12). Lithostratigraphically, the sample was located in the Emsian within 2 metres of the Pragian/Emsian boundary. In the absence of biostratigraphy based on conodonts a higher stratigraphic resolution was not available. Extrapolating the strontium isotope ratio for sample RA-22 back to the reference curve, it would plot close to the Pragian/Emsian boundary at approximately 390.3 Ma, that is within the *dehiscens* conodont biozone.

12. CONCLUSIONS

1) The Lower Devonian data sets collected for this study most likely are primary and reflect the isotopic chemistry of the Lower Devonian sea water.

2) The strontium isotope curve derived from this data set can yield high precision stratigraphy for the Pragian and Emsian, with a potential resolution approaching 1-2 Ma. For the Lochkovian, on the other hand, the potential is low because the strontium curve has a flat slope.

3) The oxygen isotope data indicate that the terminus of the Hercynian ocean located in the present-day New York State may have had ambient water temperatures about 9°C higher than the coeval shelf areas of modern Spain, Russia and the Ukraine.

REFERENCES

AGER, D.V. (1981) *The Nature of the stratigraphic record.* 2nd ed.,John Wiley & Sons. Halsted Press, 122p.

ALDIS, D.S.; GROSSMAN, E.L.; YANCEY, T.E. and MACLERRAN, R.D. (1988). Isotope stratigraphy and paleodepth changes in Pennsylvanian cyclical sedimentary deposits. *Palaios*, 3: 487-506.

ALONSO, J.L.; ALVAREZ-MARRON, J. And PULGAR, J.A. (1988). Mapa geologico de la parte Sudoccidental de la zona Cantabrica. Oviedo, 41 p.

ANATI, D.A. and GAT, J.R. (1989). Restricted marine basins and marginal sea environments. In: *Handbook of Environmental Isotope Geochemistry, 3.* Fritz, P. And Fontes, J.C. (eds.), Elsevier, Amsterdam: 29-73.

ANDERS, M.H., KRUEGER, S.W. and SADLER, P.M. (1987) A new look at sedimentation rates and the completeness of the stratigraphic record. *Journal of Geology* **95**, 1-14.

BLATT, H. and JONES, R.L. (1975). Proportions of exposed Igneous, Metamorphic and Sedimentary Rocks. *Geological Society of America Bulletin*, 86: 1085-1088.

BLATT, H.; BERRY, W.B.N. and BRANDE, S. (1991). *Principles of Stratigraphic Analysis*. Blackwell Scientific Publications, 412 p.

BOGGS, S. (1987). *Principles of Sedimentology and Stratigraphy*. Merrill Publishing Co., 784 p.

BOUCOT, A.J. (1975). *Evolution and extinction rate controls*. Elsevier, Amsterdam, Oxford and New York, xv+427 p.

BOUCOT, A.J. (1985). Late Silurian-early Devonian biogeography, provincialism, evolution and extinction. In *Evolution and environment in the Late Silurian and Early Devonian*. W.G. Chaloner and J.D. lawson (eds.). Phil. Trans. R. Soc. Lond. B., 309:323-339.

BOUCOT, A.J.; JOHNSON, J.G. and TALENT, J.A. (1969). Early Devonian brachiopod zoogeography. *The Geological Society of America*, Special Paper 119: 68p.

BRAND, U. (1989a). Biogeochemistry of Late Paleozoic North American brachiopods and secular variation of seawater composition. *Biogeochemistry*, 7: 159-193.

BRAND, U. (1989b). Global climate changes during the Devonian-Mississippian: Stable isotope biogeochemistry of brachiopods. *Paleogeo. Paleoclim. Paleoecol.*, 75: 311-329.

BRAND, U. and VIEZER, J. (1980). Chemical digenesis of a multicomponent carbonate system -1: Trace elements. *Journal of Sedimentary Petrology*, 50, No. 4: 1219-1236.

BIRCK, J.L. (1986). Precision K-Rb-Sr isotopic analysis: Application to Rb-Sr chronology. *Chemical Geology*, 56: 73-83.

BROCK, T.D. (1985). Life at high temperatures. *Science*, 230: 132-138.

BROECKER, W.S. (1963). Radioisotopes and large-scale oceanic mixing. In *The Sea*, M.N. Hill (ed.), New York: Interscience, 3:88-108.

BRUHN, F.; BRUCKSCHEN, P. and VEIZER, J. (1994) Isotopic composition and diagenetic alteration of Lower Carboniferous brachiopod shells: Constraints from proton microprobe (PIXE) trace element analysis. *Mineralogical Magazine*. 58A: 128-129.

BRUHN, F.; BRUCKSCHEN, P.; RICHTER, D.K.; MEIJER, J.; STEPHAN, A. and VEIZER, J. (1994). Diagenetic history of sedimentary carbonates: constraints from combined cathodoluminescence and trace element analysis by micro-pixe. *Nucl. Inst. Meth. in Physics Res. B*, 32:83-95.

BUHL, D.; NEUSER, R.D.; RICHTER, D.K.; RIEDEL, D.; ROBERTS, B.; STRAUSS, H. and VEIZER, J. (1991). Nature and nurture: Environmental isotope story of the river Rhine. *Naturwissenschaften*, 78: 337-346.

BURKE, W.H.; DENISON, R.E.; HETHERINGTON, E.A.; KOEPRICK, R.B.; NELSON, H.F. and OTTO, J.B. (1982). Variations in seawater $^{87}Sr/^{86}Sr$ throughout Phanerozoic time. *Geology*, V. 10 : 516-519.

CARLS, P. (1988). The Devonian of Celtiberia (Spain) and Devonian paleogeography of SW Europe. In Devonian of the world. M.J. McMillan, A.F. Embry and D.J. Glass (eds.). *Memoirs of the Canadian Society of Petroleum Geologists* 14: 421-466.

CARPENTER, S.J. and LOHMANN, K.C. (1995). $\delta^{18}O$ and $\delta^{13}C$ values of modern brachiopod shells. *Geochimica et Cosmochimica Acta*, 59:3749-64.

CHLUPÁČ, I. (1953). Stratigraphical investigation of the border strata of the Silurian and the Devonian in Central Bohemia. *Sbornik Ustr. Ust. Geol.*, 20:277-380.

CLARKSON, E.N.K. (1993). *Invertebrate Palaeontology and Evolution*. Third edition. Allen & Unwin, London, 382 p.

CLAUSER, N. (1981). $^{87}Sr/^{86}Sr$ ratios of the Barremain and early Aptian seas. *In: Init. Rep. Deep Sea Drill. Proj.*, Thiede, J.; Vallier, T.L., et. al., LXII, 781-783.

COMPSTON, W. (1960). The carbon isotopic composition of certain marine invertebrates and coals from the Australian Permian. *Geochimica et Cosmochimica Acta*, 18: 1-22.

COX, A. (Ed.), (1973). *Plate tectonics and geomagnetic reversals.* W.H. Freeman, San Francisco, 702p.

CRAIG, H. (1961). The measurements of oxygen isotope paleotemperatures. *In: Stable Isotopes in Oceanographic Studies and Paleotemperatures.* E. Tongiorgi (ed.), Spoleto 1965, CNR, Pisa, 1-24.

CRAIG, H. and GORDON, L. (1965). Deuterium and oxygen-18 variations in the ocean and marine atmosphere. In: *Stable Isotope in Oceanographic Studies and Paleotemperatures*, Tongiorgi E. (ed.), Spoleto 1965, CNR, Pisa, 9-130.

DEGENS, E.T. and EPSTEIN, S. (1962). Relationship between O^{18}/O^{16} ratios in coexisting carbonates, cherts, and diatomites. *Bulletin of American Association of Petroleum Geology.* 46: 534-542.

DIENER, A.; EBNETH, S.; VEIZER, J. and BUHL, D.(1996). Strontium isotope stratigraphy of the Middle Devonian: i-brachiopods and conodonts. *Geochimica Cosmochimica Acta.* 60:639-652.

DINELEY, D. (1984). *The Devonian System*. Elsevier, Amsterdam, Oxford and New York, 219p.

DINGUS, L. (1984). Effects of stratigraphic completeness on interpretations of extinction rates across the Cretaceous-Tertiary boundary. *Paleobiology*, 10(4): 420-438.

DUMONT, A.H. (1848). Memoire sur les terrains ardennais et rhenan de l'Ardenne du Rhin, du Brabant et du Condros. *Mem. Acad. r. Belg.* Seconde partie, 221-451.

FAIRBANKS, R.G. and MATHEWS, R.K. (1978). The marine oxygen isotope record in Pleistocene coral, Barbados, West Indies. *Quaternary Research*, 10:181-196.

FAURE G. (1986) *Principles of isotope geology*. 2nd edn. J. Wiley & Sons, New York, 589pp.

FAURE, G. and POWELL, J.L. (1972). *Strontium Isotope Geology*. Springer-Verlag, Heidelberg, 188p.

FERRONSKY, V.I. and BREZGUNOV, V.S. (1989). Stable isotopes and ocean mixing. In: *Handbook of Environmental Isotope Geochemistry. 3.* Fritz, P. And Fontes, J.C. (Eds.), Elsevier, Amsterdam: 1-27.

FRIEDMAN, L. and O'NEIL, J.L. (1977). Compilation of stable isotope fractionation factors of geochemical interest. In: Data of Geochemistry. *U.S. Geological Survey Professional Paper* 440-KK, 6th ed.

FURSICH, F.T. and HURST, J.M. (1974). Environmental factors determining the distribution of brachiopods. *Palaeontology*, 17, Part 4: 879-900.

GAGAN, M.K.; CHIVAS, A.K. and ISDALE, P.J. (1994). High resolution isotopic records from corals using ocean temperatures and mass-spawning chronometers. *Earth and Planetary Science Letters*, 121: 549-558.

GAO, G. (1992). The implications of the oxygen isotopic composition of Lower Devonian micritic limestone, Oklahoma (abstract). *Geological Society of America Annual Meeting, Abstracts with Programs*, 24: 37.

GARCIA-ALCALDE, J.L. (1986). Pradoiinae, nouvelle sous-famille de brachiopodes Athyrididés du Dévonien d'Europe. *Biostratigraphie du Paleozoique*, 4: 65-76.

GARCIA ALCALDE, J.L. (1992). El Devónico de Santa María del Mar (Castrillón, Asturias, España). *Revista Española de Paleontología*, 7(1):53-79.

GAT, J.R. (1980). The isotopes of hydrogen and oxygen in participation. In: *Handbook of Environmental Geochemistry*, 1, Fritz, P. and Fontes, J.C. (eds.), Elsevier, Amsterdam, 116-168.

GLEN, W. (1982). *The road to Jaramillo: Critical years of revolution in the earth sciences*. Stanford University Press, Stanford, California. 459p.

GOLDBERG, E.D. (1963). The oceans as chemical systems. In *The Sea*, M.N. Hill (ed.). New York: Interscience, 2: 3-25.

GOREAU, T.J. (1977). Seasonal variations of trace metals and stable isotopes in coral skeleton: Physiological and environmental controls. *In: Proceedings: Third International Coral Reef Symposium*. Fisher Island Station, Miami, pgs. 425-430.

GROSSMAN, E.L.; ZHANG, C. and YANCEY, T.E. (1991). Stable-isotope stratigraphy of brachiopods from Pennsylvanian shales in Texas. *Geological Society of America Bulletin*, 103: 953-965.

GROSSMAN, E.L.; MII, H. and YANCEY, T.E. (1993). Stable isotopes in the Late Pennsylvanian brachiopods from the United States: Implications for Carboniferous paleoceanography. *Geological Society of America Bulletin*, 105: 1284-1296.

HARLAND, W.B.; ARMSTRONG, R.L.; COX, A.V.; CRAIG, L.E.; SMITH, A.G.; SMITH, D.G. (1990). *A geological time scale:1989.* Cambridge University Press, 263p.

HAYS, P.D. and GROSSMAN, E.L. (1991). Oxygen isotopes in meteoric calcite cements as indicators of continental paleoclimate. *Geology*, 19: 441-444.

HECKEL, P.H. and WITZKE, B.J. (1979). Devonian world palaeogeography determined from distribution of carbonates and lithic palaeoclimatic indicators. *In: The Devonian System*, M.R. House; C.T. Scrutton; and M.G. Bassett (eds.), Special Papers in Palaeontology No.23: 99-124.

HELDBERG, H.D.(ed.), (1976). International stratigraphic guide: A guide to Stratigraphical classification, terminology, and procedure. *International Subcommission on Stratigraphic Classification of IUGS Commission on Stratigraphy.* John Wiley & Son, New York, 200p.

HESS, J.; RENDER, M.L. and SCHILLING, J.C. (1986). Evolution of the ratio of Strontium-87 to Strontium-86 is sea water from the Cretaceous to present. *Science*, 231: 979-984.

HOFFMAN, A.; GRUSZCYNSKI, M. and MALKOWSKI, K. (1991). On the interrelationship between temporal trends in ^{13}C, ^{18}O and ^{34}S in the world ocean. *Journal of Geology*, 99: 355-370.

HUDSON, J.D. and ANDERSON, T.F. (1989). Ocean paleotemperature and isotopic compositions through time. *Trans. R. Soc. Edinb. Earth Sci.*, 80: 183-192.

JOACHIMSKI, M.M. and BUGGISCH, W. (1993). Anoxic events in the late Frasnian-Cause of the Frasnian-Famennian faunal crisis? *Geology*, 21: 675-678.

JOHNSON, J.G. (1979). Devonian brachiopod biostratigraphy. *In: The Devonian System*. House, M.R.; Scrutton, C.T.; and Bassett, M.G. (eds.), Special papers in Geology, No.23: 291-306.

JOHNSON, J.G. and BOUCOT, A.J. (1973). Devonian brachiopods. *Atlas of Palaeobiogeography*, A. Hallam (ed.), Elsevier, Amsterdam, London, New York, 89-106.

KARHU, J. and EPSTEIN, S. (1986). The implication of the oxygen isotope records in coexisting cherts and phosphates. *Geochimica et Cosmochimica Acta*, 50: 1745-1754.

KILLINGLEY, J.S. (1983). Effects of diagenetic recrystallization on $^{18}O/^{16}O$ values of deep-sea sediments. *Nature*, 301: 594-597.

KNAUTH, L.P. and EPSTEIN, S. (1976). Hydrogen and oxygen isotope ratios in nodular and bedded cherts. *Geochimica et Cosmochimica Acta*, 40: 1095-1108.

KORVIN, G. (1992). Fractals in Flatland: a romance of <2 dimensions. In *Fractal Models in the Earth Sciences*. (ed. G. KORVIN). Chap. 5 pp. 87-118. Elsevier.

KROOPNICK, P.; WEISS, R.F. and CRAIG, H. (1972). Total CO_2, ^{13}C and dissolved oxygen in the deep ocean-^{18}O at GEOSECS II in the North Atlantic. *Earth and Planetary Science Letters*, 16: 103-110.

KROOPNICK, P. M. and CRAIG, M. (1976). Oxygen isotope fractionation in dissolved oxygen in the deep sea. *Earth Plan. Sci. Lett.*, 32:375-388.

KROOPNICK, P.M.; MARGOLIS, S.V. and WONG, C.S. (1977). $\delta^{13}C$ variations in marine carbonate sediments as indicators of the CO_2 in the oceans. *In The Fate of Fossil Fuel CO_2 in the oceans*. N.R. Anderson and A. Malahoff (eds.). Plenum Press. 295-321.

LAVOIE, D. (1993). Early Devonian marine isotope signatures: Brachiopods from the Upper Gaspe Limestones, Gaspe Peninsula, Quebec, Canada. *Journal of Sedimentary Petrology*, 63, No. 4: 620-627

LIVERMORE, R.A.; SMITH, A.G. and BRIDEN, J.C. (1985). Paleomagnetic constraints on the distribution of continents in the late Silurian and early Devonian. *In Evolution and environment in the Late Silurian and Early Devonian*. W.G. Chaloner and J.D. lawson (eds.). Phil. Trans. R. Soc. Lond. B., 309:29-56.

LONGMAN, M.W. (1982). Carbonate digenesis as a control on stratigraphic traps. *AM. Assoc. Petroleum Geologists Education Course Notes Ser.*, 21: 159 p.

LOWENSTAM, H.A. (1961). Mineralogy, O^{18}/O^{16} ratios, and strontium and magnesium contents of recent and fossil brachiopods and their bearing on the history of the oceans. *Journal of Geology*, 69: 241-260.

LUDVIGEN, R.; WESTROP, S.R.; PRATT, B.R.; TUFFNELL, P.A. and YOUNG, G.A. (1986). Dual biostratigraphy: zones and biofacies. *Geoscience Canada*, 13:139-154.

MACKINNON, D.I. (1974). The shell structure of spiriferide brachiopods. *Bull. British Museum*, 25: 187-261.

MCCREA, J.M. (1950). On the isotope chemistry of carbonates and a paleotemperature scale. *Journal of Chemistry and Physics*, 18: 849-857.

MCCONNAUGHEY, T. (1989). ^{13}C and ^{18}O isotopic disequilibrium in biologic carbonates: II In vitro stimulation of kinetic isotope effects. *Geochimica et Cosmochimica Acta*, 53: 163-171.

MCDOUGALL, I. (1977). *The present status of the geomagnetic polarity time scale. In The Earth: Ist origin, structure, and evolution* (a volume in honour of J.C. Jaeger and A.L. Hales): M.W. McElhinney (ed.). Academic Press, New York, 543-66.

MCSHEA, D.W. and RAUP, D.M. (1986) Completeness of the geological record. *Journal of Geology* **94**, 569-574.

MENENDEZ-BEDIA, I. (1976). Biofacies y litofacies de la Formacion Moniello-Santa Lucia (Devonico de la Cordillera Cantabrica, NW de España). *Trab. Geol. Univ. Oviedo*, 9.

MEYERS, W.J. (1974). Carbonate cement stratigraphy of the Lake Valley Formation (Mississippian), Sacramento Mountains, New Mexico. *Journal of Sedimentary Petrology*, 44: 837-861.

MIALL, A.D. (1994). Sequence stratigraphy and chronostratigraphy: Problems of definition and precision in correlation and their implications for global eustasy. *Geoscience Canada*, 21(1): 1-26.

MOORE, R.C. (1965). *Treatise on Invertebrate Paleontology, Part H: Brachiopoda.* The Geological Society of America and The University of Kansas Press, 1; 521 p.

MOREL, P. and IRVING, E. (1978). Tentative paleocontinental maps for the early Phanerozoic and Proterozoic. *Journal of Geology*, 86: 535-561.

MORRISON, O.J. and BRAND, U. (1986). Palaeocene No. 5: Geochemistry of recent marine invertebrates. *Geoscience Canada*, 13:237-254.

MUEHLENBACKS, K. and CLAYTON, R.N. (1976). Oxygen isotope composition of the oceanic crust and its bearing on seawater. *Journal of Geophysical Research*, 81: 4365-4369.

NEWELL, R.E. and DOPPLICK, T.G. (1979). Questions concerning the possible influence of anthropogenic CO_2 on atmospheric temperature. *Journal of Applied Meteorology*, 18, No. 6:22-25.

NIKIFOROVA, O.I. (1968). A guide to the geological excursion on Silurian and Lower Devonian deposits of Podolia (Middle Dnestr River). *International Symposium on Silurian-Devonian Boundary and Lower and Middle Devonian Stratigraphy*. Leningrad, VSEGEI. 57p.

NORTH AMERICAN COMMISSION ON STRATIGRAPHIC NOMENCLATURE (NACSN) (1983). North American Stratigraphic Code. *American Association of Petroleum Geology* , Bull. 67: 841-875.

ODIN, G.S. (1982). Introduction: uncertainties in evaluating the numerical time scale, *In: Numerical Dating in Stratigraphy*. G.S. Olin (ed.), Wiley, Chichester, England:3-16.

PALMER, M.R. and ELDERFIELD, H. (1985). Strontium isotope composition of sea water over the past 75 Myr. *Nature*, 314:526-528.

PETERMAN, Z.E.; HEDGE, C.E. and TOURTELOT, H.A. (1970). Isotopic composition of strontium in seawater throughout Phanerozoic time. *Geochimica et Cosmochimica Acta*, 34: 105-120.

POPP, B.N.; ANDERSON, T.F. and SANDBERG, P.A. (1986). Brachiopods as indicators of original isotopic compositions in some Paleozoic limestones. *Geological Society of America Bulletin*, 97: 1262-1269.

PRASADA, R.C. and GREEN, D.C. (1993). Oxygen and carbon isotopes of early Permian cold-water carbonates, Tasmania, Australia, *Journal of Sedimentary Petrology*, 52, No. 4: 1111-1125.

QING, H. and VEIZER, J. (1994). Oxygen and carbon isotopic composition of Ordovician brachiopods: Implications for coeval seawater. *Geochimica et Cosmochimica Acta*, 58: 4429-4441.

RAILSBACK, L.B. (1990). Influence of changing deep ocean circulation on the Phanerozoic oxygen isotope record. *Geochimica et Cosmochimica Acta*, 54: 1501-1509.

RICKARD, L.V. (1962). Late Cayugan (Upper Silurian) and Helderbergian (Lower Devonian) stratigraphy in New York. *N.Y. State Mus. And Sci. Serv. Bull.* 386. **132p.**

RICKARD, L.V. (1981). The Devonian system of New York State. In. Devonian biostratigraphy of new York. Part I. (W.A. Oliver and G. Klapper eds.) *International Union of Geological Sciences Subcommission on Devonian Stratigraphy*. 5-22.

RONOV, A.B.; KHAIN, V.E.; BALUKOVSY, A.N. and SESLAVINSKY, K.B. (1980). Quantitative analysis of Phanerozoic sedimentation. *Sedimentary Geology*, 25: 311-325.

RUSH, P.F. and CHAFETZ, H.S. (1990). Fabric-retentive, non-luminescent brachiopods as indicators of original $\delta^{13}C$ and $\delta^{18}O$ composition: A test. *Journal of Sedimentary Petrology*, 60, No. 6: 968-981.

SADLER, P.M. (1981). Sediment accumulation rates and the completeness of the stratigraphic sections. *Journal of Geology* **89**, 568-584.

SCHINDEL, D.E. (1982). Resolution analysis: A new approach to the gaps in the fossil record. *Paleobiology* **8**(4), 340-353.

SCHOCH, R.M. (1989). *Stratigraphy: Principles and Methods*. Van Nostrand Reinhold Publications, 375 p.

SCOTESSE, C.R. (1994). *Continental drift*. The PALEOMAP project. 75p.

SCOTESSE, C.R.; BAMBACH, R.K.; BARTON, C.; VAN DER VOO, R. and ZIEGLER, A.M. (1979).Paleozoic base maps. *Journal of Geology*, 87: 217-277.

SHARMA, T. and CLAYTON, R.N. (1965). Simultaneous determinations of the concentration and isotope ratio of sulfate and sulfide-sulfur and carbonate-carbon in geological samples. *Geochemical Journal*, 17:185-196.

SKINNER, B.J. and PORTER, S.C. (1987). *Physical Geology*. John Wiley & Sons. 750 p.

STILLE, P.; CHAUDHURI, S.; KHARAKA, Y.K. and CLAUER, N. (1992). Neodymium, Strontium, Oxygen and Hydrogen isotope compositions of waters in present and past oceans: A

review. *In : Isotope signatures and sedimentary records.* N. Clauer and S. Chaudhuri (eds.), Springer-Verlag, Heidelberg, 43: 389-410.

TARUTANI, T.; CLAYTON, R.N. and MAYEDA, T.K. (1969). The effects of polymorphism and magnesium substitution on oxygen isotope fractionation between calcium carbonate and water. *Geochimica et Cosmochimica Acta*, 36: 1237-1253.

THUNDELL, R.C.; WILLIAMS, D.F. and HOWELL, M. (1987). Atlantic-Mediterranean water exchange during the Late Neogene. *Paleoceanography*, 2: 661-678.

VEIZER, J. (1983). Trace elements and isotopes in sedimentary carbonates. *Rev. Mineral*, 11: 265-300.

VEIZER, J. (1989). Strontium isotopes in seawater through time. *Annual Review of Earth and Planetary Sciences*, 17: 141-167.

VEIZER, J. (1992). Depositional and diagenetic history of limestones : Stable and radiogenic isotopes. *In: Isotopic signatures and sedimentary records.* N. Clauer and S. Chaurdhuri (eds.), Springer-Verlag, Heidelberg, 43: 13-48.

VEIZER, J. and COMPSTON, W. (1974). $^{87}Sr/^{86}Sr$ composition of seawater during the Phanerozoic. *Geochimica et Cosmochimica Acta.* 38: 1461-1484.

VEIZER, J.; HOLSER, W.T. and WILGUS, C.K. (1980). Correlation of $^{13}C/^{12}C$ and $^{34}S/^{32}S$ secular variations. *Geochimica et Cosmochimica Acta*, 44:579-587.

VEIZER, J.; FRITZ, P. and JONES, B. (1986). Geochemistry of brachiopods: Oxygen and carbon isotopic records of Paleozoic oceans. *Geochimica et Cosmochimica Acta*, 50: 1679-96.

WADLEIGH, M.A. and VEIZER, J. (1992). $^{18}O/^{16}O$ and $^{13}C/^{12}C$ in lower Palaeozoic articulate brachiopods: Implications for the isotope composition of seawater. *Geochimica et Cosmochimica Acta*, 56: 431-443.

WALKER, J.C.E. and LOHMANN, K.C. (1989). Why the oxygen isotope composition of seawater changes with time. *Geophysical Research Letters*, 16, No. 4: 323-326.

WEFER, G. (1983). Die Verteilung stabiler Sauerstoff-und Kohlenstoff-Isotope in Kaulschalen mariner organismen - *Grundlage einer Isotope Palokologie*. Habilitationsschrift, Univ. Kiel, 151p

WICKMAN, F.W. (1948). Isotope ratios-A clue to the age of certain marine sediments. *Journal of Geology*, 16: 1-66.

WILLIAMS, A. (1968). Evolution of the shell structure of articulate brachiopods. *Special Papers in Palaeontology*, 2: 55 p.

ZAIKA-NOVATSKY, V.S. (1983). The main features of the Middle Dneister area geological structure. In. *The Silurian of Podolia: The guide to excursion.* D.E. Aisenverg (ed.) Kiev: Naukova Dumka: 58-82.

ZIEGLER, A.M.; SCOTESE, C.R.; MCKERROW, W.S.; JOHNSON, M.E. AND BAMBACH, R.K. (1977). Paleozoic paleogeography. *Annual Review of the Earth and Planetary Science*, 7: 473-502.

APPENDIX 1

Lab Technique-picking

Equipment

Hourglass
Dental Pick (stainless steel)
Binocular Microscope
Sonic Bath
Non-static paper
10% diluted HCl
Ethanol
Distilled Water
Tooth Brush

Method

A) Using tooth brush and water, remove loose dirt and other loose material from the sample and let dry

B) Identify sample to order level.

C) Place sample under microscope visually inspect the sample. Using dental pick and non-static paper, separate shell material and place in hour glass.

D) Clean separated material in distilled water and sonic bath. This should help separate any remaining matrix and/or possible contaminants. Let sample dry.

E) Under the microscope, separate slivers of the secondary fibrous layer using the dental pick and place material in a small closable container (2.5 ml flat bottomed plastic container).

Samples which have a coating of Fe or other material are immersed in a diluted 20% 1N HCl solution for approx. 1 minute and then bathed in deionized water. The splinters are then picked again.

F) For samples that look potentially altered prepare a polished thin section for Catholuminescence or check under SEM.

G) Between samples clean equipment in diluted HCl and ethanol to remove any residual carbonate and other possible contaminants

Cathodoluminescence

Equipment

Nikon Technosyn cold Cathode Luminescence
Model 8200 MK II

Method

A) Place polished thin section in slide chamber. Close chamber and seal(knob on left side of stage).

B) Making sure the seal is tight, turn on the vacuum pump (turn lever behind the control box clockwise).

C) Wait until the green **vac ready light** goes on then flick the **kV ON switch** down. Adjust the **kV signal** until the signal reaches 12 (make sure that the gun current does not exceed 600 microamps, this could destroy the machine)

D) Turn on the light (base of microscope) and move the slide to the desired position (knob to the right of the stage).

E) Once in the desired position, turn off the light and look for luminescence (eye sensitivity will improve if you let your eyes adjust to the dark for a few seconds)

F) To change slide, turn off the pump and **kV ON switch**, then slowly release the knob on the left side of the stage. Lift the top tray and remove the slide.

G) Turn off the power to the control box but not the pump when finished.

Scanning Electron Microscope (SEM) procedure

Equipment:

Jeol 6400 digital scanning electron microscope set at 15 kv and 3000X.
Anatec Lim. spatter coater.
Polaroid camera

Procedure:

A) Small splinters were taken from a series of samples and attached to a metal thin section sized plate using black double sided sticky tape. A visual map was also made of the location of each sample.

B) The metal plate was then coated with 100 Angstroms of gold/palladium dust over 10 minutes.

C) The metal plate was then placed in the SEM and a vacuum was produced in the sample chamber.

D) Each sample was visually assessed for textural preservation and quick video images produced. For exceptional images a Polaroid and negative slide was also taken.

Preliminary Phosphorus Acid Preparation Technique

A) Acid (99.98 % ultra-pure) from small ~50 ml bottles. The top was sealed in wax. This wax was first removed in order to remove possible contamination. Contamination from the wax would result in the formation of black flakes in the acid during the final preparation stage.

B) Once the acid (in powder form) was ready to pour it was mixed with (Phosphorus Pentoxide) P_2O_5 and dissolved. The devolving process was carried out at 180° C for a few minutes. It is at this stage that black flakes will appear if there is any contamination. It is best to prepare only a few 50 ml bottles at a time in order to limit any possible contamination (to make sure it doesn't spread and contaminate all 10 bottles).

C) The colour of the acid once completely dissolved should be pale yellow. The final stage is to leave the acid standing for between 2-3 weeks to allow sufficient time for proper mixing (the acid has to be completely homogeneous). Make sure that no possible source of contamination will occur to the acid during this time.

Mass spectrometer & ICP Preparation

Equipment

Morter and pestle
weighing scale, 0.0001 g (model 1602 MP8 by Sartorius)
reaction vessels
diluted Nitric acid
Falcon tube rack
Non-static paper
Distilled water

Method

A) Powder at least 5 mg of picked material using a morter and pestle. Place in a new 2.5 ml container.

B) Weigh at between 2-5 mg of crushed material using non-static paper. Record weight accurately.

C) Place the weighed material into the bottom section of a reaction vessel insuring that all measured material is used.

D) Pour 1 ml of Ultra pure 99% H_2PO_4 (prepared from Preliminary Phosphorus Acid Preparation Technique) slowly into the upper side section. Make sure that no acid gets in contact with the sample.

E) Repeat procedure for all samples being analysed during run.

Oxygen and Carbon isotope extraction

Cleaning the Reaction Vessel

A) Wash out the reaction vessels in water to remove the last sample residue

B) Clean the interior of the vessels for at least 15 min in 50% dilute nitric acid.

C) Rinse out the reaction vessels in deionized water

D) Bring down to the isotope lab and dry in drying oven for at least 1 hour at 150°C.

E) Remove using clamps and let cool.

Preparation of Cajon fitting "Break seals"

A) Get long glass tubes from the back of the lab. (Near the second door).

B) Using a permanent pen and ruler, mark off the tubes at approx 22 cm intervals.

C) At every second marking cut with glass cutter.

D) Turn on torch (first gas then oxygen). Oxygen first or too much oxygen produces small explosion. The inner blue flame should be approx 1 cm long.

E) Take one of the glass tubes and taking the middle point (marked) melt in half by continually rotating. Once soft twist slowly and pull apart a bit until the middle burns away.

F) Take the cut end and put into the flame for a few seconds in order to smooth the edges.

Transfer Procedure (Reaction vessel → ICP holding tube)

Equipment:

10 pipettes with rubber tops
2x100 or 250 ml beakers (cleaned in deionized H_2O)
ICP tubes
Small plastic squirter
Plastic 1 litre squirt container

Standards: (run every 8-10 samples)

LMS1-3 (internal standard ICP)
WATMET (internal ICP machine running standard)
WATMAJ (internal ICP machine running standard)
CA500 (internal ICP machine running standard)

Make sure that all equipment has been sterilized using 20-50% diluted nitric acid. LMS (standards) and Blanks should follow the same procedure as the samples, including being evacuated on the isotope extraction line.

A) After the H_3PO_4 reacted sample has been isotopically analysed, prepare the sample for transfer by placing the reaction vessels in a testtube holder making sure that the acid is as little disturbed as possible.

B) In one of the beakers, place the 10 pipettes making sure that the beaker is filled with deionized water

C) Place the small squirter in the second beaker, again making sure that the beaker is filled with deionized water

D) Take ten reacted samples (in their reaction vessels) and making sure that they stay fairly upright, place one of the glass pipettes in each reaction vessel and remove as much solution as can be taken up in one squeeze of the pipette. Avoid taking up the unreacted acid it the upper side holding cell.

E) Once the reacted acid has been taken up, put the pipette in a corresponding ICP tube. Make sure that the tube is labelled with the sample number.

F) Drain the sample into the tube then place the pipette almost out of the tube and let it drain for a couple minutes.

G) Drain out any remaining acid.

H) Using the plastic 1 litre squirter, dilute the acid to close to 10 ml (visual measurement). Then with the small squirter, add drop by drop, deionized water until the diluted sample is at as close to 10 ml as possible.

I) Close the ICP sample container with top and shake a few times. Let sit until used in ICP.

J) Clean equipment.

K) Repeat procedure for all the samples.

ICP machine use

Equipment:

Thermo Jarrell Ash ATOMSCAN 25 spectrometer. An inductively coupled argon plasma (ICAP) spectrometer.

A) Turn on the Argon gas (green knob) above gas tank. Make sure that the pressure reaches at least 60 psi before proceeding.

B) Turn on computer and type "**STNRUN**".

C) Press the reset button (blue button beside computer) on main machine after **STNRUN** has initialized.

D) On computer control panel press **Ctrl "F3"**. This initializes the system. Type in **"STARTER"** only if not at prompt **"ENTER"**. Wait approx 10 minutes for the ICP to startup.

E) Set up standards **"Calcite"** and blank. Press **F3)** Standardize and the **(F1)** runs the standard (note be sure to have the analysis tube in the sample (Blank, Calcite). Press **"F9"** between standards.

F) After the two standards are done, type **"F9"** done/save twice (or 3X). This should save both standard setups and prepare for sample analysis.

G) You are ready to analyse samples, press **"F1"** analyse. For the first sample type in the date and then press **"F1"** again. This starts analysis. Repeat for all the analyses.

Down-loading data from ICP to disk (procedure)

H) Type **(F9)** main menu and go to **IMS** prompt and **RETURN** on **REPORT WRITER**.

I) Press **(F6)** LIST-> Type corresponding number and **RETURN** or alternatively press **(F1)** if there is only one file. Press **(F9)** DONE/KEEP.

J) On the next screen under METHOD highlight **CALCITE-** or use **(F6)** LIST, then DELETE ALL **(F2)** and type the number for the method you want I.E. TYPE 1 for CALCITE-. Press RETURN then **(F9)** DONE/KEEP.

K) Under the heading SAMPLE NAME type the sandard name for the samples followed by a wildcard **(*)**. I.E. **NOV15***. Type **(F9) CONTINUE** to next screen.

L) **Sort option** (PRIMARY SORT->press **SPACE BAR**-> CHRONOLOGICALLY.

M) Finally send report to printer (DEFAULT) and press **(F9)**. You can then either go to LOTUS 123 and import the file or go to Excel and import the file. The second method is more compiicated.

To SHUT-DOWN the system. Procedure

N) Ctrl**(F6)** PANEL-> **(F7)** SHUTDOWN

O) Turn off screen

P) Turn off gas (GREEN KNOB) on Argon gas tank.

APPENDIX 2

Table 1. Sample location, outcrop number (from text), estimated age, conodont biozonation, brachiopod identification and chemical analysis for 121 Lower Devonian brachiopod samples.

Number	Sample Location	Outcrop Number	Sample Id.	AGE(Ma)	Conodont biozone	Brachiopod Identification	Ca %	Mg %	Ba ppm	Fe ppm	Mn ppm	Na ppm	Sr ppm
1	Spain	3	SL-8	386.01	*patulus*	Spirifera	38.81	0.15	47	1378	72	10216	1071
2	Spain	3	SL-8	386.01	*patulus*	Spirifera	38.77	0.15	53	1393	27	10785	1067
3	Spain	3	SL-7	386.10	*patulus*	Spirifera	38.72	0.30	38	1536	113	8731	738
4	Spain	3	SL-7	386.10	*patulus*	Spirifera	38.76	0.28	41	1122	93	8858	832
5	Spain	3	SL-5	386.37	*patulus*	Rhynchonellida	38.98	0.23	35	916	41	7069	1087
6	Spain	3	SL-4	386.41	*patulus*	Rhynchonellida	39.22	0.10	26	711	10	6711	1026
7	Spain	3	SL-3	386.61	*patulus*	Spirifera	38.91	0.27	41	976	30	6805	1129
8	Spain	3	SL-2	386.68	*patulus*	Rhynchonellida	39.26	0.09	21	731	16	6406	1020
9	Spain	3	SL-10	387.33	*patulus*	Rhynchonellida	38.77	0.11	25	776	31	6305	1021
10	Spain	3	SL-9	387.37	*patulus*	Rhynchonellida	39.31	0.11	25	580	17	5217	851
11	Spain	3	SL1-2	387.49	*patulus*	Strophomenida	39.31	0.08	25	565	11	6172	872
12	Spain	3	SL1-4	387.51	*patulus*	Spirifera	39.19	0.10	52	2279	67	1528	832
13	Spain	3	SL1-5	387.51	*patulus*	Spirifera	39.01	0.08	41	915	1	9911	701
14	Spain	3	SL1-3	387.59	*serotinus*	Spirifera	39.17	0.16	28	886	39	6085	942
15	Spain	3	SL1-4	387.59	*serotinus*	Spirifera	39.21	0.13	30	691	1	5873	965
16	Spain	3	SL1-1	387.64	*serotinus*	Rhynchonellida	39.01	0.25	26	745	29	6111	1171
17	Spain	3	SL-1	387.69	*serotinus*	Strophomenida	37.47	0.37	100	3251	65	21735	1132
18	Russia	1	RA-22	388.20	*serotinus*	Rhynchonellida	39.29	0.10	26	601	16	6112	618
19	Spain	1	SL4-7	388.21	*serotinus*	Spirifera	39.02	0.11	36	1351	368	7399	1015
20	Spain	4	SL4-6	388.28	*serotinus*	Spirifera	39.13	0.13	21	802	112	7020	1153
21	Spain	4	SL4-5A	388.38	*serotinus*	Spirifera	39.03	0.28	22	818	107	5526	1096
22	Spain	1	SL4-5B	388.38	*serotinus*	Spirifera	38.82	0.23	21	2667	389	6952	912
23	Spain	2	LV2-21a	388.49	*serotinus*	Rhynchonellida	38.67	0.28	23	3575	576	6732	1024
24	Spain	2	LV2-21B	388.49	*serotinus*	Rhynchonellida	38.12	0.35	76	6681	939	9172	971
25	Spain	1	SL4-2	388.49	*serotinus*	Spirifera	39.14	0.12	31	1821	215	5951	951
26	Spain	1	SL4-3	388.51	*serotinus*	Spirifera	39.28	0.10	19	705	126	5823	1161
27	Spain	2	LV2-20	388.61	*serotinus*	Spirifera	37.85	0.26	33	11139	870	6371	818

Table 1. Continued

Number	Sample Location	Outcrop Number	Sample Id	AGE(Ma)	Conodont biozone	Identification order	Ca %	Mg %	Ba ppm	Fe ppm	Mn ppm	Na ppm	Sr ppm
28	Spain	2	LV2-19	389.17	*gronbergi*	Spirifera	38.33	0.17	31	5070	570	8216	980
29	Spain	1	AH-10	389.30	*gronbergi*	Spirifera	39.22	0.16	21	750	66	5177	1316
30	Spain	2	LV2-17	389.61	*gronbergi*	Spirifera	39.26	0.14	16	1111	131	4931	935
31	Spain	2	LV2-15	389.92	*dehiscens*	Spirifera	38.91	0.25	21	1201	15	6757	1166
32	Spain	2	LV2-14	389.95	*dehiscens*	Spirifera	38.97	0.20	22	689	21	7691	1531
33	Spain	2	LV2-13	389.98	*dehiscens*	Spirifera	38.68	0.15	13	1213	11	12119	1182
34	Spain	2	LV2-12	390.11	*dehiscens*	Spirifera	38.50	0.20	42	1397	117	13211	1335
35	Spain	2	LV2-10	390.16	*dehiscens*	Spirifera	38.41	0.25	40	1728	296	13018	1063
36	Spain	2	LV2-9A	390.18	*dehiscens*	Spirifera	39.01	0.19	31	806	117	7044	1738
37	Spain	2	LV2-9B	390.18	*dehiscens*	Spirifera	38.92	0.15	26	2051	518	7486	1178
38	Spain	2	LV2-8A	390.21	*dehiscens*	Rhynchonellida	38.76	0.37	37	1128	178	6561	1180
39	Spain	2	LV2-7	390.26	*dehiscens*	Spirifera	38.21	0.36	56	1778	209	13711	1070
40	Spain	2	LV2-5	390.32	*dehiscens*	Spirifera	38.85	0.25	22	737	167	8316	1138
41	Spain	2	LV2-4B1	390.35	*dehiscens*	Rhynchonellida	38.65	0.19	43	1258	80	11656	1210
42	Spain	2	LV2-4B2	390.35	*dehiscens*	Rhynchonellida	39.05	0.29	29	560	73	5166	1159
43	Spain	2	LV2-4C	390.35	*dehiscens*	Rhynchonellida	38.99	0.22	48	617	62	7117	1523
44	Spain	2	LV2-4D	390.35	*dehiscens*	Rhynchonellida	39.08	0.21	83	694	89	6200	1296
45	Spain	2	LV2-4E	390.35	*dehiscens*	Rhynchonellida	39.07	0.25	138	725	75	5398	1192
46	Spain	2	LV2-4F	390.35	*dehiscens*	Rhynchonellida	39.05	0.21	376	628	101	5611	1158
47	Spain	2	LV2-3B	390.38	*dehiscens*	Rhynchonellida	38.59	0.41	21	2610	171	6201	1211
48	Russia	4	RA-18	391.15	*pumila*	Pentamerida	39.43	0.12	17	369	12	4220	712
49	Russia	4	RA-20	391.15	*pumila*	Pentamerida	39.28	0.11	26	621	26	6196	618
50	Russia	4	RA-19	393.11	*lindleyi*	Pentamerida	39.33	0.11	19	498	17	5631	720
51	Russia	1	RA-10	394.11	*sulcatus*	Rhynchonellida	39.24	0.11	26	677	11	6017	758
52	Russia	2	RA-15	394.95	*sulcatus*	Pentamerida	39.36	0.11	18	459	15	5121	965
53	Russia	1	RA-13	394.97	*sulcatus*	Rhynchonellida	38.97	0.12	36	1977	27	8183	702
54	Russia	1	RA-9	395.76	*sulcatus*	Rhynchonellida	39.31	0.10	23	561	16	5550	733
55	Russia	1	RA-8	396.03	*sulcatus*	Pentamerida	38.80	0.10	41	1095	23	12099	685
56	Ukraine	1	UA-1	396.62	*patulus*	Rhynchonellida	37.96	0.16	36	6005	2019	8189	1195
57	New York	1	AH-8	398.10	*patulus*	Rhynchonellida	39.09	0.15	17	960	28	7321	968
58	New York	1	AH-11	398.39	*patulus*	Spirifera	39.28	0.11	22	1039	17	5010	1111
59	New York	1	AH-12	398.51	*patulus*	Spirifera	38.32	0.11	69	1810	50	16916	1178

Table 1. Continued

Number	Sample Location	Outcrop Number	Sample Id	AGE(Ma)	Conodont biozone	Identification order	Ca %	Mg %	Ba ppm	Fe ppm	Mn ppm	Na ppm	Sr ppm
60	New York	1	AH-15	398.86	*[illegible]*	Spirifera	39.19	0.13	27	706	18	6162	1561
61	New York	1	AH-16	398.96	*[illegible]*	Spirifera	38.71	0.21	45	1156	10	10060	1113
62	New York	1	AH-18	399.25	*[illegible]*	Strophomenida	38.66	0.10	45	1749	90	6152	2011
63	Ukraine	2	UA-3	399.59	*[illegible]*	Rhynchonellida	38.50	0.26	45	3288	687	9198	1437
64	Ukraine	2	UA-4	399.70	*[illegible]*	Rhynchonellida	38.29	0.12	38	4162	910	7752	1581
65	Rusia	1	RA-5	399.82	*[illegible]*	Pentamerida	39.13	0.22	26	567	15	6121	833
66	New York	1	AH-25A	399.95	*[illegible]*	Spirifera	39.16	0.11	30	631	21	6528	1372
67	New York	1	AH-25B	399.95	*[illegible]*	Spirifera	39.26	0.12	25	700	21	5237	1507
68	New York	1	AH-28	400.14	*[illegible]*	Spirifera	38.85	0.31	26	1149	60	5865	1835
69	New York	1	AH-29	400.20	*[illegible]*	Strophomenida	38.40	0.41	38	4183	119	6582	1536
70	New York	1	AH-30	400.26	*[illegible]*	Strophomenida	38.77	0.38	35	1171	139	5900	1668
71	New York	1	AH-31	400.26	*[illegible]*	Strophomenida	38.87	0.32	32	891	131	5880	2111
72	Ukraine	2	UA-5	400.32	*[illegible]*	Rhynchonellida	38.19	0.37	31	3807	2231	9217	1007
73	Ukraine	2	UA-6a	400.41	*post-woodwardi*	Rhynchonellida	37.75	0.50	45	5836	771	11566	1689
74	New York	1	AH-35	400.66	*post-woodwardi*	Spirifera	39.17	0.14	23	1112	77	5620	1475
75	New York	1	AH-36	400.72	*post woodwardi*	Spirifera	39.08	0.20	21	978	69	5908	1501
76	New York	1	AH-38	400.81	*post woodwardi*	Spirifera	39.25	0.15	20	581	47	5240	1370
77	New York	1	AH-39	401.00	*post woodwardi*	Strophomenida	38.81	0.18	37	1173	72	9239	1450
78	New York	1	AH-40	401.06	*post woodwardi*	Strophomenida	37.80	0.18	113	2613	122	21190	1503
79	New York	1	AH-43	401.23	*post woodwardi*	Rhynchonellida	38.83	0.11	28	2988	201	8255	1290
80	New York	1	AH-45	401.30	*post woodwardi*	Rhynchonellida	38.19	0.18	42	1822	60	13219	1359
81	Ukraine	3	UA-7a	402.56	*post woodwardi*	Spirifera	37.83	0.21	61	1821	130	20949	1117
82	Ukraine	4	UA-7b	403.50	*post woodwardi*	Strophomenida	38.30	0.11	35	1669	310	11010	1783
83	Ukraine	4	UA-8	403.57	*post woodwardi*	Spirifera	38.81	0.30	33	819	91	7031	1901
84	Ukraine	4	UA-9	403.66	*post woodwardi*	Spirifera	38.66	0.31	27	957	159	8817	2016
85	Ukraine	4	UA-10	403.75	*post woodwardi*	Spirifera	38.92	0.21	21	780	88	7211	1887
86	Ukraine	4	UA-11	403.85	*post woodwardi*	Spirifera	38.88	0.23	19	1039	129	7585	1790
87	Ukraine	4	UA-12	403.93	*post woodwardi*	Spirifera	38.79	0.37	17	1202	250	5967	1741
88	Ukraine	4	UA-14	404.22	*post woodwardi*	Spirifera	38.62	0.29	29	1370	231	9604	1616
89	Ukraine	4	UA-16	404.52	*woodwardi*	Spirifera	36.73	0.47	65	11911	1584	18362	1333
90	Ukraine	4	UA-18b	404.86	*woodwardi*	Rhynchonellida	38.61	0.12	24	1827	249	9231	988
91	Ukraine	4	UA-19a	404.88	*woodwardi*	Spirifera	38.76	0.27	24	900	255	8443	1925
92	Ukraine	5	UA-19	405.50	*woodwardi*	Rhynchonellida	38.66	0.24	31	1126	117	10260	1867

Table 1. Continued

Number	Sample Location	Outcrop Number	Sample Id	AGE (Ma)	Conodont biozone	Identification order	Ca %	Mg %	Ba ppm	Fe ppm	Mn ppm	Na ppm	Sr ppm
93	Ukraine	5	UA-20	405.60	*w.s. kwg.th*	Rhynchonellida	39.03	0.14	22	1031	77	8361	712
94	Ukraine	6	UA-25a	406.21	*w.s. kwg.th*	Rhynchonellida	38.77	0.27	20	1201	271	7671	2110
95	Ukraine	6	UA-25b	406.21	*w.s. kwg.th*	Rhynchonellida	39.03	0.21	20	671	169	6590	1632
96	Ukraine	6	UA-25c	406.21	*w.s. kwg.th*	Rhynchonellida	38.83	0.22	39	1508	219	7903	1791
97	Ukraine	6	UA-25d	406.21	*w.s. kwg.th*	Rhynchonellida	38.80	0.17	11	986	178	9855	1660
98	Ukraine	6	UA-25e	406.21	*w.s. kwg.th*	Rhynchonellida	38.96	0.18	11	831	202	7627	1693
99	Ukraine	6	UA-25f	406.21	*w.s. kwg.th*	Rhynchonellida	38.71	0.20	42	1107	248	10033	1605
100	Ukraine	6	UA-25g	406.21	*w.s. kwg.th*	Rhynchonellida	38.80	0.26	31	1139	431	7671	1761
101	Ukraine	6	UA-26*	406.30	*w.s. kwg.th*	Rhynchonellida	38.10	0.30	52	1548	105	16162	1717
102	Ukraine	6	UA-26b	406.30	*w.s. kwg.th*	Rhynchonellida	38.72	0.23	39	2123	287	8281	1804
103	Ukraine	6	UA-27	406.44	*w.s. kwg.th*	?	38.76	0.11	37	1583	173	10728	1149
104	Ukraine	7	UA-28	406.59	*w.s. kwg.th*	Rhynchonellida	38.51	0.36	32	1311	613	9662	1812
105	Ukraine	8	UA-32	406.59	*w.s. kwg.th*	Rhynchonellida	38.72	0.23	42	1077	169	9619	1722
106	Ukraine	8	UA-30	406.73	*w.s. kwg.th*	Rhynchonellida	38.61	0.14	90	1375	126	13025	806
107	Ukraine	9	UA-31	406.76	*w.s. kwg.th*	Spiriferа	38.82	0.19	28	1233	96	9169	1585
108	Ukraine	9	UA-34	406.76	*w.s. kwg.th*	Rhynchonellida	38.82	0.19	28	1233	96	9169	1585
109	Ukraine	9	UA-35	406.87	*w.s. kwg.th*	Rhynchonellida	38.73	0.25	32	2291	299	8167	939
110	Ukraine	9	UA-36	406.94	*w.s. kwg.th*	Rhynchonellida	38.68	0.32	27	1651	152	6416	1118
111	Ukraine	9	UA-37	407.00	*w.s. kwg.th*	Rhynchonellida	39.09	0.16	19	768	55	7319	890
112	Ukraine	10	UA-10	407.34	*w.s. kwg.th*	Strophomenida	38.53	0.17	32	1821	112	12952	1268
113	Ukraine	10	UA-10a	407.34	*w.s. kwg.th*	Rhynchonellida	38.77	0.31	28	816	80	8001	1521
114	Ukraine	11	UA-33	407.42	*w.s. kwg.th*	Rhynchonellida	39.31	0.10	23	685	26	5307	820
115	Ukraine	11	UA-41	407.50	*w.s. kwg.th*	Rhynchonellida	38.81	0.23	28	1053	71	8712	1623
116	Ukraine	11	UA-42	407.57	*w.s. kwg.th*	Rhynchonellida	39.28	0.07	21	753	52	6613	751
117	Ukraine	12	UA-44	407.70	*w.s. kwg.th*	?	38.31	0.20	38	4317	171	12227	1170
118	Ukraine	12	UA-45	407.73	*w.s. kwg.th*	Rhynchonellida	37.57	0.16	62	2832	66	21500	1116
119	Ukraine	12	UA-47	408.50	*w.s. kwg.th*	Rhynchonellida	38.99	0.18	8	105	2	9619	238
120	Ukraine	13	UA-48	409.20	*eosteinhornicus*	Rhynchonellida	39.00	0.11	17	959	19	7819	1783
121	Ukraine	13	UA-49	409.20	*eosteinhornicus*	Spiriferа	38.71	0.22	37	1772	132	9182	1763

Average	38.80	0.22	39	1705	197	8506	1283
Standard Dev.	0.41	0.10	37	1912	334	3668	486

APPENDIX 2

Table 2. Isotope results.

Number	Sample Id.	$\delta^{18}O$ ‰ (PDB)	$\delta^{13}C$ ‰ (PDB)	$^{87}Sr/^{86}Sr$	±1 σ	Normalized*
1	SL-8	-6.84	1.46	0.707861	7.00E-06	0.707853
2	SL-8					
3	SL-7	-5.37	1.04			
4	SL-7					
5	SL-5	-4.51	0.95			
6	SL-4	-4.64	1.17	0.707815	7.00E-06	0.70782
7	SL-3	-5.52	0.91			
8	SL-2	-3.77	0.71	0.707823	8.00E-06	0.707828
9	SL-10	-4.5	0.75	0.707922	7.00E-06	0.707927
10	SL-9	-3.49	1.28			
11	SL1-2	-4.97	1.43	0.707874	8.00E-06	0.707879
12	SL1-4	-5.19	1.48			
13	SL1-5					
14	SL1-3	-4.69	1.46			
15	SL1-4					
16	SL1-1	-7.08	1.17			
17	SL-1			0.708031	8.00E-06	0.708018
18	RA-22	-4.27	2.54	0.708386	8.00E-06	0.708378
19	SL4-7	-3.98	0.28			
20	SL4-6	-3.55	0.24	0.70793	8.00E-06	0.707935
21	SL4-5A	-2.57	0.16	0.707964	7.00E-06	0.707969
22	SL4-5B					
23	LV2-21a	-6.86	-0.54	0.708043	8.00E-06	0.708048
24	LV2-21B	-6.40	-0.36			
25	SL4-2	-3.04	-0.25			
26	SL4-3	-3.27	-0.24	0.707945	8.00E-06	0.707937
27	LV2-20			0.708043	8.00E-06	0.70803
28	LV2-19	-4.63	-1.49	0.708051	7.00E-06	0.708043
29	AH-10					
30	LV2-17	-4.05	0.61	0.70812	6.00E-06	0.708125
31	LV2-15	-6.05	1.43	0.708291	8.00E-06	0.708278
32	LV2-14					
33	LV2-13	-4.87	2.75			
34	LV2-12	-4.64	1.72	0.70829	6.00E-06	0.708277
35	LV2-10	-5.35	1.22			
36	LV2-9A	-4.58	1.26			
37	LV2-9B	-6.44	-1.46			
38	LV2-8A	-3.50	1.76	0.708339	7.00E-06	0.708344
39	LV2-7	-5.11	1.56			
40	LV2-5					
41	LV2-4B1	-5.62	1.43			
42	LV2-4B2	-5.81	1.54			
43	LV2-4C	-4.78	1.46			

* Normallized to NBS 987 standard value of 0.71023

Table 2. Continued

Number	Sample Id.	$\delta^{18}O$ ‰ (PDB)	$\delta^{13}C$ ‰ (PDB)	$^{87}Sr/^{86}Sr$	±1 σ	Normalized*
44	LV2-4D	-5.93	1.46	0.708362	7.00E-06	0.708349
45	LV2-4E	-5.39	1.88			
46	LV2-4F	-5.85	1.54			
47	LV2-3B	-4.65	0.25			
48	RA-18	-3.43	1.77	0.708312	8.00E-06	0.708304
49	RA-20	-4.65	2.19			
50	RA-19	-4.80	1.78	0.708373	8.00E-06	0.708365
51	RA-10	-5.24	1.53	0.708568	8.00E-06	0.708573
52	RA-15	-1.89	2.93			
53	RA-13	-5.42	2.20			
54	RA-9	-3.47	2.27	0.708567	8.00E-06	0.708559
55	RA-8	-3.82	1.72	0.708576	7.00E-06	0.708581
56	UA-1	-2.16	-0.45			
57	AH-8	-6.92	1.02	0.708691	8.00E-06	0.708683
58	AH-11	-6.85	0.15	0.708627	7.00E-06	0.708619
59	AH-12	-7.40	0.53			
60	AH-15	-7.12	1.39	0.708689	6.00E-06	0.708687
61	AH-16	-7.17	1.04			
62	AH-18	-8.23	0.73	0.708717	8.00E-06	0.708709
63	UA-3	-4.76	-0.83	0.708883	7.00E-06	0.708882
64	UA-4	-4.34	-0.14			
65	RA-5	-3.73	1.44			
66	AH-25A	-7.51	1.32	0.708682	7.00E-06	0.70868
67	AH-25B	-7.22	1.63			
68	AH-28	-7.70	1.16	0.708677	7.00E-06	0.708669
69	AH-29	-7.94	1.13			
70	AH-30	-7.96	1.30			
71	AH-31	-8.61	2.12	0.708707	8.00E-06	0.708705
72	UA-5	-4.41	-1.07			
73	UA-6a	-4.56	-0.33	0.708743	7.00E-06	0.708742
74	AH-35	-8.51	2.86	0.708683	6.00E-06	0.708681
75	AH-36	-8.55	2.79			
76	AH-38	-7.68	2.95			
77	AH-39	-8.50	3.33	0.708731	8.00E-06	0.708729
78	AH-40	-8.84	3.03			
79	AH-43	-8.63	2.40	0.709488	7.00E-06	0.709486
80	AH-45	-7.04	3.29	0.708691	8.00E-06	0.708689
81	UA-7a	-5.22	-0.13	0.708788	8.00E-06	0.708783
82	UA-7b	-5.17	0.40			
83	UA-8	-3.74	2.09	0.708678	7.00E-06	0.708673
84	UA-9	-4.35	1.21			
85	UA-10	-3.60	1.89	0.708681	8.00E-06	0.708676
86	UA-11	-4.09	1.79			
87	UA-12	-4.30	1.33	0.708697	8.00E-06	0.708684

* Normallized to NBS 987 standard value of 0.71023

Table 2. Continued

Number	Sample Id.	$\delta^{18}O$ ‰ (PDB)	$\delta^{13}C$ ‰ (PDB)	$^{87}Sr/^{86}Sr$	±1 σ	Normalized*
88	UA-14	-4.50	1.37	0.708703	6.00E-06	0.708698
89	UA-16	-3.74	2.02			
93	UA-18b					
90	UA-19a	-4.42	2.25	0.708676	8.00E-06	0.708671
91	UA-19	-4.40	1.82			
92	UA-20	-3.09	3.38	0.70871	8.00E-06	0.708697
94	UA-25a	-3.48	2.21	0.7087	7.00E-06	0.708695
95	UA-25b	-3.70	2.24			
96	UA-25c	-3.79	2.28			
97	UA-25d	-3.91	1.98			
98	UA-25e	-4.05	1.79			
99	UA-25f	-3.67	2.17			
100	UA-25g	-3.74	2.11			
101	UA-26*	-4.15	2.49			
102	UA-26b	-3.41	2.11			
103	UA-27	-3.33	3.42			
104	UA-28	-6.25	2.32	0.708699	8.00E-06	0.708694
105	UA-32	-4.66	1.87			
108	UA-30	-3.87	2.78			
106	UA-34	-4.08	1.39	0.708687	8.00E-06	0.708674
107	UA-34	-4.08	1.39	0.708696	8.00E-06	0.708691
109	UA-35	-3.84	1.97	0.708731	8.00E-06	0.708726
110	UA-36	-4.77	0.18			
111	UA-37	-3.82	1.65	0.708699	7.00E-06	0.708686
112	UA-40	-5.53	2.48			
113	UA-40a	-4.56	3.06	0.708739	8.00E-06	0.708726
114	UA-43	-3.46	3.71			
115	UA-41	-4.25	3.54	0.708721	7.00E-06	0.708716
116	UA-42	-2.73	5.50			
117	UA-44	-6.16	1.64	0.708717	8.00E-06	0.708704
118	UA-45	-4.70	3.15			
119	UA-47	-6.40	0.27			
120	UA-48	-6.36	-0.56			
121	UA-49	-5.85	0.40	0.70871	8.00E-06	0.708705
	Average	-5.07	1.48	0.7084816		0.708477
	Standard Dev.	1.6	1.17	0.0004		3.50E-04

* Normallized to NBS 987 standard value of 0.71023

APPENDIX 2

Table 3. Blanks and standards taken along with samples during ICP analysis

Run	Sample	Ca %	Mg %	Ba (ppm)	Fe (ppm)	Mn (ppm)	Sr (ppm)
april13-1	BL(1)	0.00	0.00	0.04	1.89	0.09	0.08
april13-2	BL(2)	0.00	0.00	0.01	1.44	0.11	0.02
april13-3	BL-1	0.00	0.00	0.00	1.19	0.04	0.01
april13-4	BL-2	0.00	0.00	0.00	0.96	0.04	0.01
april13-5	BL-3	0.00	0.00	0.04	1.83	0.08	0.06
april13-6	BL-3	0.00	0.00	0.01	1.08	0.04	0.01
april13-7	BL-4	0.00	0.00	0.01	0.91	0.04	0.01
april13-8	BL-5	0.00	0.00	0.01	0.89	0.04	0.01
april13-9	BL-6	0.00	0.00	0.02	1.42	0.07	0.02
april13-10	BL-7	0.00	0.00	0.04	1.44	0.07	0.02
april13-11	BL-8	0.00	0.00	0.02	1.43	0.10	0.02
april13-12	BL-9	0.00	0.00	0.04	1.46	0.08	0.06
april13-13	BL-10	0.00	0.00	0.03	1.64	0.07	0.02
april26-1	BL-11	0.00	0.00	0.05	1.21	0.06	0.06
april26-2	BL-12	0.00	0.00	0.05	1.03	0.03	0.05
april26-3	BL-13	0.00	0.00	0.06	1.15	0.07	0.11
april26-4	BL-14	0.00	0.00	0.06	0.97	0.03	0.04
april26-5	BL-15	0.00	0.00	0.07	1.34	0.04	0.09
april26-6	BL-16	0.00	0.00	0.05	1.74	0.02	0.02
april26-7	BL-17	0.00	0.00	0.09	1.83	0.08	0.18
	Average	0.00	0.00	0.03	1.34	0.06	0.04
	Standard Dev	0.00	0.00	0.02	0.32	0.03	0.04
april13-1	LMS(1)	39.09%	0.19%	38	1056	331	476
april13-2	LMS(2)	39.15%	0.23%	30	953	317	518
april13-3	LMS-1	39.19%	0.23%	27	1076	372	501
april13-4	LMS-2	39.18%	0.18%	38	1027	278	465
april13-5	LMS-3	39.15%	0.21%	33	1118	361	490
april13-6	LMS-4	39.28%	0.20%	22	788	335	500
april13-7	LMS-5	39.24%	0.19%	22	859	335	490
april13-8	LMS-6	39.01%	0.17%	36	1035	298	455
april13-9	LMS-7	39.16%	0.20%	26	1139	342	519
april13-10	LMS-8	38.71%	0.22%	39	1507	335	514
april26-1	LMS-9	39.10%	0.21%	23	1154	357	528
april26-2	LMS-10	38.94%	0.18%	28	1353	311	463
april26-3	LMS-11	39.19%	0.21%	17	1198	348	534
april26-4	LMS-12	39.15%	0.22%	19	897	306	472
april26-5	LMS-13	39.09%	0.20%	25	995	306	475
april26-6	LMS-14	39.05%	0.20%	24	1129	326	517
april26-7	LMS-15	39.02%	0.22%	33	1189	356	536
april26-8	LMS-11	39.06%	0.21%	26	1111	348	546
april26-9	LMS-12	38.99%	0.21%	29	1135	334	504
	Average	39.09%	0.21%	28	1090	331	500
	Stand Dev	0.0013	0.0002	7	166	24	27
Recommended value *		38.99	0.18	18.00	559	286	436

* Recommended values taken from XRF, Dept. of Geology, University of Ottawa.